

**Identifying 1 Mya Fire in Wonderwerk Cave
with Micromorphology and Fourier-Transform
Infrared Microspectroscopy**

by

Megan L. Thibodeau

B.A., Boston University, 2013

Thesis Submitted in Partial Fulfillment of the
Requirements for the Degree of
Master of Arts

in the

Department of Archaeology
Faculty of Environment

© **Megan L. Thibodeau 2016**

SIMON FRASER UNIVERSITY

Summer 2016

All rights reserved.

However, in accordance with the *Copyright Act of Canada*, this work may be reproduced, without authorization, under the conditions for "Fair Dealing." Therefore, limited reproduction of this work for the purposes of private study, research, criticism, review and news reporting is likely to be in accordance with the law, particularly if cited appropriately.

Approval

Name: Megan L. Thibodeau
Degree: Master of Arts
Title: *Identifying 1 Mya Fire in Wonderwerk Cave
with Micromorphology and Fourier-Transform Infrared
Microspectroscopy*

Examining Committee: **Chair:** Dr. Dongya Yang
Professor
Dept. of Archaeology, Simon Fraser University,

Dr. Francesco Berna
Senior Supervisor
Assistant Professor

Dr. Mark Collard
Supervisor
Professor

Dr. Panagiotis Karkanas
External Examiner
Director
The Malcolm H. Wiener Laboratory for
Archaeological Science
American School of Classical Studies
at Athens

Date Defended/Approved: July 22, 2016

Abstract

The role of fire in the evolution of humans is an important yet unanswered question in palaeoanthropology, but there is a striking lack of archaeological evidence for the presence or absence of anthropogenic fire-use by early hominins. This is partially due to the difficulty of identifying fire residues, such as wood ash. I demonstrated that Fourier Transform Infrared Microspectroscopy integrated with micromorphological analysis can distinguish microscopic amounts of pyrogenic calcite which include wood ash, from non-pyrogenic calcites. The ν_3 (CO_3) peak, an absorption of energy by one of the three C-O bonds, is quantifiably more narrow in pyrogenic calcites. With the protocol, I evaluated potential evidence of anthropogenic fire at 1 Mya in Wonderwerk Cave, a South African archaeological site. The results confirmed the earlier identification of ashed plant remains in Stratum 10, thus supporting the association of fire and anthropogenic activity in Wonderwerk Cave in the Earlier Stone Age.

Keywords: origin of fire; human evolution; Wonderwerk Cave; micromorphology; Fourier-Transform Infrared Spectroscopy; wood ash

For my dad

Acknowledgements

This thesis would not have been possible without the help of many people. I especially would like to thank my senior supervisor, Dr. Francesco Berna, for the opportunity to work on this amazing project at Wonderwerk Cave and enormous amounts of advice, encouragement, and support over the past few years. I am also very grateful to Dr. Mark Collard for his continued support, excellent advice, and constructive feedback.

Many thanks to Michael Chazan, for allowing me to sample from Wonderwerk Cave, and to the entire Wonderwerk and Kathu Pan team, for three fun and amazing field seasons.

The members of the Human Evolutionary Studies Program (HESP) and the 2013 SFU archaeology graduate cohort offered advice, ideas, and support, especially during the research design phase.

I would also like to thank my fifth grade teacher Mr. Myette, who taught me that I could enjoy writing, even if I would never admit that.

I am grateful for the financial support I received from the Social Sciences and Humanities Research Council (SSHRC), HESP, and Simon Fraser University.

Last but not least, I would like to thank my family. Mom, Dad, and Jill: you may not understand the science-y bits, but I couldn't have finished without your encouragement and love.

Table of Contents

Approval.....	ii
Abstract.....	iii
Dedication.....	iv
Acknowledgements.....	v
Table of Contents.....	vi
List of Tables.....	viii
List of Figures.....	ix
List of Acronyms.....	xii
Chapter 1. Introduction.....	1
1.1. Thesis Objectives.....	4
1.2. Thesis Outline.....	5
Chapter 2. Background.....	7
2.1. Identifying the Use of Fire in the Archaeological Record.....	7
2.1.1. Past Methods of Fire Identification.....	7
2.1.2. Soil micromorphology and FTIR.....	9
2.2. Early Evidence of Anthropogenic Fire.....	11
2.2.1. Koobi Fora.....	12
2.2.2. Chesowanja.....	14
2.2.3. Swartkrans Cave.....	15
2.2.4. Wonderwerk Cave.....	16
Chapter 3. Materials and Methods.....	21
3.1. Materials.....	21
3.1.1. Control Samples.....	21
3.1.2. OSC.....	23
3.1.3. Wonderwerk.....	24
3.2. Methods.....	26
3.2.1. Processing.....	26
3.2.2. Micromorphology.....	27
3.2.3. Identification of Wood Ash with FTIR.....	27
3.2.4. Fourier Transform Infrared Microspectroscopy (FTIR-m).....	29
3.2.5. FTIR-m Spectral Analysis.....	30
Chapter 4. Identifying Pyrogenic Calcite.....	33
4.1. Experimental Results.....	33
4.2. Summary of Experimental Results.....	37
4.3. V3 (CO ₃) Peak Width Protocol to Identify Potential Ash.....	39
Chapter 5. Identifying Archaeological Wood Ash.....	43
5.1. Known Archaeological Wood Ash.....	43

5.1.1.	Oscurusciuto Archaeological Ash	43
5.1.2.	Wonderwerk LSA Combustion Feature	45
5.1.3.	Discussion of Known Archaeological Ash	50
5.2.	WW Control Samples	52
5.3.	Wonderwerk Cave ESA Potential Ash Results.....	55
Chapter 6. Discussion and Conclusions.....		81
6.1.	General Findings	81
6.2.	Reliability of v_3 (CO_3) Width as Proxy for Formation Process	83
6.3.	Implications of Fire at Wonderwerk.....	85
6.4.	Potential Future Research	89
6.5.	Conclusions.....	90
References.....		92

List of Tables

Table 3.1	Control Samples and preparation methods for heated samples	22
Table 3.2	Oscurusciuto Samples	24
Table 3.3	Wonderwerk Sample	25
Table 4.1	Descriptive statistics of v3 (CO ₃) peak widths for areas in control samples	35
Table 4.2	Identification Criteria for Wood Ash	41
Table 4.3	Categorization of v3 (CO ₃) Peak Widths.....	42
Table 5.1	Descriptive statistics of v3 (CO ₃) peak widths for OSC archaeological ash samples	48
Table 5.2	Descriptive statistics of v3 (CO ₃) peak widths for WW LSA combustion feature samples.....	48
Table 5.3	Descriptive statistics of v3 (CO ₃) peak widths for WW control samples	53
Table 5.4	Descriptive statistics of v3 (CO ₃) peak widths for areas in WW05-04 60	
Table 5.5	Descriptive statistics of v3 (CO ₃) peak widths for areas in WW11-07 66	
Table 5.6	Descriptive statistics of v3 (CO ₃) peak widths for areas in WW11-09 75	
Table 5.7	Descriptive statistics of v3 (CO ₃) peak widths for areas in WW11-10A	79
Table 6.1	Classification of Unknown Archaeological Samples	83

List of Figures

Figure 2.1	Map showing the location of Wonderwerk Cave	17
Figure 2.2	Plan of Wonderwerk Cave generated by laserscanning with locations of excavation areas. Red star marks where the evidence of fire was found.....	18
Figure 3.1	(a) Map showing the location of Oskurusiuto rockshelter (b) Stratigraphy of Oskurusiuto. The earliest permanent occupation is SU 13.	24
Figure 3.2	East profile of Square R28 showing lithostratigraphic units at left, and the location of micromorphology samples. The blue rectangle indicates the sample with evidence of fire that was collected in 2005. Red rectangles indicate the samples analyzed that were collected in the 2011 season.	26
Figure 3.3	Top: typical calcite spectra with v3 (CO ₃) (~1420 cm ⁻¹), v2 (~875 cm ⁻¹), and v4 (~713cm ⁻¹) peaks indicated. Bottom: FTIR-m reflectance spectra of Chalk-900°C with the v3 (CO ₃) peak indicated. The horizontal and vertical lines demonstrate how the height and width were measured. The length (in wavenumbers) of the horizontal line at 75% of the v3 (CO ₃) peak is the width at 75% of the height (intensity) of the v3 (CO ₃) peak (W3/4M).	32
Figure 4.1	Typical spectra of v3 (CO ₃) peak shapes in different calcite types. a. Sparite has the widest peak, with the maximum intensity at around 1500. b. Chalk has a medium, rounded peak with the highest intensity at lower wavenumbers. c. Experimental Ash 900°C is the narrowest, with a sharp peak and highest intensity located around 1400.	34
Figure 4.2	Comparison of v3 (CO ₃) widths by material for the control samples	36
Figure 5.1	(a) Photomicrograph of a cluster of ash rhombs in WW14-01 – Area 1 PPL, XPL (b) Photomicrograph of a cluster of ash rhombs in WW14-01 – Area 2. PPL, XPL.....	46
Figure 5.2	v3 (CO ₃) widths of OSC and WW known archaeological ash examples compared to control samples	49
Figure 5.3	v3 (CO ₃) widths of definitively un-burnt calcite materials in Wonderwerk Cave compared to control samples.	54

Figure 5.4	(a) Thin section WW05-04 from Layer 10 with three microstratigraphic units. Examples of ashed plant fragments identified in Berna et al. (2012) are indicated letters and close-ups are provided in b - f. (b) Micrograph of ashed plant fragment with identifiable ash rhomb cluster (Area 1). (c) Micrograph of ashed plant fragment (Area 2). (d) Micrograph of ashed plant fragment (Area 3). (e) Micrograph of ashed plant fragments and wood ash rhombs dispersed in sediment (Area 4). (f) Micrograph of ashed plant fragment with possible charring (Area 5). 57	57
Figure 5.5	(a) Photomicrograph of WW05-04 Area 1. PPL (b) Same as a except XPL. (c) Photomicrograph of Area 1 with FTIR map superimposed. The extent of the map is shown by the black box. The colors indicate different v_3 (CO_3) widths. Empty squares indicate areas without calcite or without enough signal to identify the material. 58	58
Figure 5.6	(a) Photomicrograph of WW05-04 Area 4. PPL (b) Same as a except XPL. (c) Photomicrograph of Area 1 with FTIR map superimposed. The extent of the map is shown by the black box. The colors indicate different v_3 (CO_3) widths. Empty squares indicate areas without calcite or without enough signal to identify the material. Note that the orange and yellow squares with wider v_3 (CO_3) peaks cluster on the edge of the ashed plant fragment. 59	59
Figure 5.7	v_3 (CO_3) widths in WW05-04 areas compared to the control samples 61	61
Figure 5.8	(a) Photomicrograph of WW11-07 – Area 6. PPL (b) Same in XPL. 63	63
Figure 5.9	(a) Thin section WW11-07 from Layer 10. Areas with potential ashed plant fragments are indicated by the boxes and close-ups are provided in b - f. (b) Micrograph of ashed plant fragment with extensive calcitic infilling (Area 1). (c) Micrograph of ashed plant fragment (Area 2). (d) Micrograph of ashed plant fragment (Area 3). 64	64
Figure 5.10	Photomicrograph of WW11-07 Area 1. PPL (b) Same as a except XPL. The green oval indicates the area of larger, more crystalline calcite in the center of the sample. The blue box indicates subsection 1a. (c) Photomicrograph of Area 1 with FTIR map superimposed. The extent of the map is shown by the white box. Empty squares indicate areas without calcite or without enough signal to identify the material. The colors indicate different v_3 (CO_3) widths. Note the clusters of green (geogenic v_3 (CO_3) widths) match the location of the larger, more crystalline section. (d) Photomicrograph of subsection 1a which excludes the intrusive calcite in the center. FTIR map superimposed. The extent of the map is shown by the blue box. 65	65
Figure 5.11	v_3 (CO_3) widths in WW11-07 areas compared to the control samples 67	67

Figure 5.12	(a) Thin section WW11-09 from Layer 10. Areas with potential ashed plant fragments are indicated by the boxes and close-ups are provided in b - e. (b) Micrograph of ashed plant fragment with possible charring (Area 1). (c) Micrograph of ashed plant fragment (Area 2). (d) Micrograph of ashed plant fragment with extensive calcitic infilling of voids (Area 3). (e) Micrograph of ashed plant fragments (Area 4).	70
Figure 5.13	(a) Photomicrograph of WW11-09 Area 1. PPL (b) Same as a except XPL. The green oval indicates an area with thick calcite coating. (c) Photomicrograph of Area 1 with FTIR map superimposed. The extent of the map is shown by the black box. Empty squares indicate areas without calcite or without enough signal to identify the material. The colors indicate different v_3 (CO_3) widths. Note the clusters of green (geogenic v_3 (CO_3) widths) on the edges in areas with calcitic coating and/or infilling.	71
Figure 5.14	(a) Photomicrograph of WW11-09 Area 2. PPL (b) Same as a except XPL. (c) Photomicrograph of Area 2 with FTIR map superimposed. The extent of the map is shown by the black box. Empty squares indicate areas without calcite or without enough signal to identify the material. The colors indicate different v_3 (CO_3) widths. Note the clusters of green (geogenic v_3 (CO_3) widths) on the edges in areas with calcitic coating and/or infilling. (d) Close-up of the section in the blue box. There are large calcite crystals infilling the void on the edge of the ashed plant fragment.	72
Figure 5.15	(a) Photomicrograph of WW11-09 Area 3. PPL (b) Same as a except XPL. (c) Photomicrograph of Area 3 with FTIR map superimposed. The extent of the map is shown by the black box. Empty squares indicate areas without calcite or without enough signal to identify the material. The colors indicate different v_3 (CO_3) widths. Note the clusters of green (geogenic v_3 (CO_3) widths) on the edges in areas with calcitic coating and/or infilling.	73
Figure 5.16	(a) Photomicrograph of WW11-09 Area 4. PPL (b) Same as a except XPL. (c) Photomicrograph of Area 4 with FTIR map superimposed. The extent of the map is shown by the black box. Empty squares indicate areas without calcite or without enough signal to identify the material. The colors indicate different v_3 (CO_3) widths. Note the clusters of green (geogenic v_3 (CO_3) widths) on the edges in areas with calcitic coating and/or infilling.	74
Figure 5.17	v_3 (CO_3) widths in WW11-09 areas compared to the control samples	76
Figure 5.18	(a) Thin section WW11-10A from Layer 10. Areas with calcite are indicated by the boxes and close-ups are provided in b – c. (b) Micrograph of micritic calcite fragment (Area 1). (c) Micrograph area with very fine calcite particles mixed with clays (Area 2).	78
Figure 5.19	v_3 (CO_3) widths in WW11-10A areas compared to the control sample	80

List of Acronyms

ESA	Early/Earlier Stone Age
FTIR	Fourier-Transform Infrared Spectroscopy
FTIR-m	Fourier-Transform Infrared Microspectroscopy
kya	Thousand years ago
LSA	Late/Later Stone Age
MSA	Middle Stone Age
Mya	Million years ago

Chapter 1.

Introduction

The control of fire has long been considered a pivotal moment in the development of modern human behaviour (Oakley 1956; Goudsblom 1986; Rolland 2000; Sandgathe et al. 2011; Dunbar and Gowlett 2014). Pyrotechnology has a wide-ranging and valuable assortment of applications for humans and all ethnographically documented societies have used and controlled fire on a regular basis. Beyond offering heat and light, fire gives protection from predators, increases the length of day, and promotes social bonding (Clark and Harris 1985; Bellomo 1994; Dunbar 2014). Cooking makes inedible materials edible, decreases foodborne illnesses, and increases the calorific value of a food (Wrangham et al. 1999; Carmody and Wrangham 2009; Boback et al. 2007). It can help preserve food (e.g. through smoking), alter the environment to favor useful plants and animals, clear land for agriculture, and improve the physical properties of tools (Daniau et al. 2010; Bird et al. 2008; Bellomo 1994; Brown et al. 2009).

Despite its importance, there is no consensus for when and how early hominins began to interact with and then control fire. Currently, estimates for habitual use of fire range from 1.9 million years ago (Mya) to 350 thousand years ago (Kya) to as recently as 30 Kya (Wrangham et al. 1999; Barbetti 1986; Roebroeks and Villa 2011; Sandgathe et al. 2011). The wide range of proposed dates is due to the lack of secure archaeological evidence associating hominins and fire use (Clark and Harris 1985; James 1989; Gowlett 2006).

Without solid archaeological evidence, archaeologists have attempted to identify aspects of human behaviour that could not occur without the control of fire or that may be adaptations that require the use of fire. The appearance of these traits in the fossil and archaeological record could then be considered a minimum early date for the control of

fire. Proposed traits considered to require obligatory fire-use include habitation in glacial climates, occupation of caves, and cooking (Oakley 1961; Wrangham et al. 1999). For much of the 20th century, archaeologists and palaeoanthropologists assumed fire was a prerequisite for hominin survival in glacial climates and thus it was inferred that habitual use of fire began prior to human occupation of Europe (Oakley 1961; James 1989; Parfitt et al. 2005). Another hypothesis dated the control of fire to the earliest occupation of caves, arguing that fire was required to drive off predators (Oakley 1961). However, recent surveys of archaeological evidence of fire-use in site did not find consistent indications of fire-use until after occupation of glacial climates and caves by hominins (Roebroek and Villa 2011; Sandgathe et al 2011).

In 1999, the Cooking Hypothesis stimulated a great deal of interest in the debate when it argued that the biological and paleontological evidence necessitated that hominins were cooking food habitually by 1.89 Mya. There is no example of a human society that does not eat cooked food on a regular basis, suggesting that humans are obligate cooks. (Wrangham et al. 1999). In the cooking hypothesis, this dependency began sometime before 1.89 Mya, when *Homo erectus* evolved three traits: a larger brain, a smaller gut, and smaller teeth with respect to their antecessors habilines and australopiths. Wrangham argues this suite of morphologies is only possible if hominids switched from devoting a large amount of energy to the intestinal tissue, which allows the digestion of raw foods, to the brain because food is predigested as a result of cooking (Wrangham et al. 1999; Aiello and Wheeler 1995). Cooked food provides a significant increase of calorific value and reduction of chewing time and subsisting on raw food has serious negative effects on reproductive abilities in women (Boback et al. 2007; Koenig et al. 1999; Organ et al. 2011; Wrangham et al. 1999; Wrangham and Conklin-Brittain 2003; Zink et al. 2014). While the biological and paleontological evidence may support this hypothesis, there is little archaeological evidence to show that humans used fire at all, let alone habitually controlled of fire at this early date (Gowlett and Wrangham 2014; Roebroek and Villa 2011).

An essential part of evaluating theories about the role of fire in human evolution, and the cooking hypothesis in particular, is testing whether it fits with the evidence of fire-use in the archaeological record. Because the cooking hypothesis is built on

interpretations from biological and paleontological evidence, the archaeological evidence is a related, but distinct line of evidence that has the potential to support the conclusions or suggest that another explanation better explains the adaptations in early humans. However, there is a scarcity of archaeological evidence due to the difficulty of identifying ancient fire residue. Until recently, there was a lack of emphasis on proving the presence or absence of fire-use in later sites due to the assumption fire-use had already been established in early hominin site as well as the lack of microarchaeological techniques to identify ancient fire-residues in most sites (Sandgathe et al. 2011). Because most early prehistoric archaeologists assumed fire-use began in the MSA or earlier, fire residues were often only remarked upon in sites where it was especially prevalent or unusual and there are few efforts to quantify the intensity or frequency of fire use throughout an occupation. Even when evidence of fire is deliberately searched for, identifying hominin use of fire in the Early Stone Age (ESA) is difficult because you must not only identify residues of fire, which are often ephemeral and subject to taphonomic processes, but also demonstrate that the fire is associated with hominin behaviour, and not the result of natural fire on the landscape.

Currently, the evidence for the use of fire is sufficiently ambiguous that we cannot rule out claims of habitual fire use by 1.89 Mya nor claims that as recently as 30 kya habitual fire use was not universal (Wrangham et al. 1999; Roebroeks and Villa 2011; Sandgathe et al. 2011). Due to this problem, there is a growing interest in emphasizing the secure identification and contextualization of fire residues in archaeological sites (Sandgathe et al. 2011). This has led to an approach that prioritizes a thorough understanding of depositional and taphonomic processes, in order to establish the context and relationship between the evidence of fire and hominin activity (Bellomo 1993, 1994; Karkanas et al. 2007; Sergant et al. 2006; Isaac 1982). Karkanas et al (2007) lists four criteria that are required for secure attribution of fire to humans: “(1) burnt artifacts are in primary depositional setting, (2) artifacts such as bones and lithics are indeed burnt, (3) the surrounding sediment is composed of ash and/or its stable derivatives (e.g., siliceous aggregates, wood ash, phytoliths), and (4) other minerals (such as clays) are burnt as well.”

This study focuses on Karkanas' (2007) third criterion: the presence of in situ wood ash or its derivatives. The presence of ashed plant remains is one of the strongest lines of evidence to pinpoint the location of a fire and thus link a fire with hominin activity. Perceptible quantities are unlikely to survive movement, especially by natural processes such as wind, and so ash deposits usually mark the location of the fire, or post-fire anthropogenic cleaning. However, ash is easily destroyed by taphonomic processes and is very difficult to identify in ancient sediments.

1.1. Thesis Objectives

The goal of this thesis is to demonstrate a new method of identifying ashed plant remains and use the method to evaluate the evidence for potential anthropogenic fire residues from a 1 Mya hominin occupation in Wonderwerk Cave.

Recently, robust evidence of in situ fire associated with ESA assemblages was found at Wonderwerk Cave in South Africa. Micromorphological analysis identified what appears to be intact ashed plant remains. The presence of these intact ash fragments suggests that a fire occurred inside the cave, which is a secure anthropogenic context with limited potential for wildfires (Berna et al. 2012). However, the identification of these ash deposits has been complicated by the presence of micritic pseudomorphs of plant tissues which can resemble wood ash in micromorphological analysis (Goldberg et al. 2015). While the identification of wood ash originally reported remains uncontested, based on the clear micromorphological characteristics of wood ash as well as corroboration from other lines of evidence for fire, a secure method to distinguish between the two would provide another proxy to support the identification of fire and greatly aid future research on the presence of fire throughout the cave.

This thesis addresses this problem in three parts. First, I demonstrate a new analytical protocol that is capable of identifying microscopic amounts of ashed plant remains by integrating archaeological soil micromorphology and infrared spectroscopy. My new protocol expands on previous work using Fourier-Transform Infrared Spectroscopy to distinguish pyrogenic calcite, which includes wood ash, from other forms of calcite.

To test the ability of this protocol to accurately identify archaeological ash, I used two examples of known combustion features from prehistoric sites: Oscurusciuto and Wonderwerk Cave. Oscurusciuto is a Middle Palaeolithic site in southern Italy that contains a number of ancient, well-preserved hearths (Spagnolo et al. in press). The excellent preservation and extensive sampling make Oscurusciuto a good test site for evaluating the capabilities of FTIR-m to identify wood ash. Wonderwerk Cave was continually occupied for over 1 Mya and a later stratum includes a Late Stone Age (LSA) occupation horizon that includes a combustion feature. As a known example of a burning activity in the same location as the potential ESA combustion feature, it is a good test of whether the protocol's ability to detect wood ash is affected by environmental or geological factors in Wonderwerk Cave.

Finally, I use this protocol to evaluate the evidence of intact ashed plant remains in the ESA layers at Wonderwerk Cave. The results are consistent with an identification of pyrogenic calcite and support the original identification of the ashed plant remains. This strengthens the evidence for fire in an anthropogenic context at Wonderwerk Cave, and helps to address the lack of knowledge on early hominin interactions with fire. With stronger and broader archaeological evidence of the presence and absence of wood ash, we will be able to better evaluate the different theories on the origins of fire.

1.2. Thesis Outline

This introduction established the importance of pyrotechnology in human evolution and how this study addresses the general problem of a lack of archaeological evidence of fire residues in the past, and the specific problem of identifying wood ash in Wonderwerk Cave. Chapter 2 summarizes the current potential evidence for anthropogenic fire use in the ESA and goes into more detail on the difficulties and current methods of identifying fire in prehistoric contexts. Next, in Chapter 3, I outline the control materials and archaeological samples along with the methodology I used to develop the ν_3 (CO_3) peak width protocol in order to identify wood ash. Chapter 4 presents the results of the control sample set, and demonstrates how FTIR-m can distinguish between different types of calcite. I use these results to develop the ν_3 (CO_3) peak width protocol, a method and set of criteria for evaluating potential examples of ashed plant remains. In Chapter 5, I first

test this protocol using known, confirmed examples of ash from prehistoric anthropogenic fires, and then apply the protocol to evaluating potential evidence of ashed plant remains from ESA layers in Wonderwerk Cave. Chapter 6 discusses my findings, the reliability of this new protocol, and the implications of these results for the putative association between hominins and fire at Wonderwerk Cave. Lastly, Chapter 6 concludes by proposing avenues for future research and situates this research within the broader context of understanding the role of fire in human evolution.

Chapter 2.

Background

In this chapter, I discuss the difficulty of identifying anthropogenic fire and specific techniques that have been used. This leads to an overview of two currently essential methods of identifying and contextualizing fire residues: micromorphology and Fourier-Transform Infrared Spectroscopy. These techniques are the foundation of my new protocol for identifying ashed plant remains. In order to explain how FTIR can identify wood ash, a summary of calcite formation processes, and specifically, pyrogenic calcite, is included. I end by reviewing the earlier research that first used FTIR to identify wood ash and explain how I expand on it and why my protocol is necessary.

In the second half of the chapter, I give an overview of how microarchaeological techniques were used to conclusively establish the earliest evidence for human-controlled fire at Qesem Cave. This leads to a discussion of the ways anthropogenic fire-use has been misidentified in the past. Following that, I review four African sites with evidence of potential fire-use in the ESA, including Wonderwerk Cave, and discuss the strengths and weaknesses of the evidence in each site.

2.1. Identifying the Use of Fire in the Archaeological Record

2.1.1. Past Methods of Fire Identification

In most cases, the primary challenge is not identifying combustion features in an archaeological context, but proving that it was made or used by humans. Fire has been a part of Earth's environment for almost five hundred million years and it has been a frequent natural event over the past two million years in the warm, dry savannah environments hominins evolved in (Scott 2000; Archibald et al. 2010, 2012). The African continent has the highest rate of wildfires and on average, over 130 million hectares of savannah south of the equator burn every year (Giglio et al. 2006). The base assumption must be that fire is the result of natural causes, not hominin behavior.

The most conclusive evidence of a controlled fire in archaeological sites is the presence of a constructed hearth. However, the earliest evidence of constructed hearths is not until the Middle Paleolithic (Karkanas et al. 2004; Vaquero and Pastó 2001). Even in modern hunter-gatherer populations constructed hearths are not used consistently or ubiquitously (Bird et al. 2008).

Modern ethnographic and ethnoarchaeological research has found that humans use fire in a wide variety of forms, including deliberately setting grass or forest fires to modify the landscape, and burning stumps to clear the land or preserve coals for long periods of time (Daniau et al. 2010; Mallol et al. 2007; Bird et al. 2008). Although these are examples of fire-control, they are difficult or impossible to distinguish from natural fire events. Therefore, efforts have focused on identifying characteristics specific and unique to camp or hearth fires, which are solely created by humans. Camp or hearth fires are deliberately contained and well-controlled fires within a small area that are primarily used for heat, light, cooking, and as a central social location within a camp. They can be temporary, one-time use fires, or semi-permanent fires with multiple burn periods lasting day, months, or even years. Experimental analyses of sediment from grass, stump, and campfires has found that multi-burn campfires produced alterations in the colour and magnetic properties in the sediment that were distinct from either stump or grass fire. Magnetometry survey, magnetic susceptibility, paleomagnetism analysis and others were able to distinguish between modern fired and unfired sediment, as well as campfires and other types of fires. The differences are a result of the higher temperatures and longer duration. (Bellomo 1993; Bellomo and Kean 1997; Gowlett et al. 1981; Pickering 2012). The survival of these alterations and alternative causes of alterations in sediment are less conclusive. There has been very little research done on the full range of effects grass and stump fire can cause.

Identifying unstructured hearths requires greater analytical precision and spatial analysis. Unstructured hearths occur when fire is used consistently and intensively in a small area, resulting in a large, macroscopic accumulations of ash, charcoal, and burnt bone/lithics that match a pattern of spatial behavior observed geographic and temporal regions (Vaquero and Pastó 2001; Sergant et al. 2006). However, experiments on fire residues suggest that most short-term fires leave few visible remains that survive long-

term. (Mallol et al. 2007, 2013). One solution uses spatial patterns of burnt lithics, as the indication most likely to survive, to indicate the location of hearth that lack more prominent, visible features (Sergant et al. 2006). The use of lithics limits this to regions where the stone has identifiable reactions to heat. Identifying unstructured hearths with other materials requires microarchaeological techniques such as FTIR and soil micromorphology which can identify the fire residues even when no macroscopic evidence has survived.

2.1.2. Soil micromorphology and FTIR

The ephemeral nature of fire residues and the re-evaluation of early examples of the control of fire demonstrate the necessity of multi-proxy evidence and an understanding of the post-depositional context. Two techniques that have proven crucial in identifying fire and understanding the formation and taphonomic processes are soil micromorphology and Fourier-Transform Infrared Spectroscopy (FTIR).

Micromorphology is the study of intact archaeological deposits and features processed in petrographic thin sections (Goldberg and Macphail 2006). It has proven to be valuable for analyzing fire residues through the identification of ash deposits, charred material, and burnt stone and bone. Equally importantly, the microscopic analysis of the specimens maintains the original spatial organization, which allows for the identification of natural depositional processes and anthropogenic activities to determine whether the fire residues are in-situ, a vital part of establishing the source of the fire (e.g. natural, human-made) (Goldberg and Berna 2010; Weiner 2010). For example, it is possible to identify occupational surfaces within a sequence and link deposits directly with hominin surfaces. Identifying microstratigraphic units, or microfacies, can differentiate between individual events, such as different combustion features, trampling, and hearth maintenance (Goldberg and Berna 2010; Schiegl et al. 1996). These capabilities make micromorphology an important part of identifying and contextualizing evidence of fire in archaeological sites.

Fourier-Transform Infrared Spectroscopy and Microspectroscopy (FTIR and FTIR-m) are an increasingly common part of archaeological analysis as they have been

demonstrated to be valuable for the characterization of the archaeological record and the reconstruction of site formation processes (Berna and Goldberg 2007; Berna et al. 2007; Weiner et al. 1998). They can identify the inorganic and organic compounds of raw and plastic materials (e.g., stone, plaster, adobe, glass), bones, wood, charcoal, and pigments, and characterize their preservation state (Weiner 2010). It is also applied to identify secondary minerals forming as a result of specific human activities such as food processing, pyrotechnological processes (metallurgy, pottery), livestock penning, and/or as a result of specific environmental conditions (e.g., sediment acidification and/or phosphatization) (Weiner et al. 1993; Chu et al. 2008; Thompson et al. 2009).

FTIR uses the absorption of IR energy by the bonds between atoms in a molecule to provide a way to characterize and identify different substances. The specific wavelength of energy absorbed is dependent on the type of chemical bond and the type of vibrations of the molecule (Lane 1999). It can detect different molecules as well as changes in the molecular structure and bonds within a single material, including differences caused by heat altering the molecular structure of certain materials (Lane 1999; Poduska et al. 2011). Research by Berna (2007) has demonstrated that by using FTIR it is possible to identify heat induced mineralogical alteration of clay minerals commonly found in soils. Using this, it is possible to analyze loose sediment and determine if it was subjected to heat at a specific temperature. A similar FTIR application can identify if bone has been heated (Steiner et al., 1995)

FTIR-m can complement micromorphological analysis because it can analyze individual grains that are less than 100 microns across on a micromorphological thin section, linking the compositional data from FTIR-m with the contextual data from micromorphology. Using it, it is possible to directly analyze microartifacts within a single microfacie or occupation layer (Goldberg and Berna 2010). This provides a very detailed and precise interpretation of any heated material and its association with the surrounding deposit.

2.2. Early Evidence of Anthropogenic Fire

Almost all evidence for fire-use by hominins in the ESA is based on the presence of fired soil and/or bones and/or lithics within a mixed assemblage or palimpsest (James 1989). The majority of ESA sites in Africa are either deposits of archaeological material transported and accumulated by natural processes (e.g. sinkholes, carnivore deposits) or open-air sites that are in fact palimpsests of multiple occupations without clear stratigraphy (Spagnolo et al.). The depositional history in these sites complicates the relationship of hominin activity with heat-altered material, making it difficult to conclusively establish anthropogenic control or creation of the fire. For this reason, there are few sites older than 500,000 BP with potential evidence of hominin interaction with fire and those that exist are disputed (Isaac 1982; Gowlett et al. 1982; Bellomo 1993; Brain and Sillen 1988; Berna et al. 2012; Barbetti 1986).

The earliest noncontroversial evidence of human use of fire is from 400 kya in Qesem Cave, located in the Levant. The lower layers of occupation contained individual undisturbed loci of burnt material. In the upper layers, there was a 4.5m thick section of the stratigraphy was composed of reworked wood ash mixed with burnt bone, lithic artifacts, and heated soil. The burnt bones were originally identified visually, but FTIR analysis confirmed the identification (Karkanas et al. 2007). Likewise, stable oxygen isotope analysis results were consistent with wood ash (Shahack-Gross and Ayalon 2013). Micromorphological analysis characterized the context and depositional history of the sequence (Karkanas et al. 2007). The claim for fire in Qesem used multiples lines of evidence and microarchaeological analyses to verify macroscopic, visual identification. The use of microarchaeology to confirm field interpretations is a critical part of the strength of the evidence for fire-use.

Recently, modern analytical techniques have disproven two accepted examples of early fire-use at Zhoukoudian Cave and Schöningen. Zhoukoudian Cave in eastern China was seen as the most secure evidence of fire use in the Lower Paleolithic, on the basis of meter deep ash deposits containing charcoal and burnt bone. However, the ash deposits were reanalyzed with FTIR and determined to be loess (Weiner et al. 1998). Micromorphological analysis of the site formation processes found that the layers with

charcoal and burnt bone were formed in a low-energy fluvial environment. The microfacies were a result of natural processes, not living surfaces, and the burnt material had originated outside of the cave. Because of this, the charred bones and charcoal had no relation to the artifacts they were found with (Goldberg et al. 2001; Weiner et al. 1998).

A similar story occurred at Schöningen, which was considered the best evidence for the control of fire in Europe during the Lower Paleolithic. It was based on qualitative macroscopic observations of reddened sediment in the shape of hearths (Thieme 1997, 2005). It was reanalyzed using a suite of microarchaeology techniques, including micromorphology, FTIR and FTIR-m, and thermoluminescence analysis. The results found that the reddened sediment was a result of natural post-depositional processes of iron precipitation and oxidation (Stahlschmidt et al. 2015). These misidentifications demonstrate the necessity of scientific, quantifiable techniques to confirm the presence and context of combustion features, as well as demonstrating how our capability to detect fire has improved in the past decades. Prior to the use of microarchaeological approaches, identifying fire residues was far more difficult.

2.2.1. Koobi Fora

Koobi Fora encompasses a large collection of sites located near Lake Turkana in Kenya with a rich history of hominin activity beginning in the Oldowan period. Potential 'fireplace' features were found in the FxJj20 site complex, located on the west bank of a gully that drains a headland on the Karari Escarpment. The Karari Escarpment was formed from accumulation of water-transported material deposited in broad alluvial floodplain with a number of braided streams (Isaac 1997: 44-45). FxJj20 sits on top of the Okote Tuff Complex, which has been K-Ar dated to 1.64 Ma (Isaac 1997: 147-150). It includes four different excavation areas (E, M, AB, S) and at least two different high-density artifact clusters ((Isaac and Project 1997: 147).

Two discolored, oxidized patches of sediment were found in FxJj20M and five were found in FxJj20E (Bellomo and Kean 1997: 224). The features are located at the base of

the archaeological horizon within a bed of mudstones interlayered with sand and tuffaceous silt. The discolored sediment in the features extends 30-40cm in diameter and in two cross-sectioned features, the top five centimeters were oxidized with discoloration extending 10-15 cm. (Bellomo and Kean 1997: 165). Within FxJj20M, three stone artifacts were identified as potentially heated out of 335 discolored samples (and approximately 2500 stone artifacts overall) (Bellomo 1994).

The potential fire features have been extensively analyzed and compared to experimental single and multi-burn campfires, tree stump fires, and grass fires. A magnetometer study of the excavation area found small, but clear anomalies approximately at the location of the two features in FxJj20M, but not FxJj20E. Bellomo and Kean (1997) concluded that one of the features in FxJj20M was unequivocally the result of hominin-controlled fire, as archaeomagnetic data collected from the feature produced results consistent with the experimental campfires and different from the control wildfire samples. The archaeomagnetic data from the second feature was less conclusive, as the results differed from the control samples but were not consistently within the range of results predicted by the experimental campfire. (Bellomo and Kean 1997; Bellomo 1993).

The results from the five features in FxJj20E were intriguing but not as promising as those from FxJj20M. Magnetometry data did not show any anomalies at the location of the features and archaeomagnetic results did not consistently reach the range expected from a campfire (Bellomo and Kean 1997). They suggested that higher amounts of weathering and erosion at FxJj20E could have affected the archaeomagnetic data (Bellomo and Kean 1997; Barbetti et al. 1980). A study on the phytolith remains found that in four of the features, the relative amounts of different types of phytoliths (arboreal, grass, palm, other) were consistent with the heterogeneity of phytoliths in campfires, and distinct from phytoliths found from a stump fires. The fifth feature contained a phytolith assemblage far more similar to the natural burning of a single tree. That feature had also been the most anomalous in the archaeomagnetic analyses (Rowlett 2000).

Crucial to understanding if and how hominins used fire here is determining what taphonomic processes may have disturbed the site. Although the disturbance may be

minimal when compared to other similarly ancient sites, it still complicates our capability to evaluate whether it can be definitively identified as anthropogenic and what activities may have been associated with it. Both now and in the past, the site was subject to water action, as a floodplain for the lake and transient streams (Bellomo 1993; Isaac 1997: 147). Isaac argues that the stone artifacts within both M and E are very well-preserved when compared to nearby sites of similar ages. There is a wide range of sizes, including small and angular fragments, which suggests that there was only minimal transport or disturbance of the artifacts (Isaac 1997: 155, 161). At FxJj20E, the interbedded stratigraphy of fine sand and silt indicates that there was low-energy fluvial activity. When combined with the bioturbation by roots and rodent activity, it is clear that there was some horizontal and vertical movement, estimated to be as much as 60-80 cm (Isaac 1997: 147, 161). As a result, there are no identified living surfaces and the relationship of artifacts to the features is unknown.

In comparison to most other examples of ESA fire, FxJj20 is claiming that the hearths are in-situ and thus can offer information on how hominins used fire. There is new ongoing research combining FTIR, micromorphology, and spatial analysis to improve the data and understanding of the features (Hlubik, personal communication). The data from FxJj20 is inconclusive, but does offer promising evidence that the hominins may have been using fire 1.6 Mya. Determining what the fire was used for or whether hominins had the capability of controlling or creating fire is a different problem.

2.2.2. Chesowanja

Chesowanja is an Oldowan site located on the east side of Lake Baringo in Kenya. It is below the Chesowanja Formation, which has been potassium argon dated to 1.42Ma. The largest excavation, GnJi 1/6E, contained a large assemblage of artifacts and faunal remains, including clay clasts that appear to have been burnt (Clark and Harris 1985). All the archaeological materials occurred within a silty-clay sediment with lenses of sand which was likely deposited in a low-energy fluvial environment (Gowlett et al 1981).

Fifty-one clay clasts were identified as heated to 400C based on remanent magnetism analysis (Clark and Harris 1985; Gowlett et al 1981). Similar clay clasts have

been identified as the result of heating in both more recent prehistoric fires and natural bush fires (Gowlett et al 1981; 1982; Isaac et al 1982). The close spatial association and temperature of the clay clasts suggests that the fire was anthropogenic (Gowlett et al 1981).

Since the spatial relationship between the clay clasts and the hominin artifacts is the key piece of the evidence for anthropogenic fire, understanding the taphonomy of the site is crucial. The clay clasts, along with the associated artifacts, were horizontally distributed in what may have been a small, temporary water channel, with a concentration of artifacts in the northwest corner of the excavation area. In response to criticism about the role of water transport in the arrangement archaeological materials, Gowlett et al performed analyses on the size and shape. The clay clasts have sharp edges, supporting the idea that they were not transported or were not transported a long distance (Gowlett et al 1982). Analysis on the clay clasts and artifacts did not show any statistical signs of size-sorting, which normally indicated water transport (Clark and Harris 1985; Gowlett et al 1981). Refits of stone artifacts have been found within the 40m² excavation which speaks to the lack of disturbance in the area (Gowlett and Wrangham 2013). In place of water transport, Gowlett et al (1981) proposed that the combustion was more resistant to erosion than the unburnt sediment around it and became a slight raised mound as the unburnt material was removed. Over time, it broke up and pieces of it were transported downhill only a few meters. Again, the results may indicate the use of fire by early hominins, but all non-anthropogenic possibilities are yet to be ruled out.

2.2.3. Swartkrans Cave

Swartkrans is located in Gauteng Province, South Africa, and is one of a cluster of early hominin sites in the Cradle of Humanity. It is a dolomite sinkhole located above the Blaubank River that formed as a result of a series of complex depositional and erosional events. The roof of the cave has been eroded away or destroyed by lime-mining. A reconstruction of the depositional history divided Swartkrans into five members, of which three are deposits of material containing Acheulian stone tools. Member 3 is the youngest of the deposits containing archaeological material and excavations found burnt bones throughout the deposit (Brain 1993). Member 3 is composed of sediment that was

deposited into an erosional gully. It was originally dated to between 1.0 and 1.8 million years based on faunal stratigraphy and environmental similarities to Members 1 and 2 (Brain and Sillen 1988).

The evidence for fire is based on the presence of burnt bones found in seventeen different units, and in as many as twenty successive layers within a single 1m² unit. 270 out of about 60,000 bones were identified as burnt using chemical analysis and comparison with experimental samples (Brain and Sillen 1988; Sillen and Hoering 1993). Of the burnt bones, four have cutmarks, linking them to hominin activity (Pickering 2012). Similar numbers of bones were also excavated from Member 1 and 2. Member 1 had no burnt bones and Member 2 had only 2 (out of 34,000) (Brain 1993: 238).

Because of the complicated stratigraphy of the cave, determining how the burnt bones were deposited is not clear. Brain proposed that Member 3 formed as a roofed erosional gully that was occupied by hominins who used fire either within the cave itself and at the entrance, and the burnt bones were transported downhill (Brain 2004: 240, 261; Pickering 2012). However, there is little evidence of hominin occupation within the cave, as artifacts (lithics, bone tools, modified bones) are rare (de Ruiter 2004). If burnt bones are excluded from the cultural artifact count, Member 3 has the same or less cultural artifacts when compared to Members 1 and 2. The entrance to the cave was a steep, vertical opening which would not have been ideal for hominin occupation (de Ruiter 2004: 277). Alternatively, the burnt bones may have been transported from outside of the cave along with the washed-in sediment.

Brain and Sillen argue the repeated occurrences of burnt bone within Member 3 and entirely lacking in Members 1 and 2 is strong evidence that the fire was anthropogenic in nature (1988). If the fire was a natural event, the same burnt material would have been entering the cave regularly, as the environment did not undergo any significant changes between the depositional events (Brain and Sillen 1988).

2.2.4. Wonderwerk Cave

Wonderwerk Cave is located in the Northern Cape province of South Africa, at the base of the Kuruman Hills (Figure 2.1). It is a karstic cave within a regional dolomitic

limestone formation. It has been continuously occupied from ca. 2.0 Mya until the early 20th century and is the earliest example of hominin occupation within a cave (Chazan et al. 2008, 2012; Goldberg et al. 2015). The identification of fire within the cave is based on both macroscopic and microscopic analysis of sediments and artifacts from Stratum 10 in Excavation Area 1 (Figure 2.2). Stratum 10 dates to the Jaramillo subchron, based on cosmogenic dating and its normal magnetic orientation, which fits with the early Acheulean stone tool assemblage found within the stratum. This places the evidence of fire at 1.07-0.99 Ma (Berna et al. 2012; Chazan et al. 2008).



Figure 2.1 Map showing the location of Wonderwerk Cave
Note. Map data: Google, NOAA, U.S. Navy, GEBCO, Landsat AfriGIS (Pty) Ltd.

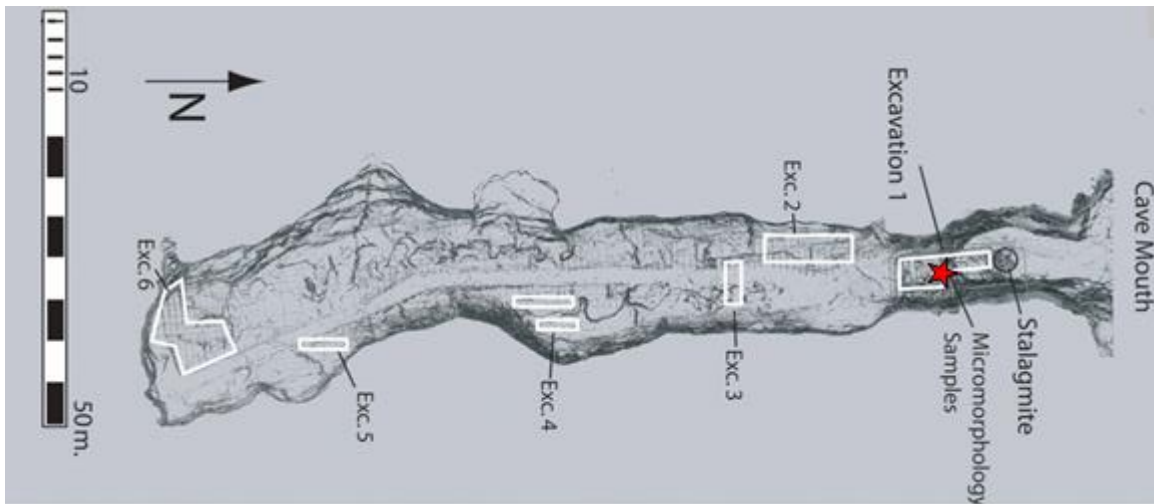


Figure 2.2 Plan of Wonderwerk Cave generated by laserscanning with locations of excavation areas. Red star marks where the evidence of fire was found

Note. Berna et al, 2012, courtesy of H. Rüter, Zamani project

The macroscopic evidence of fire consists of burnt bones and lithics, originally excavated and reported by Beaumont (2011). Almost half the bones found within the entirety of Stratum 10 (43.7%) were identified as burnt based on discoloration and the majority (80%) of the bones in the unit closest to the micromorphological samples were burnt. FTIR analysis on several of the discolored bones confirmed that they had been altered by heat and indicated that they had been heated above 400°C and sediment attached to the sampled bones had reached a temperature between 400°C and 700°C (Berna et al. 2012)

The lithic assemblage also showed signs of heat alteration. Pot-lid flakes of banded ironstone were found within the stratum, including flakes that refit to larger slabs, indicating that the fractures occurred within the cave. Pot-lid fractures happen when rocks are heated and the water trapped inside expands, causing a flake to break off. The flakes are identifiable by their round shape and lack of striking platform (Whittaker 2010). Furthermore, although all of the ironstone with pot-lid fractures were unworked, ironstone does not occur naturally within the cave and could have entered only as a manuport (Berna et al 2012). However, it is not reported whether bone and lithics from other strata show similar signs and percentages of heating.

The macroscopic evidence for anthropogenic fire is comparable to other claims of anthropogenic fire but the addition of microscopic analysis in the form of micromorphology is what makes Wonderwerk Cave one of the most robust examples and strongly supports the in-situ nature of the evidence. The micromorphological analysis on thin sections demonstrated that Stratum 10 contains a number of surfaces. Burnt bones, charcoal, and ash deposits were identified on a clearly defined occupational surface extending over a meter. FTIR analysis applied directly to the thin section indicated that the bones were in fact burnt, at approximately 500°C. Furthermore, the bones were angular, showing that they had not been transported any great distance. This is supported by the presence of ash rhombs (oxalate pseudomorphs), which are especially valuable as a marker of combustion features because ash rhombs are too fragile to survive transportation by wind or water (Canti 2003). Therefore, the preservation of ash deposits within the microfacie indicates that the fire occurred in-situ (Berna et al 2012).

The evidence that the fire residues are in-situ is a critical part of their association with anthropogenic activity. The combustion feature is located approximately 24m inside the cave, making it unlikely to be the result of a wildfire. There is no phosphate/chemical signature for guano deposits in these layers, so the fire could not have been caused by spontaneous combustion of guano. Thus, Berna et al (2012) concluded that the most likely source of the fire is anthropogenic.

The multiple lines of evidence form a strong case for in-situ anthropogenic use of fire within Wonderwerk Cave. A crucial aspect of the evidence is the role micromorphology played in establishing the presence of a surface associated with burnt materials and demonstrating that the wood ash and burnt bone were associated with the surface. Currently, the microscopic evidence cannot be definitively linked with hominin activity, because none of the burnt materials was an artifact. However, the artifacts within the stratum and unit are associated with the burnt materials, as the micromorphology indicates they are in-situ. As it is one of the only hominin sites that represents occupation and activity rather than post-depositional transport or a palimpsest of multiple occupational periods, Wonderwerk Cave offers an unprecedented look at how hominins were using fire.

Since the original publication on fire in the ESA deposits at Wonderwerk Cave, one of the authors has brought up a complication in the identification of wood ash. Analysis of newly collected samples identified fragments of micritic pseudomorphs of plant tissues. These calcified plant remains can appear similar to ashed plant remains (Goldberg et al. 2015). Rhizolites are formed when plants are soaked calcite-rich water. Calcite precipitates and replaces parts of the plant but preserving the structures, including potentially the rhomb structures associated with wood ash. While Goldberg et al. maintain the identification of wood ash in the layer based on the proximity and frequency of other evidence of burning, the presence of the calcified plant tissues complicates the issue and limits the ability to map the full extent of combustion evidence in the cave. This new complication “requires the development of analytical methods that will definitively distinguish between them and ash” (Goldberg et al. 2015: 641). It is this problem that my technique addresses.

Chapter 3.

Materials and Methods

To develop the ν_3 (CO_3) peak width protocol, I created a library of FTIR-m spectra collected in reflectance mode from common calcite types and analyzed the spectra to identify characteristic differences in absorption of infrared radiation at different wavelengths between the different types. In this chapter I describe three sets of samples used in my study: a reference collection of control samples including experimentally produced pyrogenic calcite, examples of known archaeological ash from a Middle Paleolithic hearth at Oscuriusciuto, and samples from Wonderwerk Cave which included local calcite sources, a LSA horizon with evidence of burning, and potential ashed plant remains from the ESA. The second half of this chapter details how the samples were analyzed with infrared spectroscopy and the process of developing the ν_3 (CO_3) peak width protocol.

3.1. Materials

3.1.1. Control Samples

Known samples of different types of calcites were collected and processed into micromorphological thin sections (Table 3.1). The control samples included a range of calcites formed by different processes. The geogenic calcites include sparite, micrite, chalk, and travertine. Sparite refers to mineral calcite that forms with large, organized crystals and micrite refers to mineral calcite that forms with small, fine-grained, microscopic crystals. Chalk is a common sedimentary rock composed of consolidated foraminifera shells. Sparite, micrite and chalk were taken from Ward's Natural Science collections of mineral and rock specimens. Travertine forms from the rapid precipitation of calcite from mineral springs near limestone sources (Folk 1959). The sample of travertine was collected from Sabul, an archaeological site. Marl is a sediment containing equal parts of calcite and sediment. The sample of marl used was collected from a Paleolithic lakebed in from Schöningen, Germany. It was formed when dissolved calcite in water precipitates

in a clay-rich environment, producing a micritic calcite-clay sediment (Bausch 1968). Calcrete is a pedogenic calcitic rock formed in a slow process of minerals precipitating from the soil. The sample of calcrete was collected from an open gravel pit mine in Bestwood, South Africa.

Experimental pyrogenic calcite was created in controlled burning experiments using a standard laboratory muffle oven. Subsamples of two control materials (chalk, micrite) and a sample of dry wood were heated for two hours at the goal temperature. Heating temperatures are given in Table 3.1. The heated samples were left to cool for at least one month before processing and analysis. The transformation from calcium hydroxide to calcite occurs as heated material reacts with the carbon dioxide in the air. FTIR analysis can determine the relative amounts of calcium oxide and calcite within a sample and each sample was tested with FTIR to determine when the reaction had proceeded to completion. Depending on the environment and material, the reaction can take months so in order to hasten this reaction, water and carbon dioxide were added to the heated samples. The samples were allowed to dry and tested with FTIR to determine that the reaction had proceeded to completion prior to embedding in epoxy resin.

Table 3.1 Control Samples and preparation methods for heated samples

Sample ID	Temperature	Heating Method	Duration
Sparite	Unheated	N/A	N/A
Micrite	Unheated	N/A	N/A
Calcrete	Unheated	N/A	N/A
Travertine	Unheated	N/A	N/A
Experimental Ash - 550°C	550°C	Muffle Oven	2hr
Chalk	Unheated	N/A	N/A
Marl	Unheated	N/A	N/A
Experimental Ash - 700°C	700°C	Muffle Oven	2hr
Experimental Ash - 900°C	900°C	Muffle Oven	2hr
Chalk - 700°C	700°C	Muffle Oven	2hr
Micrite - 1000°C	1000°C	Muffle Oven	2hr
Chalk - 1000°C	1000°C	Muffle Oven	2hr

Note: Duration indicates time at highest temperature and does not include time took to reach the highest temperature.

3.1.2. OSC

Oscurusciuto is a collapsed rock shelter in southern Italy with Mousterian occupation deposits. It is located on the northern side of a ravine, in Mesozoic limestone and Quaternary calcrete deposits. The layers containing anthropogenic material at Oscurusciuto cover a period of ten to fifteen thousand years, ending approximately around 40 Kya (Spagnolo et al. in press).

Anthropogenic materials were found across 60 m², with the greatest being depth of 5m. The occupational layers are capped by a level of tephra that likely marked the end of occupation and preserved the original depositional context. Within the 10 m² of excavations, multiple areas of combustion have been identified. The hearths consist of clearly defined round hollows containing ash, burnt bone, and charcoal. Two are large, independent features, 50-70 cm long at their widest point. One area has a group of six smaller hearths overlapping each other. The largest hearth is set apart and covers over 2m. The hearths are well-preserved, with visible macroscopic ash deposits (Spagnolo et al. in press). They have been extensively sampled for micromorphological and FTIR analysis by F. Berna.

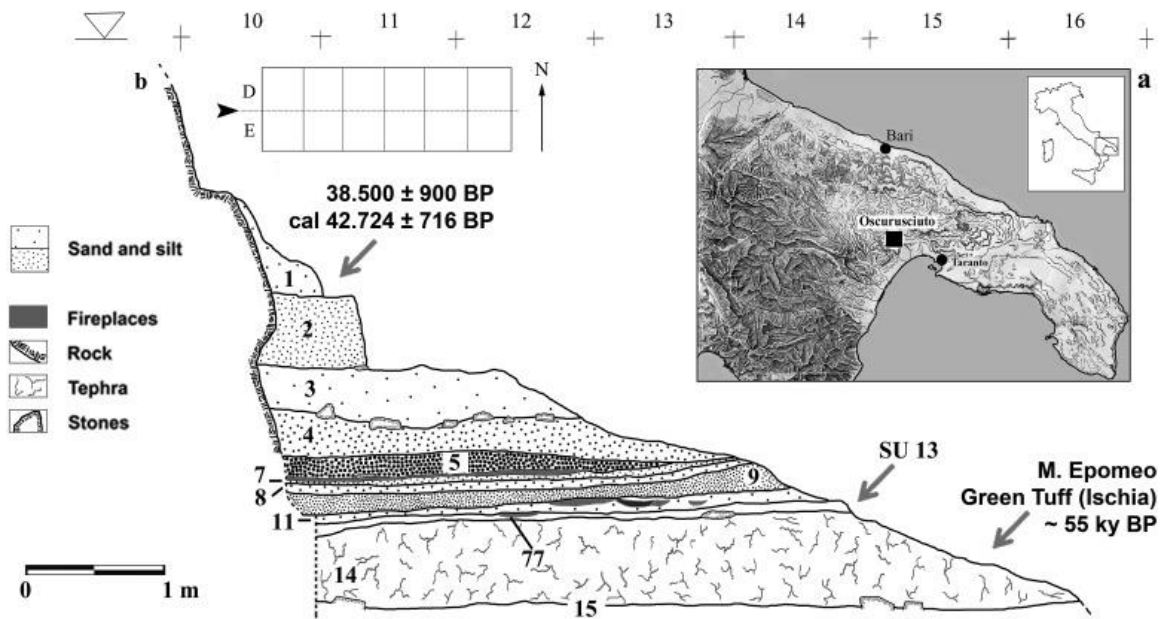


Figure 3.1 (a) Map showing the location of Oscurusciuto rockshelter (b) Stratigraphy of Oscurusciuto. The earliest permanent occupation is SU 13.

Two thin sections from individual hearths were analyzed.

Table 3.2 Oscurusciuto Samples

Thin Section ID	Stratum	Period
OSC-38	13	Middle Paleolithic
OSC-78	13	Middle Paleolithic

3.1.3. Wonderwerk

The Wonderwerk Cave samples included both ESA and LSA material. I collected the LSA sample in the 2014 field season from a macroscopic feature that was conclusively identified as a combustion feature associated with hominin activity.

Six ESA thin sections were analyzed. The samples were collected by F. Berna from the east profile of Square R28 in Wonderwerk Cave (Figure 3.2). WW05-04 was collected by F. Berna during the 2005 field season. After evidence of fire was identified in this sample (Berna et al. 2012), five more samples from the same profile and stratum were collected by F. Berna in the 2011 field season.

Table 3.3 Wonderwerk Sample

Thin Section ID	Archaeological Stratum	Location	Stratigraphic Unit	Period
WW05-04	10	E Profile, Sq. R28	4a	ESA
WW11-06	9	E Profile, Sq. R28	4a	ESA
WW11-07	9/10	E Profile, Sq. R28	4a/4b	ESA
WW11-08	10	E Profile, Sq. R28	4a	ESA
WW11-09	10	E Profile, Sq. R28	4a	ESA
WW11-10A	10	E Profile, Sq. R28	4a	ESA
WW14-01	4	W Profile, Sq. T24	3	LSA

Interpretation of archaeological samples also requires a database of local calcite controls from the site and surrounding area to understand the calcite background and what is normal variation of non-pyrogenic calcite in that site. The results of the local control samples indicate the range of variation expected from non-ash calcite in the site.

The bedrock of the area is a dolomitic limestone and the specific stratum of the local formation is primarily limestone based on FTIR sampling within the cave. Wonderwerk Limestone refers to the primary parent material within the cave. Modern Stalactite and Modern Flowstone were collected from currently active formations in the cave. Ancient Speleothem is from thin section WW11-08, which contains 2 cm fragments of biogenic speleothem.

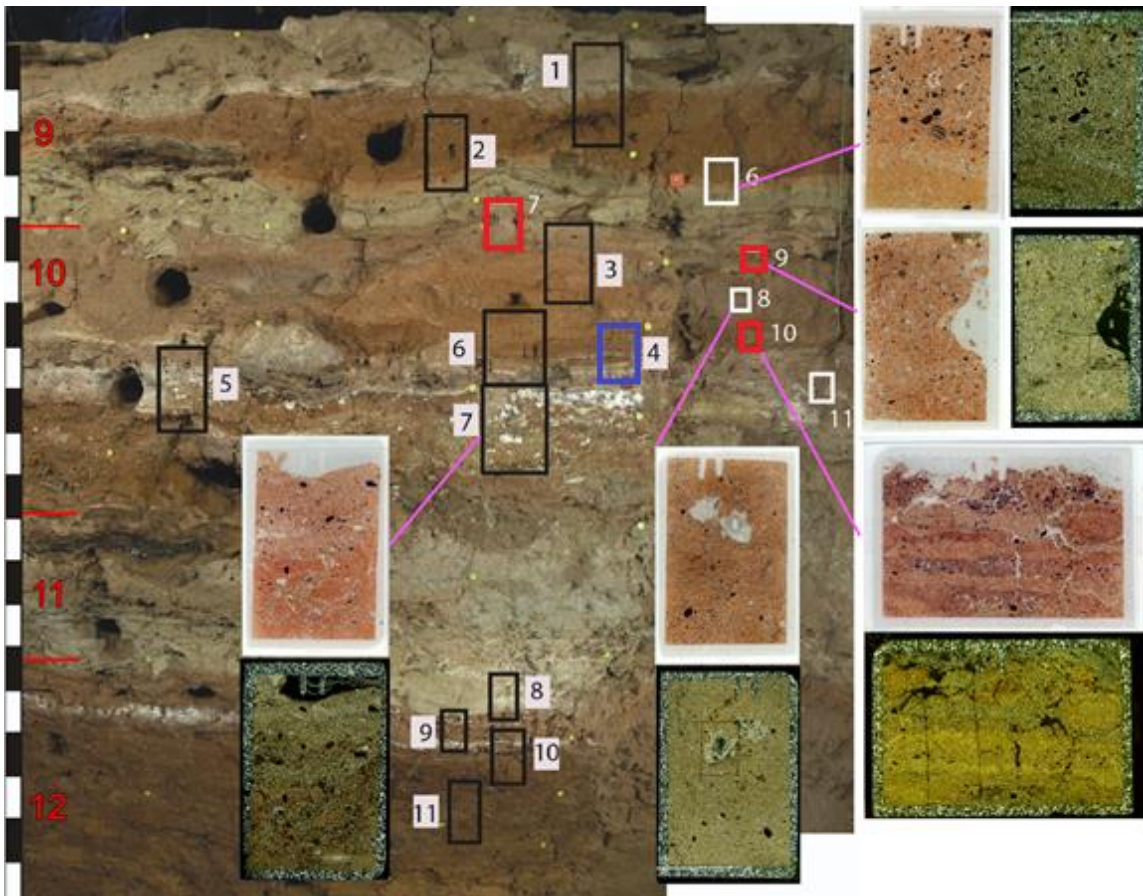


Figure 3.2 East profile of Square R28 showing lithostratigraphic units at left, and the location of micromorphology samples. The blue rectangle indicates the sample with evidence of fire that was collected in 2005. Red rectangles indicate the samples analyzed that were collected in the 2011 season.

Note. Figure from Goldberg et al. 2015

3.2. Methods

3.2.1. Processing

Micromorphological samples were processed into petrographic thin sections in the Geoarchaeology and Microstratigraphy Lab at Simon Fraser University. Micromorphological samples were impregnated with a 5:1 mixture of EpoxyCure resin and hardener, and then placed in a fume hood to cure. After one week, the samples hardened

completed in one week. The embedded samples were then bonded to glass slides and polished.

3.2.2. Micromorphology

Each archaeology sample was examined with a petrographic microscope. The focus of this analysis was to identify types of calcite and characterize the context of these sections. Areas with different types of calcite were identified for FTIR-m analysis. The primary goal was to identify potential ashed material, but also included was material identified as geogenic for the local site controls. Especial care was taken to identify any potential microfacies that could indicate a past surface and any alteration features (pedofeatures in soil micromorphology) that could indicate post depositional environmental conditions.

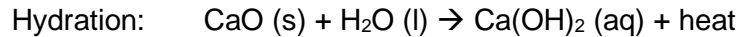
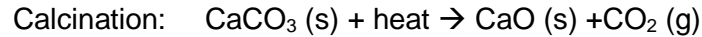
3.2.3. Identification of Wood Ash with FTIR

FTIR is capable of identifying calcite, the mineralogical component of wood ash, in loose samples. Calcite is a common component in the geological and archaeological records in the form of limestone, chalk, and other rocks and thus the presence of calcite is not sufficient to identify wood ash within sediment. It is impossible to distinguish pyrogenic calcite (ash, plaster) from other forms of calcite (sparite, limestone, chalk etc.) merely on the basis of the mineral composition.

However, variations in the particle size and morphology of material with the same molecular composition can produce predictable changes in FTIR spectra (Lane 1999). Different formation processes produce types of calcites with different particle sizes and shapes (Folk 1974). Geogenic calcite forms slowly and as a result have large, stable crystals. The most extreme example of this is sparite, which forms slowly in a saturated solution of calcite and, as a result, has a high level of atomic order and very large crystals (Addadi et al. 2003; Regev et al. 2010).

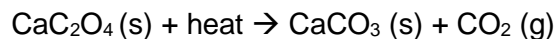
Pyrogenic calcite forms when any calcitic material is heated above 700°C, causing it to calcine and decompose into carbon dioxide gas and calcium oxide. This product takes

in liquid water or vapor to yield calcium hydroxide. The calcium hydroxide reabsorbs carbon dioxide from the air to reform as calcite.



What is important here is that the final step produces calcite at a much faster rate in any pyrogenic calcite than in other forms. Because the result of this series of reactions is chemically identical to the original material, normal chemical analyses cannot distinguish pyrogenic calcium carbonate from geogenic and biogenic forms (limestone, chalk, sparite). Despite this, there is a distinct structural difference in the materials. The speed of formation changes the size and organization of the atomic crystal structure, giving pyrogenic calcite much smaller, more disorganized crystals than geogenic. This reaction occurs in any type of calcite when heated at high temperatures, and is the method used to produce plaster. In all of these cases, the final result is a form of pyrogenic calcite (Dollimore 1987; Robert 1979).

While wood does not contain calcite, many woody plants have bipyramidal crystals of calcium oxalate (CaC_2O_4) which transform into calcite in two different ways, depending on the temperature. Low-temperature ash is produced around 500°C , when calcium oxalate spontaneously transforms directly into solid calcite by releasing one molecule of carbon monoxide:



High-temperature ash is produced when the temperature reaches above 700°C . The calcite formed at 500°C goes through the same chemical reaction described above.

After the chemical and mineralogical transformation of the oxalate into calcite, the newly formed calcite crystals maintain the original bipyramidal shape, whereas geogenic calcite forms in hexagonal crystals (Canti 2003; Stoops et al. 2010). In petrographic thin

section, the bipyramidal structure appears as a rhomb shape, which is distinct from the hexagonal crystals of geogenic calcite particles (Canti 2003). However, few pseudomorphic rhombs survive at high temperatures, as the particles tend to fuse and lose the rhomb shape (Shahack-Gross and Ayalon 2013). This means that micromorphology cannot always conclusively identify ash. Ash produced through the low temperature and the high temperature method have higher levels of disorder at the atomic level than most geogenic calcites, but high temperature ash is much more disordered than low and comparable to other forms of pyrogenic calcite (Poduska et al. 2011; Regev et al. 2010; Shahack-Gross and Ayalon 2013).

Previous research has demonstrated that infrared spectroscopy can detect differences in particle size and morphology (Lane 1999; Chu et al. 2008; Poduska et al. 2012). Specifically, the particle size can predict the spectral shape and peak size (Lane 1999). This has been used to distinguish between geogenic, biogenic, and pyrogenic calcite in archaeological sites using Fourier-Transform Infrared Spectroscopy (Chu et al. 2008; Regev et al. 2010; Poduska et al. 2011). However, the method of FTIR required is destructive and requires a small, loose fraction of material to be ground and homogenized. In the case of potential ash from over a million years ago, not enough material survives and the characteristics identified were not indicative of calcite type in the FTIR-m spectra.

I address the question of identification of ash by developing a protocol that uses FTIR microspectroscopy (FTIR-m), an application of FTIR that is integrated with micromorphology. It is a non-destructive method that can analyze particles with a diameter as small as 50 microns, on a petrographic thin section. Micromorphology is crucial to this technique because it allows the identification of potential ash that is invisible to the naked eye, in a form that FTIR-m can analyze.

3.2.4. Fourier Transform Infrared Microspectroscopy (FTIR-m)

To determine if FTIR-m spectra exhibit any characteristics that differ by calcite source, I assembled a database of various calcites, processed them into petrographic thin sections, and I collected an area map containing a minimum 100 spectra, and if possible, included the entire extent of the feature (up to 6000 spectra). For archaeological samples,

I began with micromorphological analysis and identified types of calcite particles, with an emphasis on potential examples of ashed plant remains. Each fragment or feature was treated as a separate area, and sampled individually. This was necessary to ensure that the overall variation of an area was included in the analysis and interpretation.

All spectra were collected with the Nicolet iN10 MX IR microscope in reflection with the IN10 Array Imaging Detector and using a 15X reflectochromatic condenser between 4000 - 715 cm^{-1} with an 8 cm^{-1} resolution and a minimum of 64 scans. The area sampled for each spectrum was 25 μm by 25 μm and spectra were collected every 25 μm .

A typical calcite spectra is shown in Figure 3.3. Calcite spectra have three IR absorption peaks corresponding to vibrational and rotational modes of the C-O bond in the CO_3 unit: the ν_3 (CO_3) peak at 1420 wavenumbers (asymmetric CO_3 stretch), the ν_2 peak at 874 wavenumbers (out-of-plane CO_3 bending), and the ν_4 peak at 713 wavenumbers (in-plane CO_3 bending). These peaks represent the different interactions of the C-O bonds in the carbonate functional group and each one absorbs radiation at different wavelengths (Addadi et al., 2003).

The form of each peak is affected by the type of vibration of the bond and changes in the molecular structure can influence the shape (Lane 1999; Poduska et al. 2011). Previous research found that the shape of ν_3 (CO_3) peak of calcite varied in different calcitic materials (Poduska et al., 2012). Based on these past observations and my own simple, visual comparison of spectra from the control materials, I focused my efforts on a specific feature of calcite spectrums: the ν_3 (CO_3) peak.

3.2.5. FTIR-m Spectral Analysis

For each individual spectrum, I quantified the difference in shape of the ν_3 (CO_3) peak measuring the width. Each spectrum was normalized to the maximum intensity (represented in the spectrum as the highest point of the peak) of the ν_3 (CO_3) peak, so that different intensities of spectra did not affect the comparison. I measured the width of the ν_3 (CO_3) peak at 75% of the maximum intensity (Figure 3.3). I took the measurement at 75% intensity because noise or extraneous peaks occasionally altered the peak at lower levels.

Infrared spectroscopy is a general analytical tool that cannot limit the results to a single material. It returns a combined spectrum that includes peaks from all wavenumbers where molecular bonds absorbed IR energy. This additive property of FTIR can hide or skew the peaks from calcite if there is another material included that absorbed IR energy at a nearby wavenumber. To avoid this, all spectra were reviewed before the ν_3 (CO_3) peak width was recorded. I excluded any spectra where calcite was not the main, dominant material and any spectra that contained extraneous peaks near the ν_3 (CO_3) location that rose above 75% of the ν_3 (CO_3) peak maximum (where I collected the width). FTIR-m spectra tend to have greater amounts of noise obscuring the desired signal due to the very small, precise area analyzed. The advantage of using FTIR-m is that it is capable of analyzing microfeatures that do not have enough material to be identified and processed for FTIR. Furthermore, samples have much greater contextual detail because they are chosen in conjunction with micromorphological analysis.

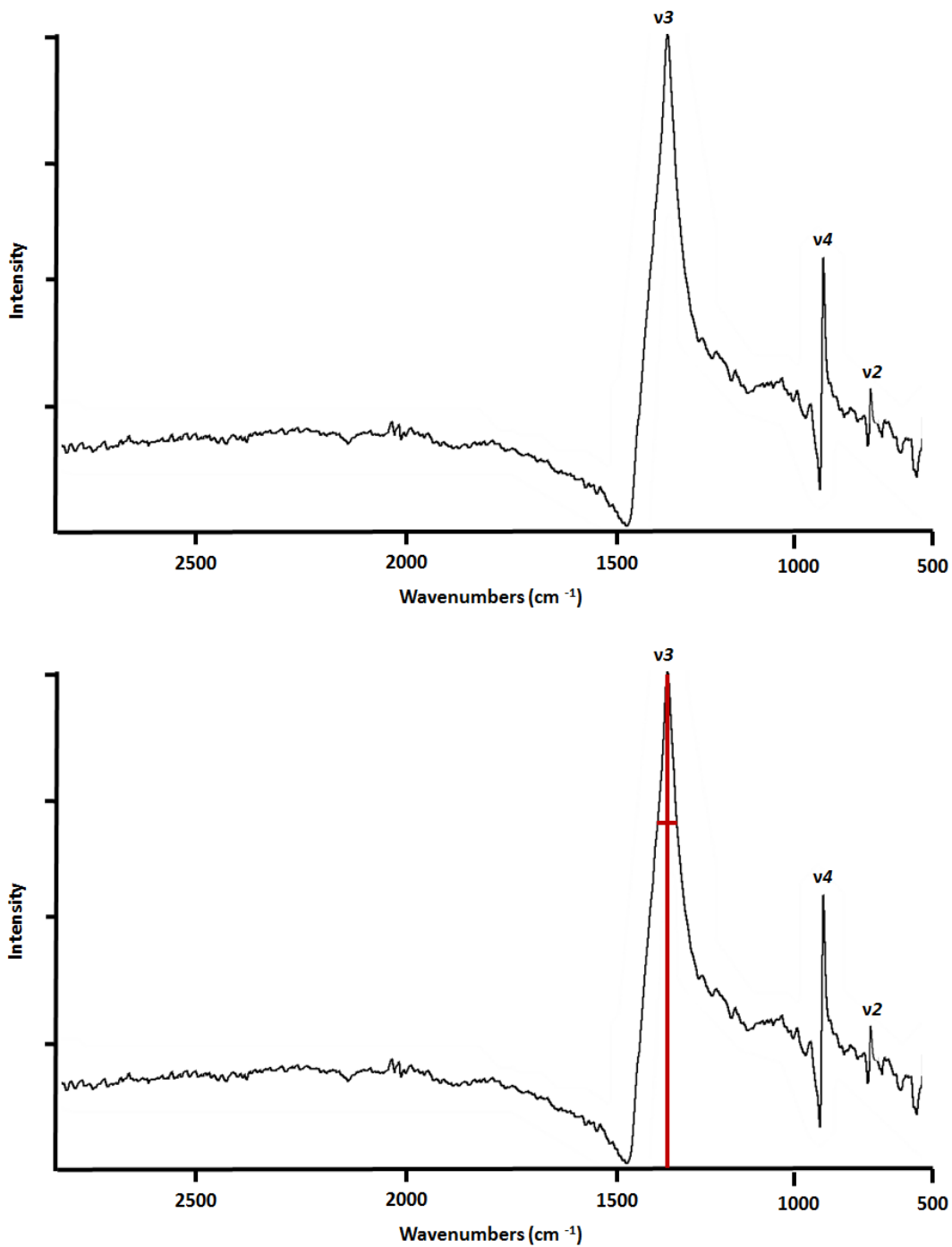


Figure 3.3 Top: typical calcite spectra with v3 (CO₃) (~1420 cm⁻¹), v2 (~875 cm⁻¹), and v4 (~713cm⁻¹) peaks indicated. Bottom: FTIR-m reflectance spectra of Chalk-900°C with the v3 (CO₃) peak indicated. The horizontal and vertical lines demonstrate how the height and width were measured. The length (in wavenumbers) of the horizontal line at 75% of the v3 (CO₃) peak is the width at 75% of the height (intensity) of the v3 (CO₃) peak (W3/4M).

Chapter 4. Identifying Pyrogenic Calcite

Here I detail the results of the FTIR-m and FTIR analyses of the control calcite samples. This leads into a potential explanation for the variation of ν_3 (CO_3) width found in different calcites. Using the results from the control samples, I developed the ν_3 (CO_3) peak width protocol, which proposes four criteria to identify ashed plant remains.

4.1. Experimental Results

Figure 4.1 is a visual comparison of FTIR-m spectra of three different types of calcite. All calcite spectra have three IR absorption peaks: the ν_3 (CO_3) peak at 1420 wavenumbers, the ν_2 peak at 874 wavenumbers, and the ν_4 peak at 713 wavenumbers (the ν_4 peak is not included in the figure). The comparison below demonstrates that different calcite types produce FTIR-m reflectance spectra that have distinct qualitative characteristics. Figure 4.1a shows a characteristic spectrum of sparite, which is one of the most crystalline calcite forms. The ν_3 (CO_3) peak is very wide and blocky (Figure 4.1a). Chalk, a material with a medium crystal size has spectra that are typically narrower with rounded peaks (Figure 4.1b). Wood ash, a highly disorganized material with small crystals has spectra with very narrow, sharp ν_3 (CO_3) peaks (Figure 4.1c).

I quantified the visual differences between the samples used the width of the ν_3 (CO_3) peak (as detailed above). The results are summarized below in Table 4.1. The range of ν_3 (CO_3) peak widths are not exclusive to each calcite sample, meaning that a measurement from a single spectra of calcite cannot limit the potential identification to a single type and depending on the width, could be found in as many as eight calcite samples. However, the average ν_3 (CO_3) peak width at 75% of maximum intensity is different for each control sample.

While unburnt materials may overlap with extreme ends of burnt materials, the heated materials have much lower minimum widths, and the average widths are less than the extremes of unheated materials. This shift in width is demonstrated in a single material. Chalk was compared in three different forms: unheated, 700°C, and 1000°C. Unheated

chalk has an average width of 100 wavenumbers, and a range from 83 to 120 wavenumbers. At 700°C, it has an average width of 79 wavenumbers and a range from 69 to 93 wavenumbers. At 1000°C, its average width is 73 wavenumbers, with a range from 55 to 90 wavenumbers.

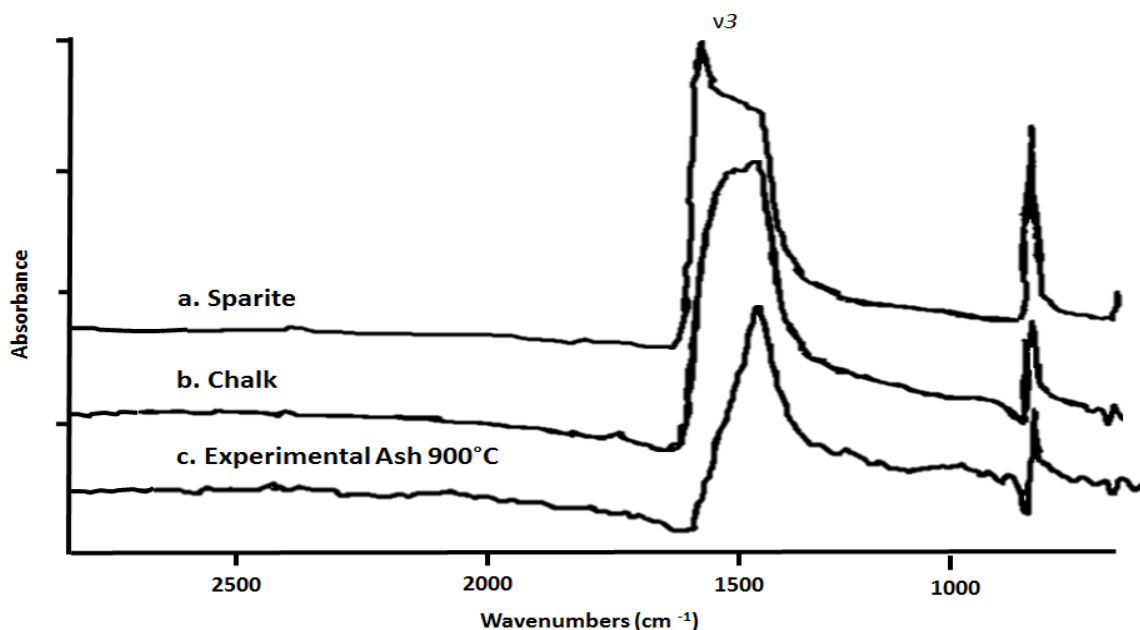


Figure 4.1 Typical spectra of v_3 (CO_3) peak shapes in different calcite types. a. Sparite has the widest peak, with the maximum intensity at around 1500. b. Chalk has a medium, rounded peak with the highest intensity at lower wavenumbers. c. Experimental Ash 900°C is the narrowest, with a sharp peak and highest intensity located around 1400.

Figure 4.2 compares the variation of v_3 (CO_3) width between materials. While there is overlap between different calcite types, a comparison of a large group of spectra from two types show that as a group, the measurements from different calcite samples cluster around different widths. This figure reveals a high degree of overlap in the average v_3 (CO_3) peak widths of pyrogenic calcites, especially when the low-temperature ash is excluded. The overlap is not shared by non-pyrogenic calcites with the exception of marl.

The wood ash from 700°C has a comparable range of width to the chalk at 700°C. Likewise, wood ash produced at 900°C has comparable v_3 (CO_3) widths to 1000°C chalk. Unburnt wood does not have calcium carbonate and therefore cannot be compared to (or mistaken for) burnt wood.

Table 4.1 Descriptive statistics of v3 (CO₃) peak widths for areas in control samples

Area ID	Average v3 (CO ₃) width at 75% intensity	n	Standard Deviation	Max v3 (CO ₃) width	Min v3 (CO ₃) width	Range	Percentage of Spectra with v3 (CO ₃) Width:				Ash in MM?
							< 78	78 - 95	95 - 125	> 125	
Sparite	157.1	101	2.6	163	148	15	0.0%	1.0%	0.00%	99.01%	No
Micrite	136.0	101	3.4	143	128	16	0.0%	1.0%	0.00%	99.01%	No
Calcrete	114.1	100	10.1	139	86	53	0.0%	2.0%	82.00%	16.00%	No
Travertine	110.2	633	15.2	155	89	66	0.6%	12.6%	70.77%	15.96%	No
Experimental Ash - 550°C	101.0	342	14.0	136	65	71	6.4%	26.9%	63.16%	3.51%	Yes
Chalk	100.2	101	7.4	120	83	37	0.0%	24.8%	75.25%	0.00%	No
Marl	87.5	298	21.0	154	63	91	41.6%	34.6%	15.77%	8.05%	No
Experimental Ash - 700°C	86.4	511	13.7	129	62	67	35.8%	36.8%	27.01%	0.39%	Yes
Experimental Ash - 900°C	83.6	101	13.4	105	50	54	29.7%	43.6%	26.73%	0.00%	Yes
Chalk - 700°C	77.9	156	13.5	122	54	68	52.9%	47.1%	0.00%	0.00%	No
Micrite - 1000°C	76.7	206	5.9	93	58	35	61.2%	38.8%	0.00%	0.00%	No
Chalk - 1000°C	72.7	103	6.9	92	62	30	80.6%	19.4%	0.00%	0.00%	No

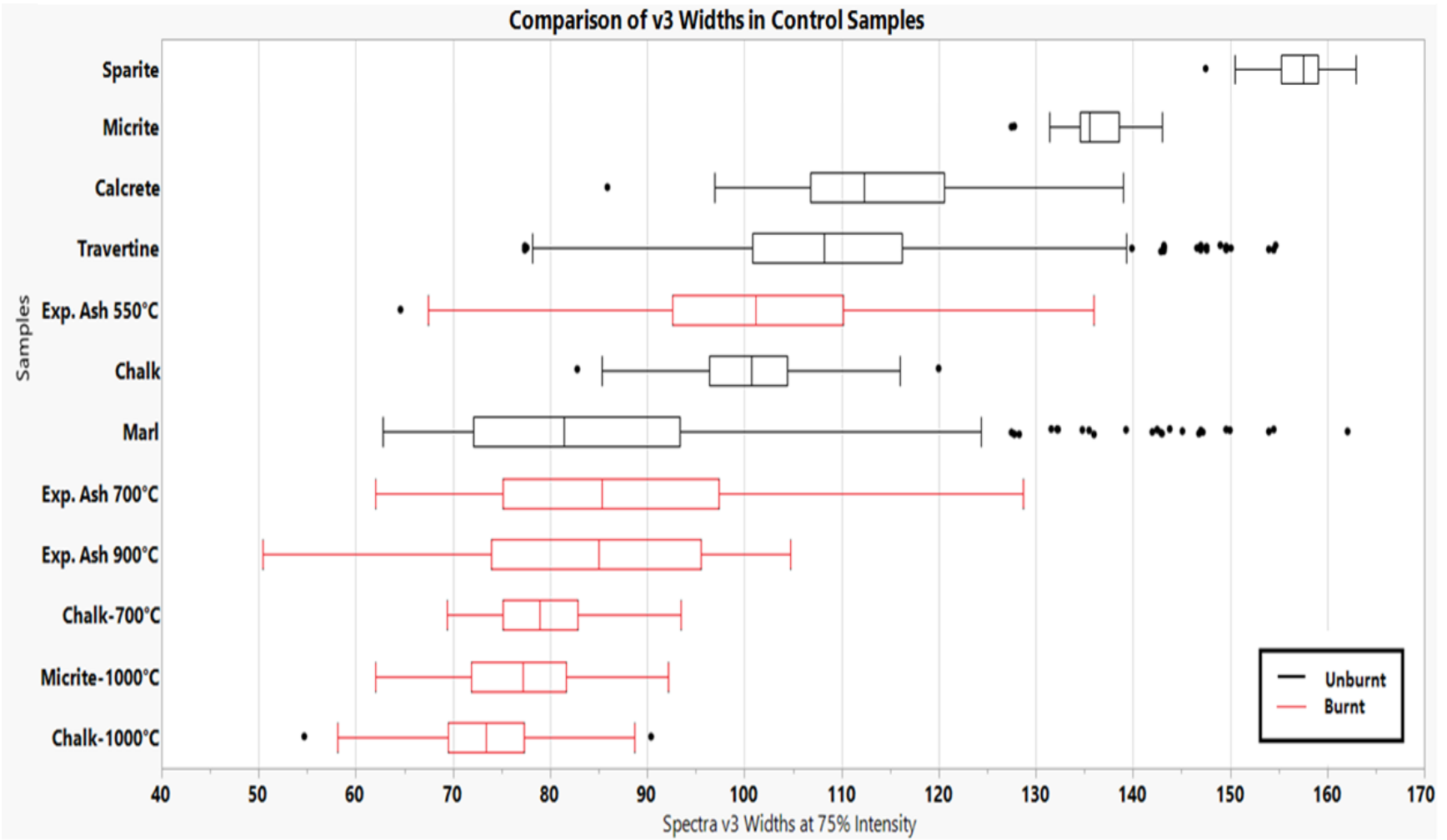


Figure 4.2 Comparison of v3 (CO₃) widths by material for the control samples

4.2. Summary of Experimental Results

The comparison of the control calcite materials indicated that there is an association between the width of the ν_3 (CO_3) peak and the type of calcite. Specifically, the range of widths of the ν_3 (CO_3) peaks in pyrogenic calcites produced at high temperatures (above 700°C) are consistently less wide than those of geogenic calcites (sparite, limestone, chalk, micrite).

The cause of the shift is likely a consequence of differing crystal size and level of atomic order. Figure 4.2 illustrates how ordering the calcite samples based on average ν_3 (CO_3) width, from wide to narrow, is consistent with an ordering of the samples according to crystallinity, atomic order, and homogeneity. In the upper right are the widest samples, which correspond to the geogenic forms. Sparite is one of the most stable forms of calcite, with large, ordered crystals. The middle section has forms of calcite with smaller crystal sizes. Micrite is a similar form of calcite to sparite, but has smaller, fine-grained crystals. They are also more heterogeneous materials, which explains the greater range of ν_3 (CO_3) widths. In the lower left corner are the most disordered materials. Examples of pyrogenic calcite all cluster at the end of the spectrum, regardless of whether they were produced from calcined geogenic material or from wood ash.

The only non-pyrogenic material with ν_3 (CO_3) widths in the pyrogenic range is marl. While the calcite in marl forms through geogenic processes, it has a disordered structure with low crystallinity because the formation is constricted by the clay particles (Bausch 1968). As it is composed of both calcite and clay, marl does not have the visual characteristics used to identify wood ash in micromorphological analysis. Furthermore, FTIR-m spectra collected in transmission can identify the presence of clay, providing another method to differentiate the two.

Experimental Ash at 550°C is the one pyrogenic sample that was not distinct from the non-pyrogenic materials. The spectra collected from ashed sections had wider ν_3 (CO_3) widths than the other pyrogenic calcite samples. This can probably be explained by

the low temperature and short period of burning. Calcium oxalate transforms directly into calcite at low temperatures (~500°C) but at higher temperatures (greater than 700°C), it transforms first to calcium oxide and then calcite (Shahack-Gross and Ayalon 2013). Without the additional stage, the wood ash maintained the structure of the calcium oxalate which was more organized than ash formed in at higher temperatures and longer periods. Regev et al noted this phenomenon of low-temperature ash having an equivalence to chalk in his 2011 paper.

The results of the three chalk samples attest to the fact that the difference in ν_3 (CO_3) width are not merely a factor of different materials, but the result of formation processes. The FTIR-m results from unheated chalk are distinct from chalk at 700°C and 1000°C. The same decrease in width is reflected in the ν_3 (CO_3) peaks of micrite when heated at 1000°C.

The differing ranges of ν_3 (CO_3) peak widths in the three chalk samples also support the explanation for the differences driving the spectral results. The structure and order of unheated chalk is heterogeneous, even within a small sample. There are areas where it is comparable to geogenic spar as well as areas of much greater disorder and smaller crystal size. When it is heated to 700°C, the maximum and minimum width drop dramatically. The overall range is also decreased, indicating that the material acquired a greater homogeneity. This is likely due to the calcination and reformation process which reforms calcite in a pyrogenic process and homogenizes the material. The overlap with the unheated material and the greater variation of chalk at 700°C than 1000°C, is a result of incomplete calcination due to a lower temperature.

In conclusion, the results of the control dataset support the theory that FTIR-m reflects variances between different sources and types of calcite, and demonstrates that the width of the ν_3 (CO_3) peak at 75% of intensity can be used to distinguish between ordered and disordered materials. The protocol is not yet precise enough to differentiate between all calcite types, but it does show a division that separates pyrogenic calcite from non-pyrogenic calcite with the exception of marls and low-temperature ash, both of which overlap too much with pyrogenic and non-pyrogenic to be distinguished.

4.3. ν_3 (CO_3) Peak Width Protocol to Identify Potential Ash

With this foundation, the next step is developing a protocol that quantifies these differences and can be used to evaluate whether an unknown sample is pyrogenic or not. Using the results from the dataset of unheated and heated control samples, I quantified the association of narrow ν_3 (CO_3) peaks with pyrogenic calcites and then identified criteria that separated pyrogenic from non-pyrogenic.

To determine what patterns of ν_3 (CO_3) peak widths were linked with pyrogenic calcite, I divided the full range of potential ν_3 (CO_3) widths in calcite into four subranges (Table 4.3). The maximum and minimum limits of each subrange were chosen at points that divided pyrogenic and non-pyrogenic materials.

The first category contains all spectra with ν_3 (CO_3) widths of 78 wavenumbers or less. No spectra with a ν_3 (CO_3) width of less than 78 wavenumbers were collected from a non-pyrogenic calcite with the exception of marl.

The second category includes spectra with ν_3 (CO_3) widths between 79 and 95 wavenumbers. This range includes spectra from non-pyrogenic materials, but those spectra were a small minority. No non-pyrogenic sample had more than 25% of spectra with widths in this range and most had a much lower percentage. In contrast, 75% of the spectra of all pyrogenic materials (except experimental ash at 550°C) had ν_3 (CO_3) widths less than 95 wavenumbers.

The third category includes spectra with ν_3 (CO_3) widths between 96 and 125 wavenumbers. This includes primarily geogenic materials with smaller crystals and less crystalline structure, along with a small minority of spectra in lower temperature samples of pyrogenic calcite.

The fourth and final category is all spectra with ν_3 (CO_3) widths of 125 wavenumbers or greater. All spectra in this category are geogenic and the most crystalline materials with the largest crystals have all or the majority of spectra in this category.

The difference in ν_3 (CO_3) width and association of wider peaks with geogenic calcites can be seen in Table 4.1, where the percentage of spectra in each of the four categories is given for the control samples.

The control samples do not encompass every potential type of calcite, and therefore 78 wavenumbers cannot be a decisive lower bound on non-marl/pyrogenic calcites. The presence of ν_3 (CO_3) widths less than 78 does not prove a sample is pyrogenic, but the absence of ν_3 (CO_3) widths less than 78 wavenumbers is strong evidence that the sample is not pyrogenic (with the possible exception of low temperature ash).

I excluded experimental ash at 550°C from the data when determining these divisions as FTIR-m does not have the capability to differentiate low-temperature ash from non-pyrogenic materials. This may exclude potential examples of low-temperature fires but it would increase the possibility of a false positive identification of pyrogenic calcite. I also excluded the data from marl because the ν_3 (CO_3) data was not distinct from pyrogenic or non-pyrogenic calcites. FTIR-m analysis of spectra collected in reflectance cannot rule out marl and identification of pyrogenic calcite based on ν_3 (CO_3) widths must incorporate micromorphology to reject the possibility of marl.

To evaluate whether an unknown sample is wood ash, I set out four criteria that integrate the FTIR-m results with micromorphology (Table 4.2). Three of the criteria are based on the results of the FTIR-m data and identify quantifiable characteristics that distinguish pyrogenic from non-pyrogenic samples. The final criterion is based on the micromorphological identification of wood ash. Samples that fulfill all four requirements strongly support an identification of wood ash. Samples that fulfill some, but not all, of the criteria are potentially wood ash. In this scenario, integrating the micromorphology results with the FTIR-m results is critical in order to understand the cause of the different ν_3 (CO_3) peak widths.

Because of the overlap in ν_3 (CO_3) peak widths, I compared large groups of spectra from each sample, rather than individual spectra. A single spectrum or small group of spectra could fit with multiple types of calcite that overlap, but groups of spectra showed what the predominant ν_3 (CO_3) widths were. The minimum number of spectra I used for a

single sample was 100, and most areas included more, up to 6000 spectra. If possible, the extent of the area was chosen to encompass an entire fragment.

Table 4.2 Identification Criteria for Wood Ash

Criteria	Basis for Criteria
Spectra with ν_3 (CO_3) width less than 78 wavenumbers	No non-pyrogenic control sample had spectra with a ν_3 (CO_3) width less than 78 wavenumbers
Average ν_3 (CO_3) width of 87 or less	All pyrogenic control samples had an average ν_3 (CO_3) width between 72 and 87 wavenumbers
75% of the spectra have ν_3 (CO_3) widths that are less than 95	At least 75% of all spectra in every pyrogenic control sample had widths less than 95 wavenumbers
Micromorphological Identification	Micromorphology is the accepted method for identifying wood ash at this scale.

Archaeological deposits are frequently heterogeneous and interpreting a deposit includes understanding how post-depositional and diagenetic processes add, remove, or alter sediments. Geogenic and pedogenic calcite often forms in small voids, or replaces less stable calcite through dissolution and re-precipitation (Regev et al. 2010; Gillieson 2009). If the environment preserves pyrogenic calcite, other forms of calcite are likely to be preserved, especially as wood ash is less stable than other forms. Therefore, including a large number of spectra in the analysis is also necessary to understand the full range of variation. Micromorphology can support the FTIR-m results and explain the relationship between different types of calcite within a single area of analysis.

To address the issues of heterogeneity, I combined the FTIR-m spectral map of a sample area with micromorphological location pictures. A grid overlying a petrographic image of the area indicates the extent of the map, the location of each spectra and categorizes the ν_3 (CO_3) peak width of each spectrum. From this, it is possible to look at the concentrations of different calcite types and match the FTIR-m results with the micromorphology (Table 4.3). When a distinct feature in the sample is identified as non-pyrogenic as part of the micromorphology analysis, that should be considered when interpreting the FTIR-m results. If the micromorphology results conclude that the feature

is unrelated to the potential ash deposits (i.e. post-depositional calcitic filling/coating, rock/mineral fragment), the data from this feature can be removed from the dataset.

Table 4.3 Categorization of v3 (CO₃) Peak Widths

N3 (CO₃) Peak Width Range	Interpretation	Color
< 78	Pyrogenic/Marl	Red
78 – 95	Likely Pyrogenic/Marl	Orange
96 - 124	Likely Geogenic	Yellow
> 125	Geogenic	Green

Chapter 5. Identifying Archaeological Wood Ash

In this chapter, I test and apply the v3 (CO₃) width protocol to archaeological samples. I begin by presenting the results of known archaeological ash samples from Oscurusciuto and Wonderwerk Cave, in order to test whether that the spectral properties of pyrogenic calcite can be preserved over millennia. The results are discussed, with a consideration of how they limit the ability of FTIR-m to identify wood ash in the ESA. Finally, I use the protocol to evaluate the examples of potential ashed plant remains from the ESA strata in Wonderwerk Cave and discuss the results for each sample.

5.1. Known Archaeological Wood Ash

5.1.1. Oscurusciuto Archaeological Ash

The results from two separate hearths in Oscurusciuto are summarized below in Table 5.1. A comparison of the different preservation and calcite precipitation can be seen in . OSC-38 contained a very distinct ash deposit with a visible macrostructure that preserved the edge of a hearth but the micromorphological analysis showed diagenetic processes that altered the microstructure (Figure 5.1). There was extensive alteration within the ash deposit in the form of calcitic void infillings and coatings. There were also fabric inclusions and crystalline areas of calcite in the fine material. These features are likely caused by the original ash or other calcitic material dissolving in water and calcite re-precipitating in the same location, a common process in caves (Gillieson 2009). There are no identifiable ash rhombs or plant structures.

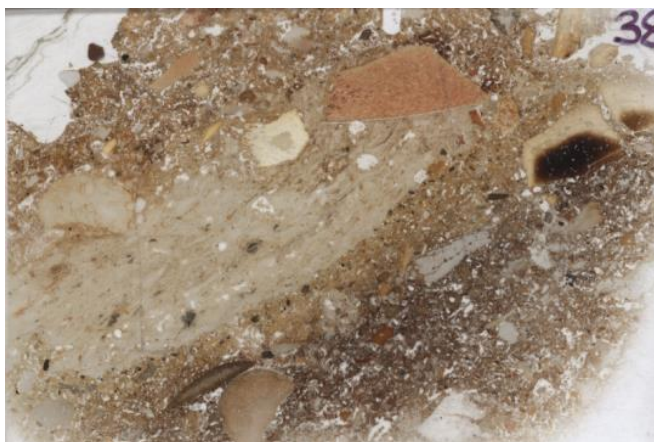


Figure 5.1 Petrographic thin section of OSC-38. The gray area on the left is wood ash, which has preserved the macrostructure of a combustion feature.

The ν_3 (CO_3) widths of the spectra in two areas mapped in OSC-38 were primarily in the geogenic range (Figure 5.4). This fits with the micromorphological conclusions of extensive reworking and calcitic precipitation within the ash microfacie.

The ash deposit in OSC-78 was a complex, heterogeneous layer with multiple interwoven microfacies of ash and clay. Within the layer were regions with varying levels of preservation, including areas with surviving rhombs.

Three areas (2, 4, 8) where I identified surviving ash rhombs were mapped. The results of the ν_3 (CO_3) peak width measurements from these areas were consistent with the micromorphological identification of ash rhombs. In all of the three areas, the average width of the ν_3 (CO_3) peak at 75% intensity is less than 78 wavenumbers, the narrowest width found in a non-pyrogeic control material. Over 75% of spectra in all three maps were below 95 wavenumbers. All three areas fulfilled the criteria for an identification of wood ash.

Areas 6 and 7 were maps taken from regions where there were no visible rhombs, but there appeared to be good preservation with minimal calcitic precipitation. The ash here was identified based on appearance and proximity to burnt materials and/or ash rhombs. Despite the lack of rhombs, the spectral analysis of Area 6 was consistent with ashed material. The average ν_3 (CO_3) width was 76 wavenumbers and 98% of the spectra were less than 95 wavenumbers. Area 6 fit all criteria for wood ash.

The original Area 7 map was highly diverse, and included multiple forms of calcite. The range of ν_3 (CO_3) widths in Area 7 extended from 50 to 165 wavenumbers, which includes geogenic and pyrogenic calcites, reflecting the heterogeneous composition. A sub-section, Area 7a, excluded the fossiliferous limestone and calcitic precipitation features. This sub-section was more consistent with pyrogenic material and fulfilled all criteria for wood ash.

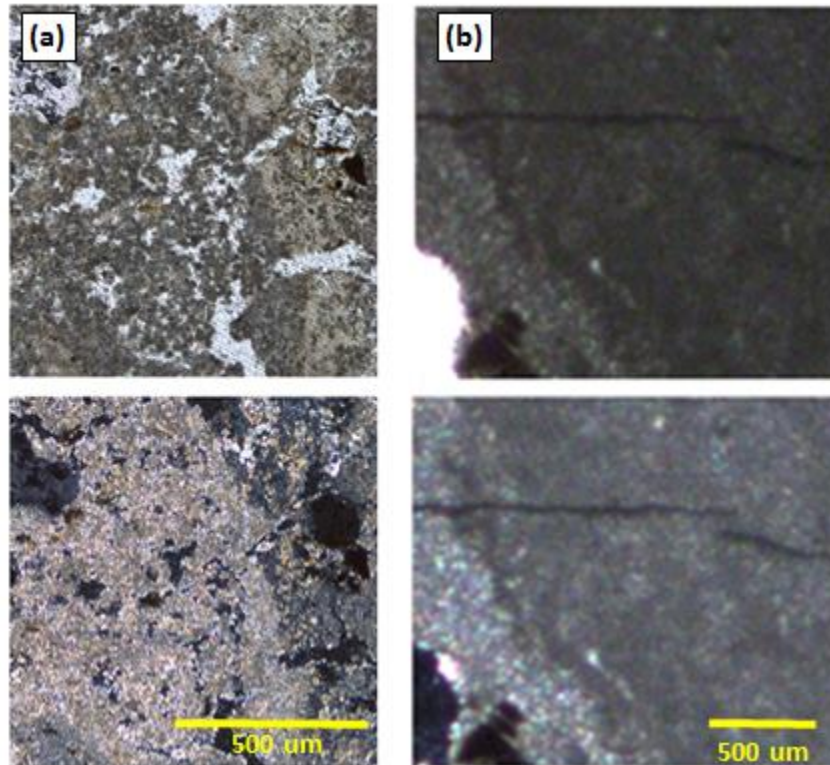


Figure 5.2 (a) Photomicrograph of a cluster of ash rhombs in OSC78 - Area 2. PPL, XPL (b) Photomicrograph of weathered wood ash in OSC38 - Area 1. PPL, XPL. The presence of preserved, distinct ash rhombs in (a) supports the FTIR-m analysis results. The ash in (b) has dissolved and re-precipitated, destroying the pyrogenic signature.

5.1.2. Wonderwerk LSA Combustion Feature

The micromorphological analysis of the LSA occupational horizon with a combustion feature in Wonderwerk Cave identified small clusters of ash rhombs in the matrix on or near the surface of the combustion feature (Figure 5.3). Overlying the areas with rhombs was a white layer of phosphate, possibly from bat guano. This has

implications for the survival of ash as the degradation of bat guano produces a phosphate-rich solution which reacts with calcitic ash, and replaces the calcite with authigenic phosphatic minerals (Schiegl et al. 1996; Weiner et al. 1993; Karkanis et al. 2000). The four areas collected for analysis were small clusters of rhombs. There were no calcitic coatings or infillings, but the rhombs themselves had birefringence indicating a possible crystalline structure.

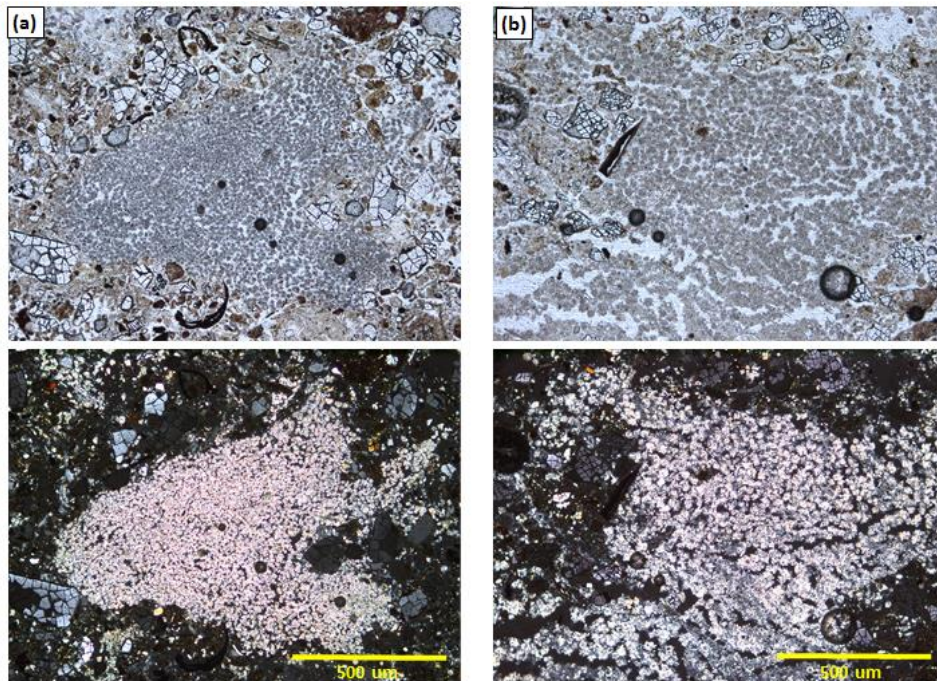


Figure 5.3 (a) Photomicrograph of a cluster of ash rhombs in WW14-01 – Area 1 PPL, XPL (b) Photomicrograph of a cluster of ash rhombs in WW14-01 – Area 2. PPL, XPL

The spectral results from Area 1 are consistent with the experimental ash samples. The average ν_3 (CO_3) peak width is 81.5 wavenumbers and over 95% of the spectra are less than 95 wavenumbers, with 35.8% less than 78 wavenumbers. It fulfills all of the criteria for wood ash.

Areas 2, 3, and 4 do not fit all the criteria. The average ν_3 (CO_3) peak width for each area is between 88 and 95 wavenumbers, above the criteria number of 85 wavenumbers. 71% of spectra in Area 2 are less than 95 wavenumbers, but only 2% are less than 78 wavenumbers. Forty-seven percent of spectra in Area 4 are less than 95

wavenumbers, but only 4% are less than 78 wavenumbers. 90% of spectra in Area 4 are less than 95 wavenumbers, but only 5% are less than 78 wavenumbers.

Table 5.1 Descriptive statistics of v3 (CO₃) peak widths for OSC archaeological ash samples

Area ID	Average v3 (CO ₃) width at 75% intensity	n	Standard Deviation	Max v3 (CO ₃) width	Min v3 (CO ₃) width	Range	Percentage of Spectra with v3 (CO ₃) Width:				Ash in MM?
							< 78	78 - 95	95 - 125	> 125	
OSC-38 - Area 1	146.94	154	5.3	157.1	127.5	30	0.0%	0.0%	0.0%	100.0%	No
OSC-38 - Area 2	123.21	383	14.5	149.6	73.5	76	1.1%	0.8%	44.7%	51.3%	No
OSC-78 - Area 2	70.86	562	8.5	117.9	51.0	67	84.88%	13.9%	1.25%	0.00%	Yes
OSC-78 - Area 4	67.94	163	9.8	102.1	51.2	51	87.12%	10.4%	48.13%	0.00%	Yes
OSC-78 - Area 6	76.85	333	6.7	97.5	58.3	39	65.77%	32.7%	1.50%	0.00%	Yes
OSC-78 - Area 7	91.12	1709	26.5	164.6	50.4	114	44.29%	27.03%	11.47%	17.20%	Mixed
OSC-78 - Area 7a	76.56	922	8.5	105.3	54.2	51	63.56%	33.4%	3.04%	0.00%	Yes
OSC-78 - Area 8	75.85	394	11.9	119.0	52.1	67	62.44%	31.5%	6.09%	0.00%	Yes

Table 5.2 Descriptive statistics of v3 (CO₃) peak widths for WW LSA combustion feature samples

Area ID	Average v3 (CO ₃) width at 75% intensity	n	Standard Deviation	Max v3 (CO ₃) width	Min v3 (CO ₃) width	Range	Percentage of Spectra with v3 (CO ₃) Width:				Ash in MM?
							< 78	78 - 95	95 - 125	> 125	
WW14-01 - Area 1	81.49	729	8.9	152.2	60.5	92	35.80%	60.1%	3.70%	0.41%	Yes
WW14-01 - Area 2	91.88	396	7.3	122.1	69.9	52	1.52%	70.2%	28.28%	0.00%	Yes
WW14-01 - Area 3	95.45	637	9.6	128.3	55.1	73	3.92%	42.7%	52.90%	0.47%	Yes
WW14-01 - Area 4	88.35	1090	6.2	115.5	65.8	50	4.86%	84.8%	10.37%	0.00%	Yes

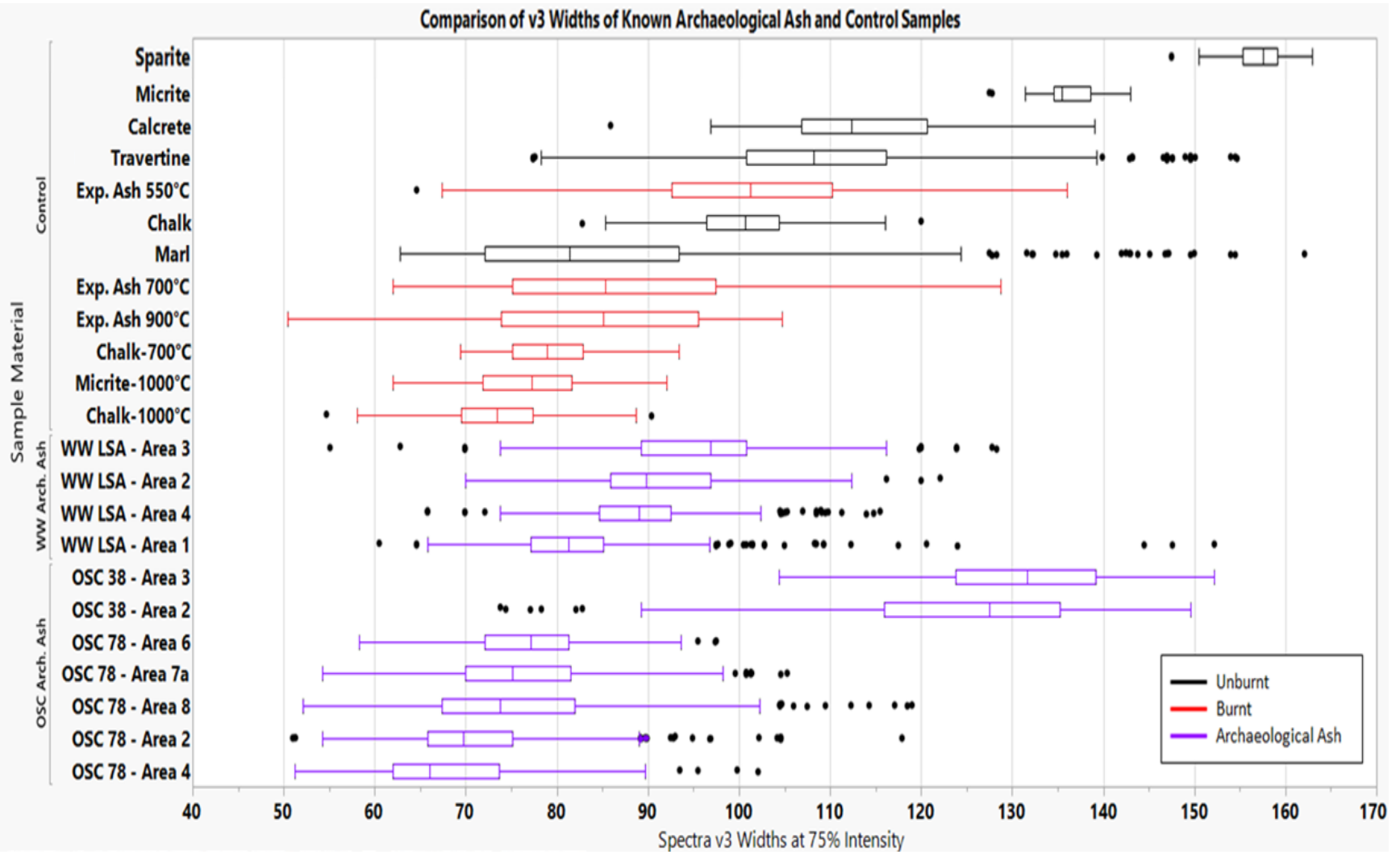


Figure 5.4 v3 (CO₃) widths of OSC and WW known archaeological ash examples compared to control samples

5.1.3. Discussion of Known Archaeological Ash

Overall, the results were mixed. The known archaeological ash samples demonstrate that the characteristics denoting wood ash could survive over time, but the preservation is not guaranteed, or even likely. Areas from the same site and even the same thin section showed different results. The results from Oscurusiuto were inconsistent within the site. One hearth (OSC38) did not fulfill the FTIR-m criteria for wood ash despite a preserved macroscopic ash deposit, while the other hearth in OSC78 was less preserved on a macroscopic scale but did contain regions of wood ash that had the FTIR-m traits for pyrogenic calcite.

This inconsistency can be resolved with the addition of micromorphological analysis. The high degree of variance in the ν_3 (CO_3) widths of these ash is a result of the heterogeneous mixture of different types of calcite within the sample. The variety of calcite types is due to both the heterogeneity of the deposit and differences in preservation and stability on a microscopic scale. The different calcite types and preservation were identified with micromorphology.

Based on these results, the amount of wood ash surviving does not reflect the preservation on the molecular scale, as OSC38 had a larger ash deposit with a surviving macroscopic structure but the extensive calcite precipitation altered or hid the pyrogenic characteristics from the FTIR-m spectral results. OSC78 had thinner ash layers but better preservation. One good indicator of preservation was recognizable rhombs. In areas with preserved rhombs, the FTIR-m results fit the profile for pyrogenic calcite.

Only one of the four areas in the Wonderwerk LSA sample fit all four criteria for wood ash. Although all four were identified as clusters of wood ash rhombs with micromorphology, results of the ν_3 (CO_3) peak width analysis were inconclusive. Three of the areas had only 2-5% of the spectra in each area are thinner than 78 wavenumbers, the geogenic minimum. One possibility is that low-temperature fire produced these ash clusters. Another possibility is that these areas had greater levels of calcite dissolution and precipitation. Figure 4.3b shows signs of crystallization in Area 2, supporting the second possibility.

The mixed outcomes from the LSA combustion feature in Wonderwerk Cave suggest that the pyrogenic properties of wood ash can survive in the cave environment, as seen in Area 1, but the persistence of the properties is not uniform, even within a very small region. In the other three areas, the rhombs confirm that the material is wood ash, but the FTIR-m results are very inconclusive and point to a low-temperature fire, or recrystallization. Because wood ash is disordered and unstable, it can dissolve and reprecipitate as larger, stable crystals (Shahack-Gross and Ayalon 2013). As mentioned above, there is a layer of phosphatic material, likely from bat guano, which can alter and destroy ash. It's possible that the ash facies that had recrystallized were more resistant to the phosphatic reaction, and thus preferentially survived.

In summary, the test of known archaeological ash offers both optimistic and pessimistic conclusions in regards to the identification of unknown wood ash. The properties of wood ash that FTIR-m identifies are fragile enough that the survival is not reliable and varies across microfacies. This is consistent with previous studies of prehistoric wood ash, where both preserved and recrystallized ash were identified in close proximity (Karkanas et al. 2007) However, examples of prehistoric wood ash do fit the criteria I laid out for the identification of wood ash with FTIR-m and micromorphology, proving that the indicators of pyrogenic calcite can be preserved.

5.2. WW Control Samples

The results of control materials from Wonderwerk Cave are summarized in Table 5.3 below. All of the samples had average ν_3 (CO_3) widths above 125 wavenumbers and average ν_3 (CO_3) widths in the geogenic range.

Wonderwerk Limestone, the cave bedrock, fell conclusively within the geogenic range of ν_3 (CO_3) widths, very close to sparite (Figure 5.11). Modern Stalactite and Modern Flowstone have extensive ranges of ν_3 (CO_3) peak widths, including overlap with exclusively pyrogenic/marl ν_3 (CO_3) widths. However, the spectra in the pyrogenic range make up less than 2% of calcite spectra, which is not indicative of pyrogenic calcites.

Ancient Speleothem had a range of widths from 54 to 166 wavenumbers, with the vast majority of the spectra clustering towards the right of the plot with the definitively geogenic materials. Other than the presence of small minority of spectra with pyrogenic ν_3 (CO_3) widths, it does not fit any of the other criteria for identifying wood ash. Only 15% of the spectra are less than 95 wavenumbers.

The non-pyrogenic Wonderwerk samples show a greater range of ν_3 (CO_3) widths than seen in the original control set, including narrow widths previously only measured in pyrogenic calcites. However, the vast majority of the spectra in all the Wonderwerk control samples fell in the geogenic range, and the samples did not meet any of the criteria to identify wood ash. Spectra from the Modern Flowstone, Modern Stalactite, and Ancient Speleothem included aragonite. These spectra were excluded for the analysis, but may have contributed to the range of variation, as aragonite is less stable than calcite and some of the calcite may have been in the transition from aragonite to calcite (Weiner 2002). These results demonstrate the importance of comparing large groups of samples.

Table 5.3 Descriptive statistics of v3 (CO₃) peak widths for WW control samples

Area ID	Average v3 (CO ₃) width at 75% intensity	n	Standard Deviation	Max v3 (CO ₃) width	Min v3 (CO ₃) width	Range	Percentage of Spectra with v3 (CO ₃) Width:				Ash in MM?
							< 78	78 - 95	95 - 125	> 125	
Wonderwerk Limestone	155.1	101	6.1	165.0	137.3	28	0.0%	0.0%	0.0%	100.0%	No
Modern Flowstone	148.2	501	16.9	165.5	66.4	99	1.6%	3.2%	2.4%	92.8%	No
Modern Stalactite	123.5	112	31.6	164.6	70.5	94	1.8%	31.3%	15.2%	51.8%	No
Ancient Speleothem	129.0	495	26.5	169.0	54.3	115	7.5%	8.7%	16.6%	67.3%	No

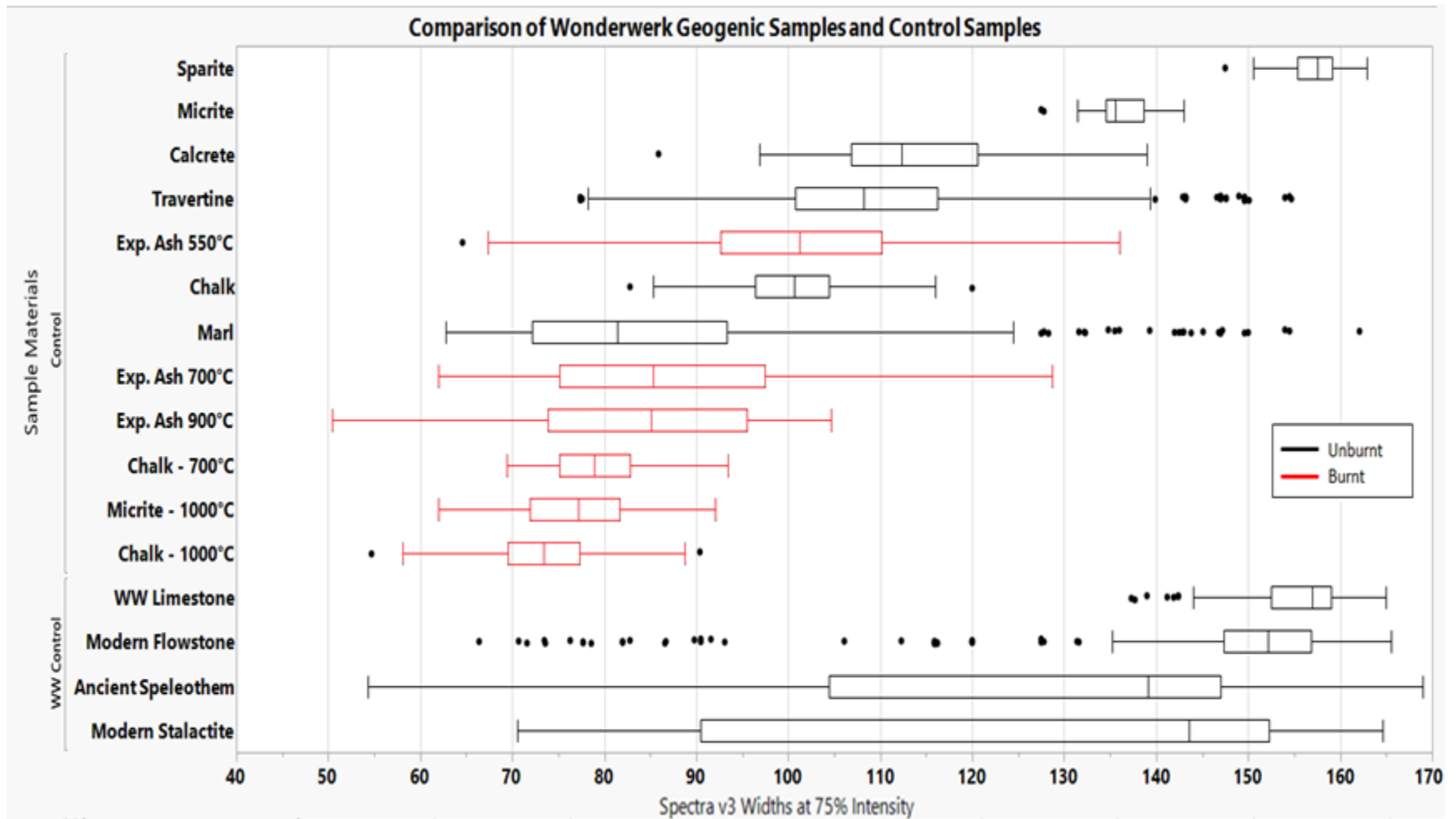


Figure 5.5 v3 (CO₃) widths of definitively un-burnt calcite materials in Wonderwerk Cave compared to control samples.

5.3. Wonderwerk Cave ESA Potential Ash Results

The data collected from the potential ashed plant fragments in the ESA samples from Wonderwerk Cave using the ν_3 (CO_3) width protocol is summarized below. The results confirmed the identification of wood ash in eleven of the sixteen areas analyzed. The results for each area of analysis is as part of a grouped based on the thin section in which they are collected.

The areas analyzed in thin section WW05-04 are shown in Figure 5.6 and the results from the FTIR-m mapping and ν_3 (CO_3) peak width analysis are summarized in Table 5.4. All five areas had a wide range of ν_3 (CO_3) widths extending from the pyrogenic range to the geogenic range. The results from Areas 2, 3, 4 and 5 meet the criteria I set out in the previous chapter for the identification of wood ash with FTIR-m data. These four areas had average ν_3 (CO_3) widths below 85 wavenumbers. In those areas 60-75% of the spectra analyzed were less than 78 wavenumbers wide, and 80-91% were less than 95 wavenumbers.

Area 1 is the exception. Despite being identified as a cluster of ash rhombs, the average ν_3 (CO_3) peak width was 89.9 wavenumbers and only 57.4% had ν_3 (CO_3) widths less than 95 wavenumbers. However, the calcitic plant material is the most fragmented of the five areas, with extensive calcitic coating and infilling (Figure 5.7). The difference from the other four areas may be due to poorer preservation.

To address the issues of heterogeneity, I combined the FTIR-m spectral map of a sample area with micromorphological location pictures. The overlaid grid in Figure 5.7 shows the location of each spectra and categorizes the ν_3 (CO_3) width. From this, it is possible to look at the concentrations of different calcite types and match the FTIR-m results with the micromorphology (Table 4.3).

Figure 5.8 demonstrates the connection between the ν_3 (CO_3) width of a spectra and location of the spectra. When the ν_3 (CO_3) width results are mapped on top of the photomicrograph of the area, the spectra with the widest ν_3 (CO_3) results are found mainly on the outer edge or cracks within the plant fragment. This suggests the calcite there is

re-precipitated calcite coatings, with a different formation process than the interior of the fragment. Consideration of the calcite coating accounts for the wide range of ν_3 (CO_3) widths in Area 4. Many of the outlier spectra are located in these areas.

In contrast to Area 1, Area 5 is the largest, most intact fragment of potential ash. The results of the ν_3 (CO_3) peak width measurements strongly support an identification of pyrogenic calcite. The large size and lack of fragmentation and voids of the unit may indicate better preservation, and less calcitic precipitation than the other areas, explaining why this area is most consistent with pyrogenic calcite.

Figure 5.9 compares the range and clustering of ν_3 (CO_3) peak widths in the WW04-05 areas to the control samples. When the WW05-04 results are compared to the control data, the WW05-04 areas have a much greater similarity to the other pyrogenic calcites (and marl) than the unburnt samples.

In summary, the predominance of spectra in the burnt range strongly support the identification of ashed plant material for Areas 2-5. Areas 2-5 fit all four criteria for wood ash identification. The FTIR-m results from Area 1 are inconclusive, but do not rule out a conclusion of wood ash. The presence of 30% of the spectra with ν_3 (CO_3) widths less than 78 wavenumbers suggest that the sample contains a heterogeneous mixture of both pyrogenic and geogenic calcites. The presence of ash rhombs identified in the micromorphological analysis supports the conclusion of wood ash. In addition, the micromorphological analysis noted the presence of geogenic calcite within the ash rhomb clusters which can explain the spectra with wider, geogenic ν_3 (CO_3) peak widths that were measured in the FTIR-m analysis. Thus, this demonstrates the importance of incorporating both the FTIR-m and micromorphology results into conclusions.

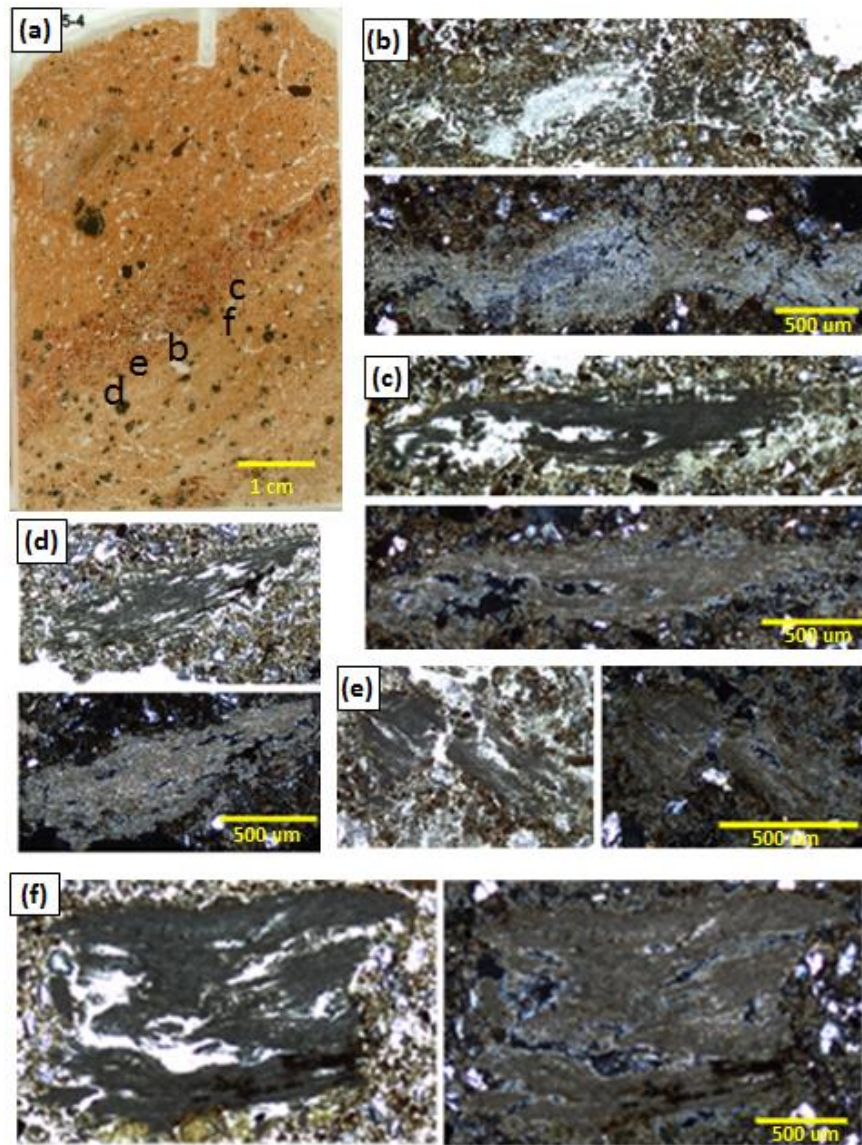


Figure 5.6 (a) Thin section WW05-04 from Layer 10 with three microstratigraphic units. Examples of ashed plant fragments identified in Berna et al. (2012) are indicated letters and close-ups are provided in b - f. (b) Micrograph of ashed plant fragment with identifiable ash rhomb cluster (Area 1). (c) Micrograph of ashed plant fragment (Area 2). (d) Micrograph of ashed plant fragment (Area 3). (e) Micrograph of ashed plant fragments and wood ash rhombs dispersed in sediment (Area 4). (f) Micrograph of ashed plant fragment with possible charring (Area 5).

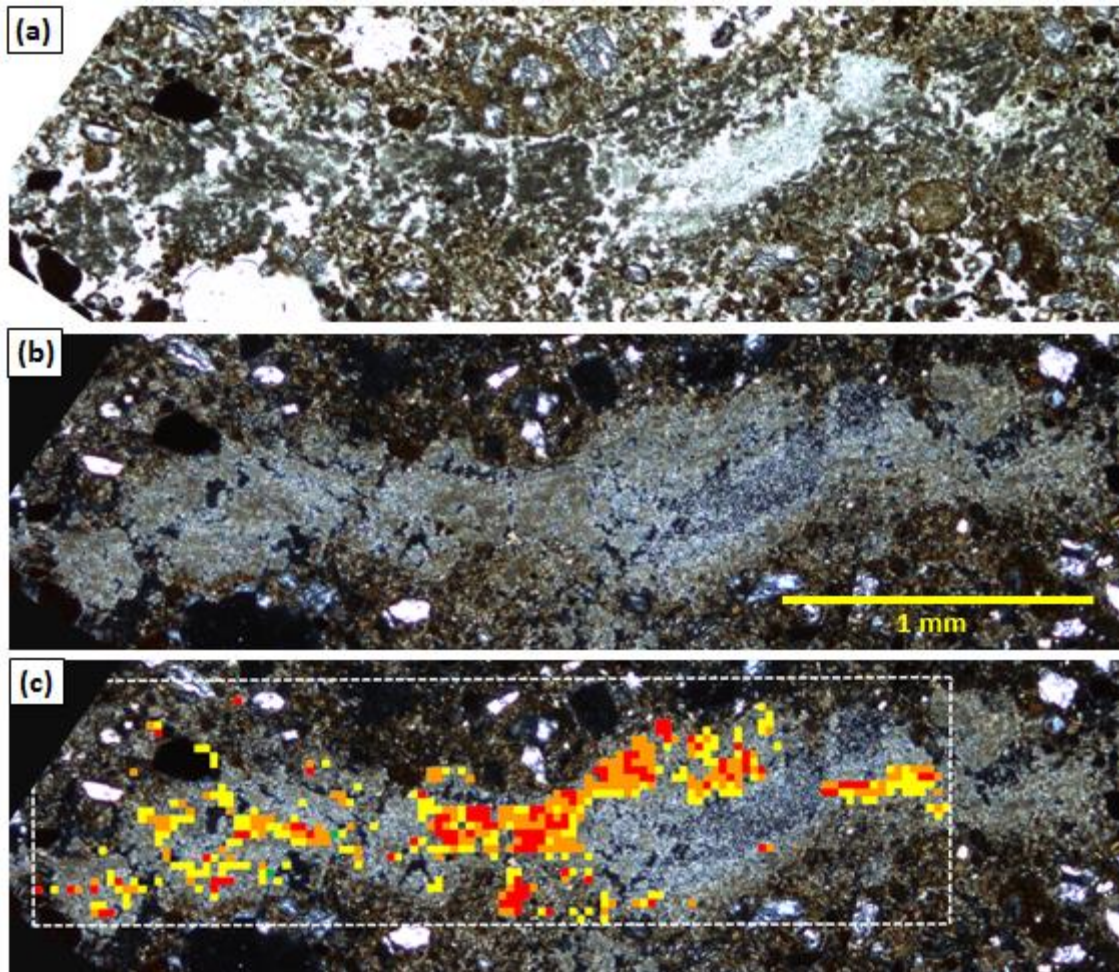


Figure 5.7 (a) Photomicrograph of WW05-04 Area 1. PPL (b) Same as a except XPL. (c) Photomicrograph of Area 1 with FTIR map superimposed. The extent of the map is shown by the black box. The colors indicate different $\nu_3(\text{CO}_3)$ widths. Empty squares indicate areas without calcite or without enough signal to identify the material.

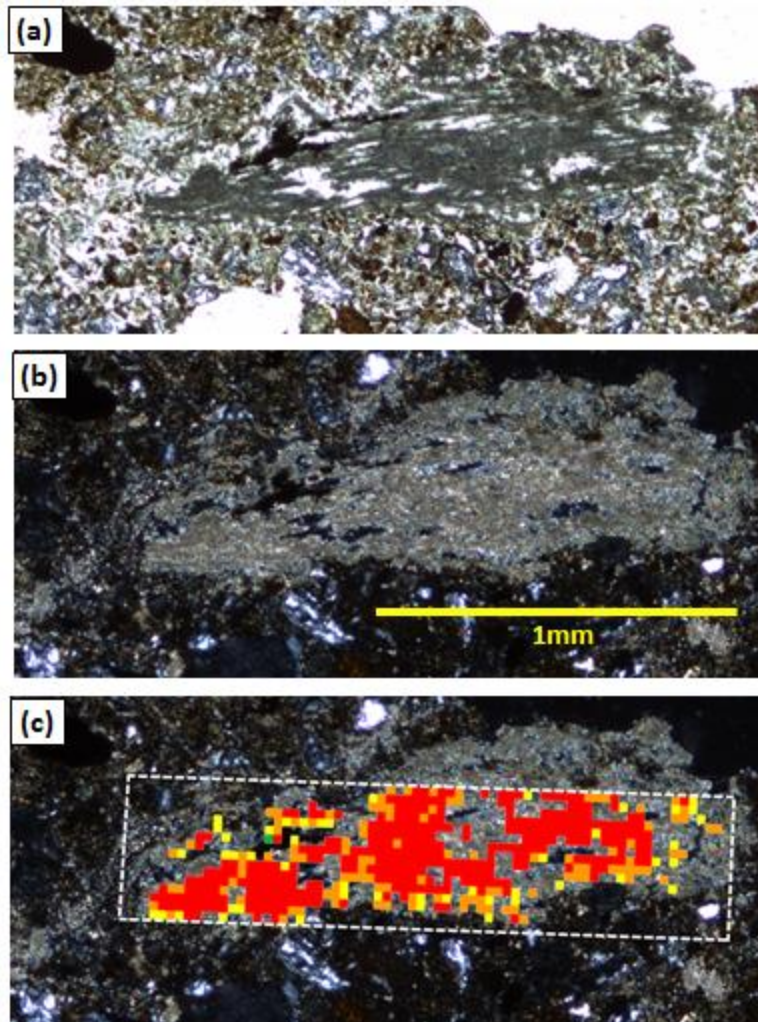


Figure 5.8 (a) Photomicrograph of WW05-04 Area 4. PPL (b) Same as a except XPL. (c) Photomicrograph of Area 1 with FTIR map superimposed. The extent of the map is shown by the black box. The colors indicate different ν_3 (CO_3) widths. Empty squares indicate areas without calcite or without enough signal to identify the material. Note that the orange and yellow squares with wider ν_3 (CO_3) peaks cluster on the edge of the ashed plant fragment.

Table 5.4 Descriptive statistics of v3 (CO₃) peak widths for areas in WW05-04

Area ID	Average v3 (CO ₃) width at 75% intensity	n	Standard Deviation	Max v3 (CO ₃) width	Min v3 (CO ₃) width	Range	Percentage of Spectra with v3 (CO ₃) Width:				Ash in MM?
							< 78	78 - 95	95 - 125	> 125	
WW05-04 - Area 1	89.9	491	13.6	129.0	58.3	71	22.4%	37.1%	40.5%	1.6%	Yes
WW05-04 - Area 2	78.0	551	17.6	139.1	50.4	89	59.2%	21.6%	19.2%	5.8%	Yes
WW05-04 - Area 3	79.4	228	12.9	115.7	57.1	59	53.1%	32.5%	14.5%	0.0%	Yes
WW05-04 - Area 4	71.7	471	15.4	127.7	46.8	81	67.1%	22.7%	10.2%	0.8%	Yes
WW05-04 - Area 5	70.1	905	15.5	143.2	46.8	96	75.5%	15.9%	8.6%	3.5%	Yes

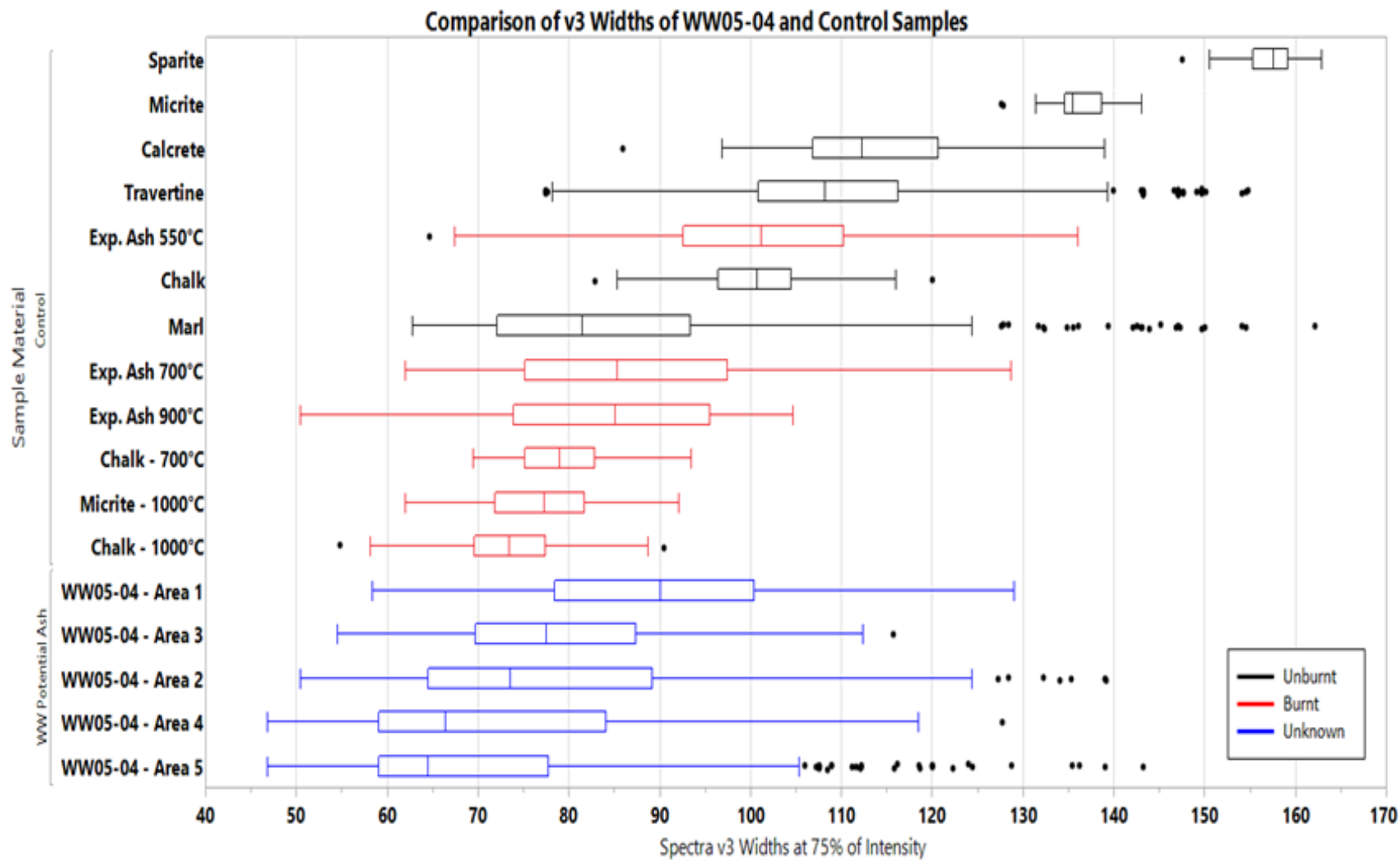


Figure 5.9 v3 (CO₃) widths in WW05-04 areas compared to the control samples

The areas analyzed in this section WW11-07 are shown in Figure 5.11 and the results from four areas in WW11-07 are summarized in Table 5.5. Area 1 is the only one to have an average ν_3 (CO_3) peak width over 86.4 wavenumbers, and 73.4% of the spectra have ν_3 (CO_3) widths less than 95 wavenumbers, less than 2% under the cut-off. The micromorphology results show a large intrusion of calcitic crystals in the center of the potential ashed plant fragment (Figure 5.12). Subsection 1a is a region within Area 1 that did not include the intrusive calcitic crystals. The Subsection 1a results from the ν_3 (CO_3) width analysis fit the four criteria to identify wood ash as laid out in the previous chapter.

The results for areas 3-5 fit all the criteria for wood ash. They were identified as wood ash in the micromorphological analysis. The average ν_3 (CO_3) peak width for all fell between 74 and 79 wavenumbers. In the same three areas, all had over 90% of spectra with less than 95 wavenumbers and 55-75% of the spectra in each area had ν_3 (CO_3) widths less than 78 wavenumbers (Table 5.5). From this, I categorized the areas as pyrogenic.

The FTIR-m results conflict with the micromorphology results in Area 6. The ν_3 (CO_3) peak data indicate that the sample is pyrogenic. The average ν_3 (CO_3) width was 72.4 wavenumbers and 97% of spectra were less than 95 wavenumbers, well within the criteria. In contrast, the micromorphological analysis identified the sample as a cemented micritic matrix containing small fragments of quartz and ironstone. The fine calcite particles have a crystallinity and birefringence that is not associated with wood ash (Figure 5.10).

A summary of the results finds support for the identification of ashed plant material with some reservations. Area 1 does not fit two of the criteria laid out for wood ash. The average ν_3 (CO_3) width is above 84 wavenumbers and more than 25% of spectra have a ν_3 (CO_3) width greater than 95 wavenumbers. However, the area does include spectra with ν_3 (CO_3) widths less than 78 wavenumbers. The micromorphological analysis suggests that this discrepancy is the result of the presence of precipitated calcitic crystals in the center of the preserved plant fragment, and the map of ν_3 (CO_3) peak widths confirms that the spectra with geogenic ν_3 (CO_3) widths are located in that area (See Figure 5.12). Subsection 1a excludes that area and the spectral results fit the criteria for wood ash. Areas 3-5 also fulfill the criteria for ashed plant fragments. The predominance

of spectra in the burnt range supports the identification of these fragment as wood ash. Area 6 has conflicting micromorphology and FTIR-m results. The FTIR-m results clearly indicate that it is pyrogenic, while the micromorphology did not identify any ash characteristics but did not conclusively identify it as marl, although that possibility was not ruled out. It is also possible that area is wood ash that lost its structural features but not the molecular characteristics that differentiate pyrogenic material from non-pyrogenic. Alternatively, geogenic calcite could form in environments or specific conditions inside Wonderwerk Cave that result in the same disorder and small particle size as pyrogenic materials. It is not currently possible to determine whether the FTIR-m or the micromorphology is correct.

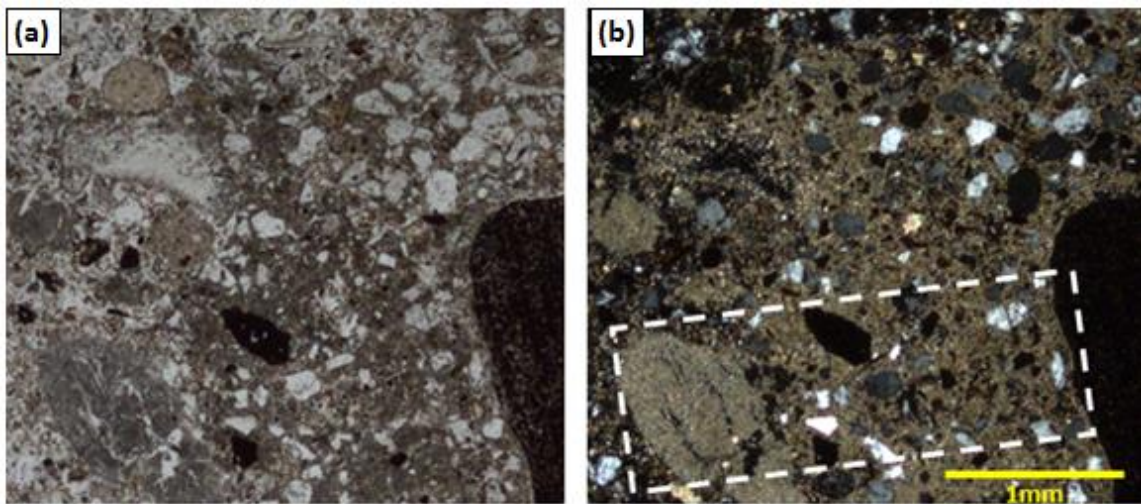


Figure 5.10 (a) Photomicrograph of WW11-07 – Area 6. PPL (b) Same in XPL.

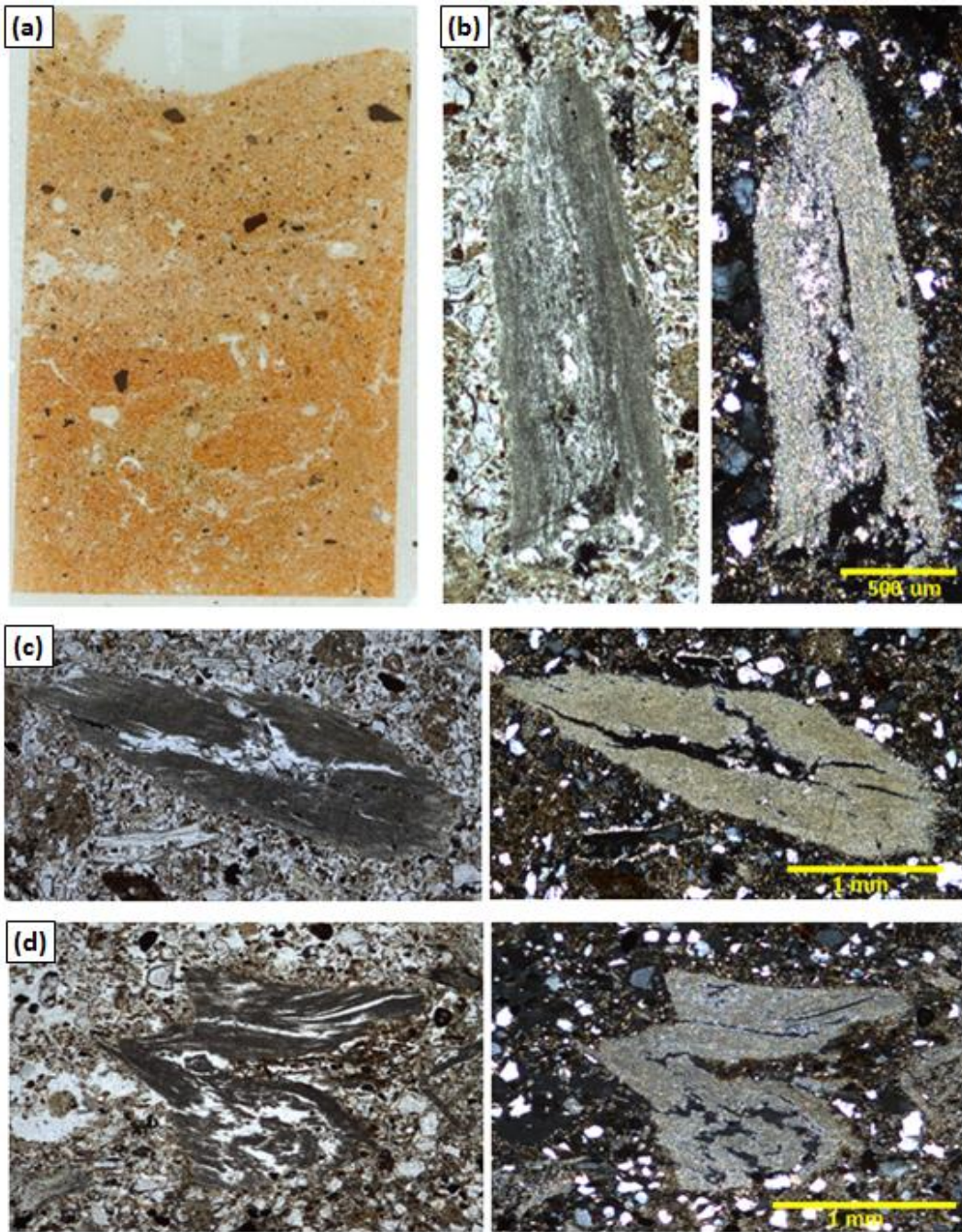


Figure 5.11 (a) Thin section WW11-07 from Layer 10. Areas with potential ashed plant fragments are indicated by the boxes and close-ups are provided in b - f. (b) Micrograph of ashed plant fragment with extensive calcitic infilling (Area 1). (c) Micrograph of ashed plant fragment (Area 2). (d) Micrograph of ashed plant fragment (Area 3).

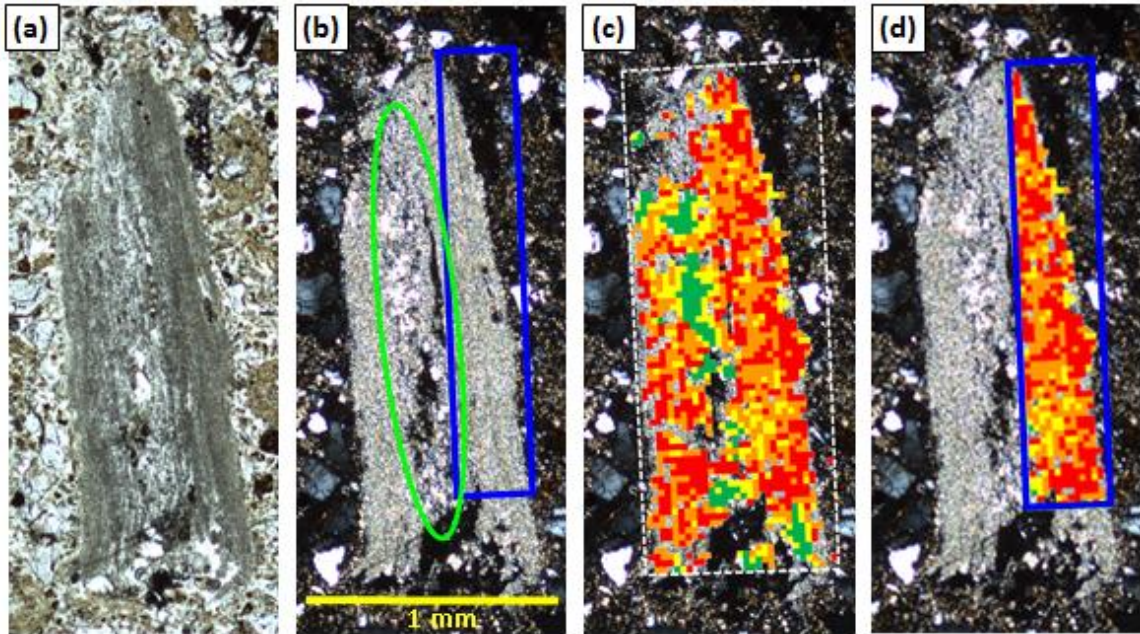


Figure 5.12 Photomicrograph of WW11-07 Area 1. PPL (b) Same as a except XPL. The green oval indicates the area of larger, more crystalline calcite in the center of the sample. The blue box indicates subsection 1a. (c) Photomicrograph of Area 1 with FTIR map superimposed. The extent of the map is shown by the white box. Empty squares indicate areas without calcite or without enough signal to identify the material. The colors indicate different ν_3 (CO_3) widths. Note the clusters of green (geogenic ν_3 (CO_3) widths) match the location of the larger, more crystalline section. (d) Photomicrograph of subsection 1a which excludes the intrusive calcite in the center. FTIR map superimposed. The extent of the map is shown by the blue box.

Table 5.5 Descriptive statistics of v3 (CO₃) peak widths for areas in WW11-07

Area ID	Average v3 (CO ₃) width at 75% intensity	n	Standard Deviation	Max v3 (CO ₃) width	Min v3 (CO ₃) width	Range	Percentage of Spectra with v3 (CO ₃) Width:				Ash in MM?
							< 78	78 - 95	95 - 125	> 125	
WW11-07 - Area 1	89.5	1323	21.3	159.1	58.9	100	36.8%	36.4%	17.0%	9.8%	Yes
Area 1 - Subsect. 1a	82.2	524	12.0	150.7	58.9	82	45.4%	39.7%	14.3%	0.4%	Yes
WW11-07 - Area 3	78.7	2131	14.7	162.5	54.2	108	67.8%	25.3%	3.5%	3.4%	Yes
WW11-07 - Area 4	77.6	1104	13.8	158.5	46.5	112	67.3%	25.3%	5.3%	2.1%	Yes
WW11-07 - Area 5	74.3	1491	10.3	159.0	49.6	109	75.3%	21.3%	3.0%	0.4%	Yes
WW11-07 - Area 6	72.4	922	11.9	169.6	52.1	118	78.9%	18.4%	2.0%	0.8%	No

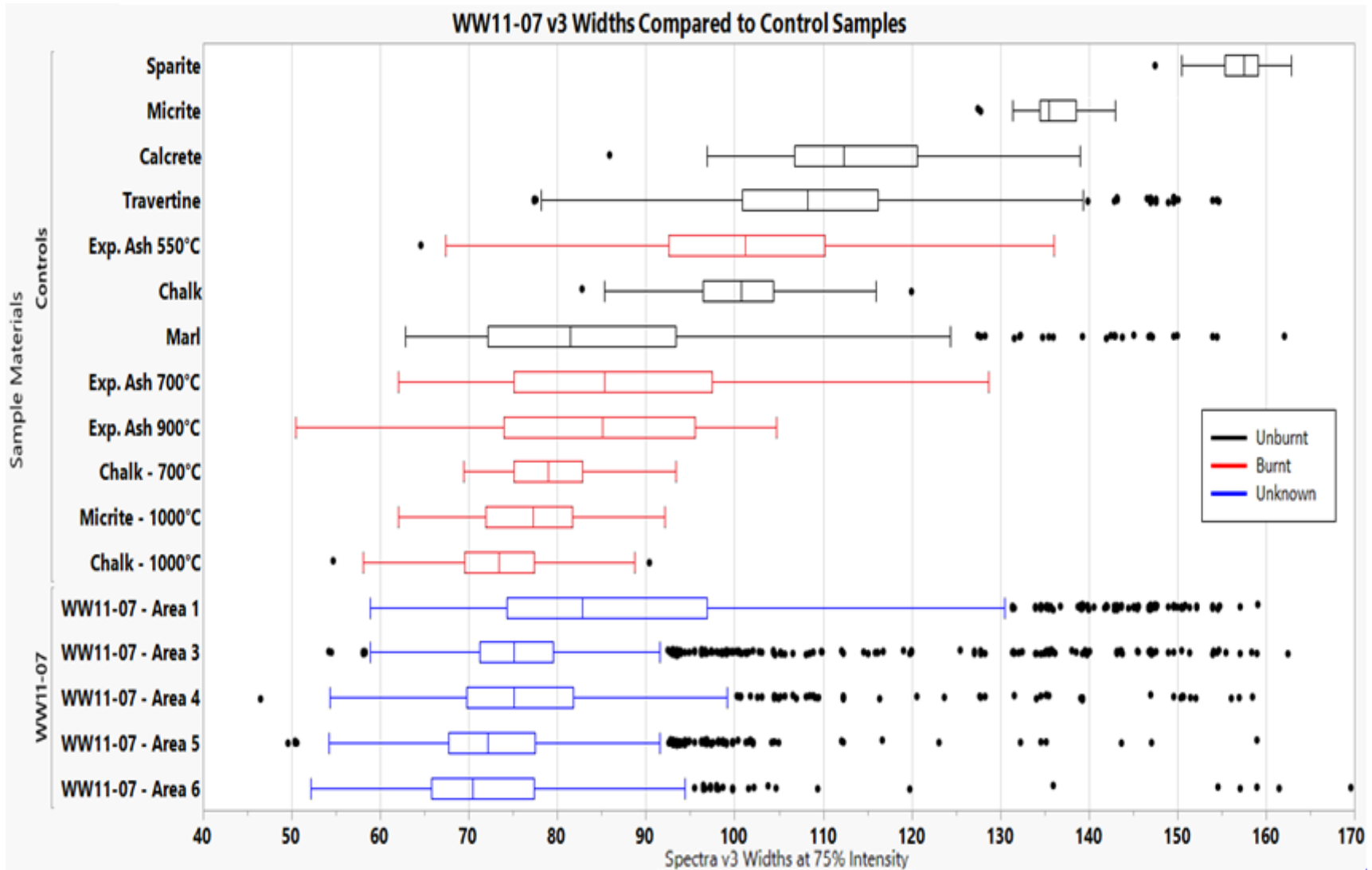


Figure 5.13 v3 (CO₃) widths in WW11-07 areas compared to the control samples

The areas of analysis in thin section WW11-09 are shown in Figure 5.14 and the results from four areas in WW11-09 are summarized in Figure 5.14 below. The average the ν_3 (CO_3) peak widths in all four areas fell between 78 and 84 wavenumbers and 55-75% of the spectra in each area had ν_3 (CO_3) widths less than 78 wavenumbers. These results match the traits identified in the control samples and fulfil the four criteria set out.

Overall, the comparison of the WW11-09 data to the control data Table 5.6 demonstrates that the archaeological samples are more similar to the burnt control results than the unburnt. The WW11-09 areas have a larger number of outliers in geogenic ν_3 (CO_3) widths. The geogenic spectra are in areas with geogenic calcite coating and/or calcite intrusions (Figure 5.15, Figure 5.16,

Figure 5.17, Figure 5.18). The results for WW11-09 support the micromorphological identification of ashed plant fragments. The predominance of spectra in the burnt range strongly supports the identification of these fragment as wood ash. The clear pyrogenic signal from all four areas analyzed in this thin section suggest that all the micritic, plant-shaped calcite fragments could be wood ash. When the location of the spectra is taken into consideration, the geogenic v_3 (CO_3) widths can be identified as an infilling, coating, or otherwise unrelated material.

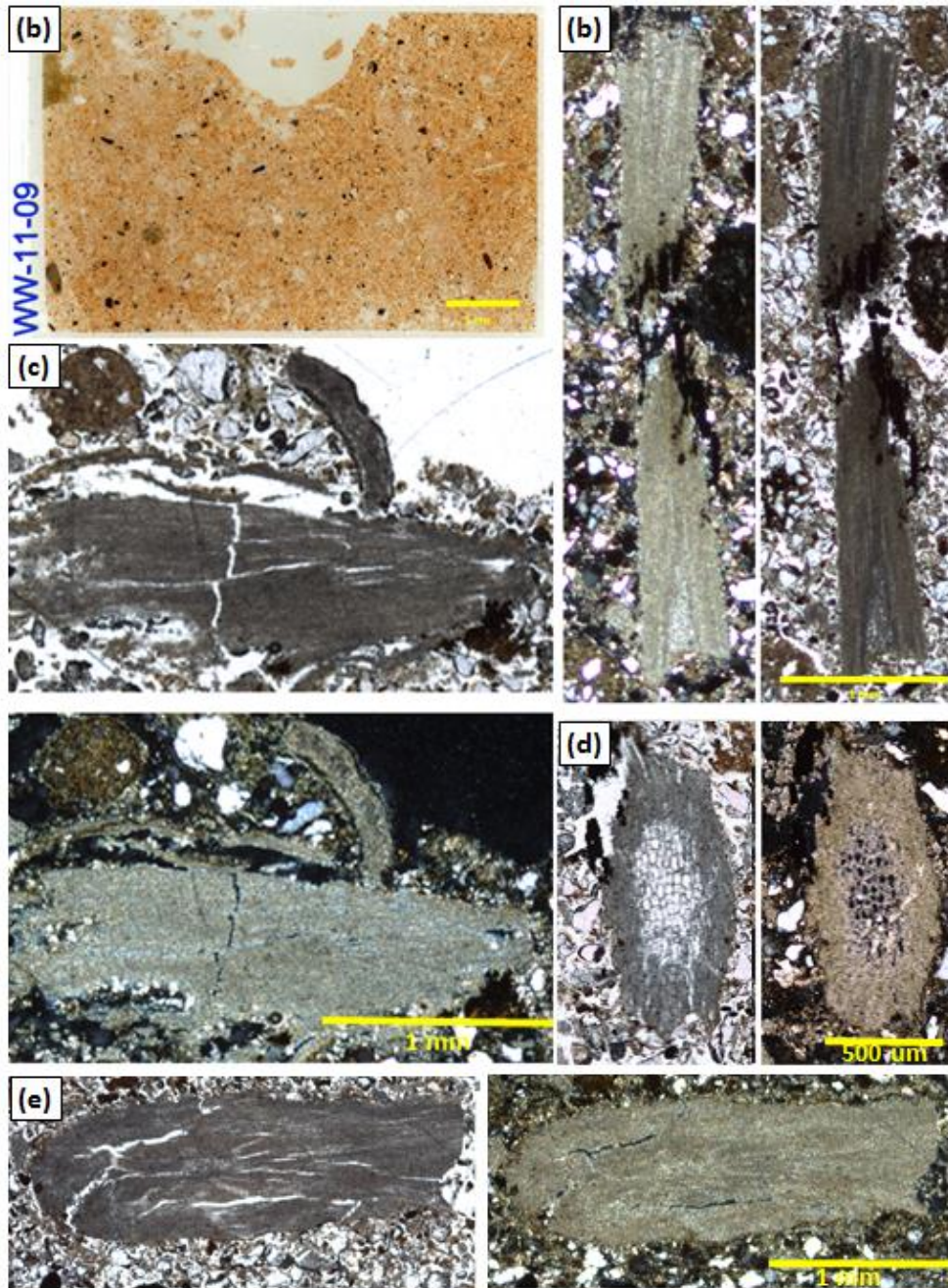


Figure 5.14 (a) Thin section WW11-09 from Layer 10. Areas with potential ashed plant fragments are indicated by the boxes and close-ups are provided in b - e. (b) Micrograph of ashed plant fragment with possible charring (Area 1). (c) Micrograph of ashed plant fragment (Area 2). (d) Micrograph of ashed plant fragment with extensive calcitic infilling of voids (Area 3). (e) Micrograph of ashed plant fragments (Area 4).

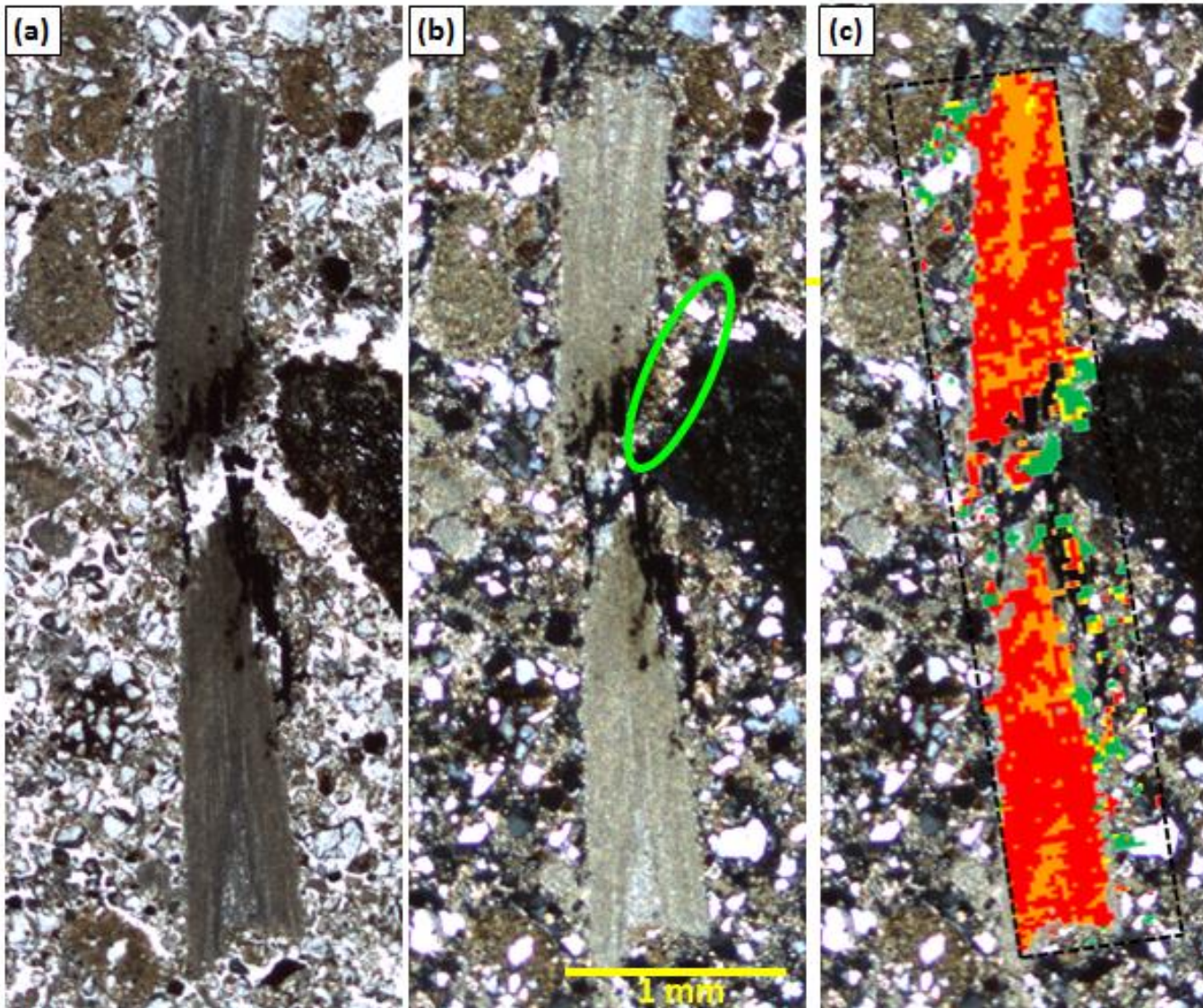


Figure 5.15 (a) Photomicrograph of WW11-09 Area 1. PPL (b) Same as a except XPL. The green oval indicates an area with thick calcite coating. (c) Photomicrograph of Area 1 with FTIR map superimposed. The extent of the map is shown by the black box. Empty squares indicate areas without calcite or without enough signal to identify the material. The colors indicate different $v_3(\text{CO}_3)$ widths. Note the clusters of green (geogenic $v_3(\text{CO}_3)$ widths) on the edges in areas with calcitic coating and/or infilling.

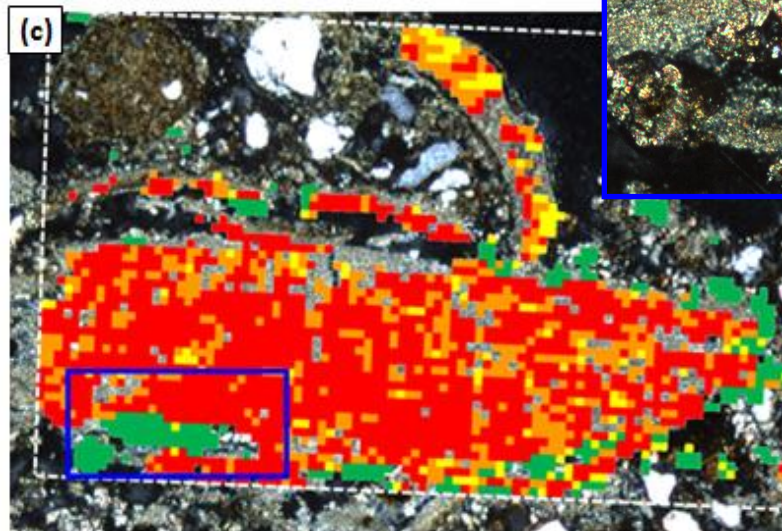
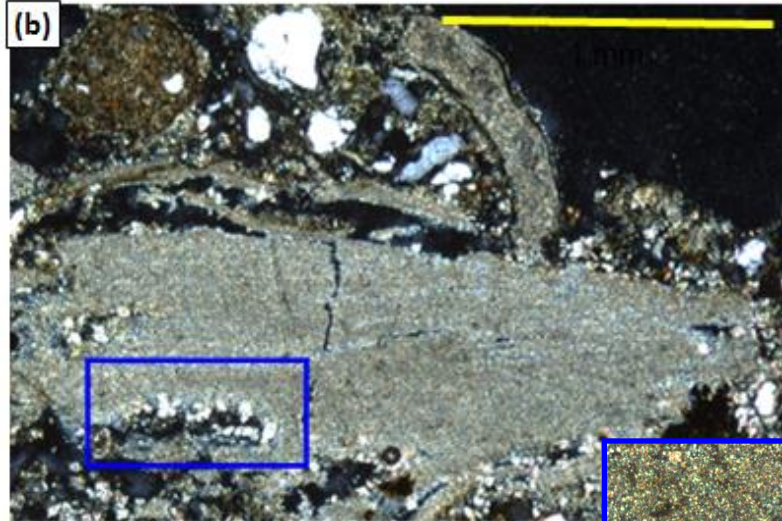
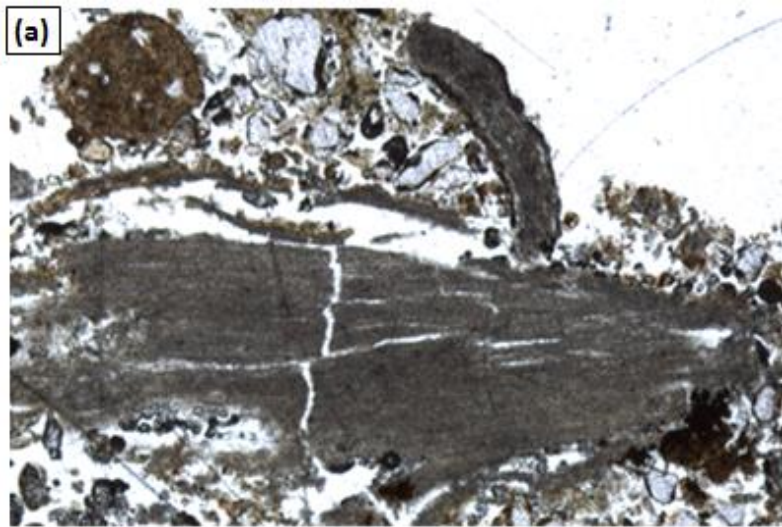
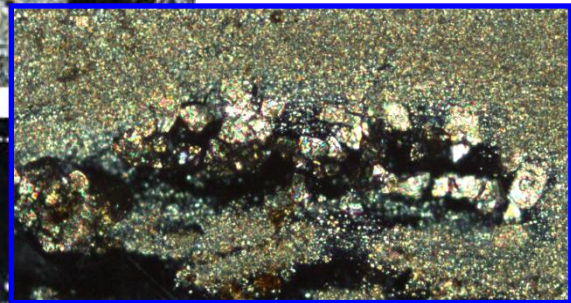


Figure 5.16 (a) Photomicrograph of WW11-09 Area 2. PPL (b) Same as a except XPL. (c) Photomicrograph of Area 2 with FTIR map superimposed. The extent of the map is shown by the black box. Empty squares indicate areas without calcite or without enough signal to identify the material. The colors indicate different v_3 (CO_3) widths. Note the clusters of green (geogenic v_3 (CO_3) widths) on the edges in areas with calcitic coating and/or infilling. (d) Close-up of the section in the blue box. There are large calcite crystals infilling the void on the edge of the ashed plant fragment.



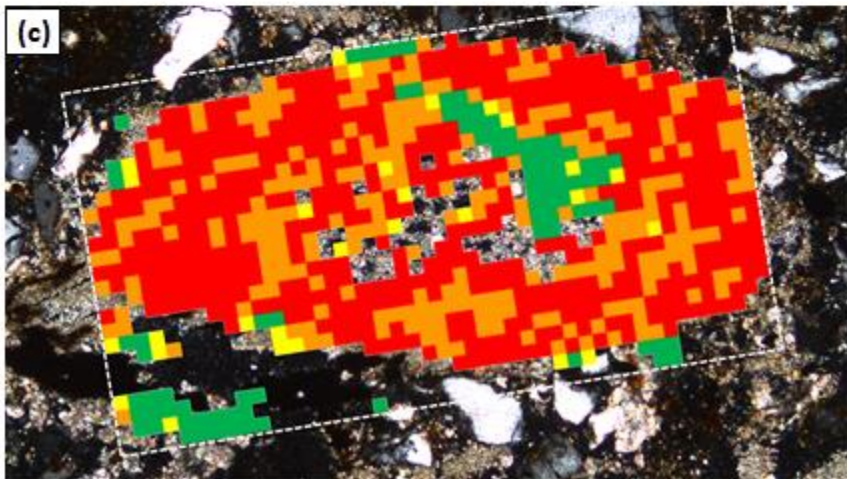
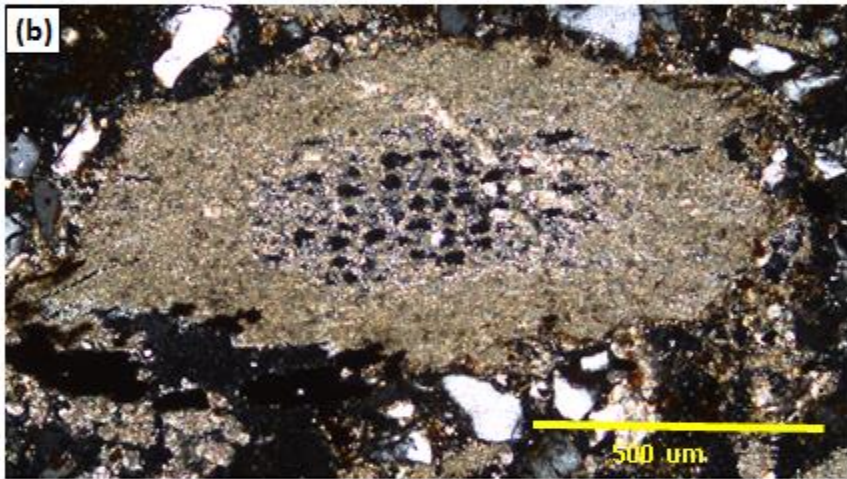
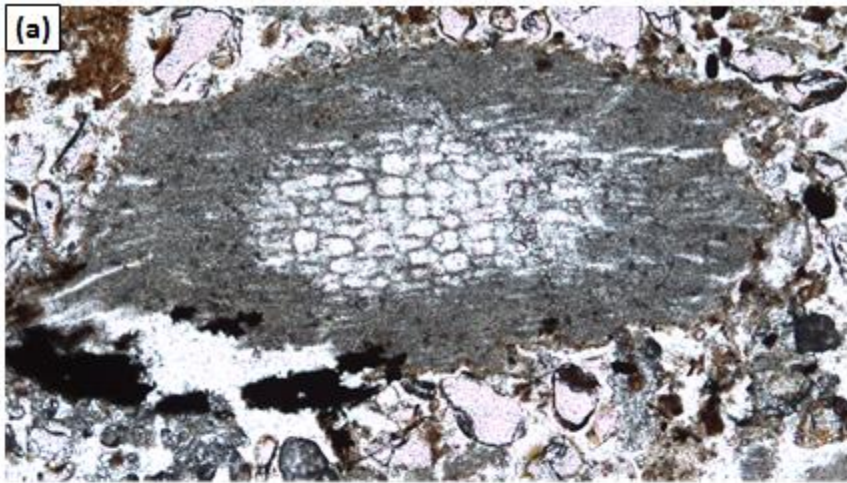


Figure 5.17 (a) Photomicrograph of WW11-09 Area 3. PPL (b) Same as a except XPL. (c) Photomicrograph of Area 3 with FTIR map superimposed. The extent of the map is shown by the black box. Empty squares indicate areas without calcite or without enough signal to identify the material. The colors indicate different v3 (CO_3) widths. Note the clusters of green (geogenic v3 (CO_3) widths) on the edges in areas with calcitic coating and/or infilling

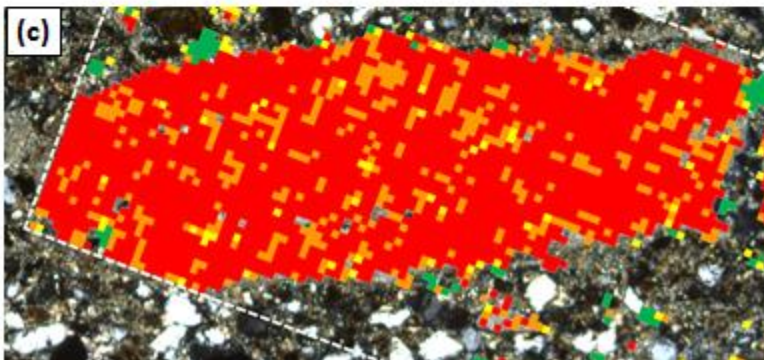
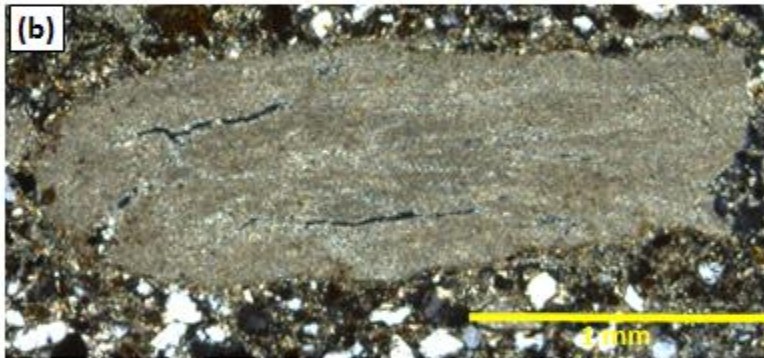
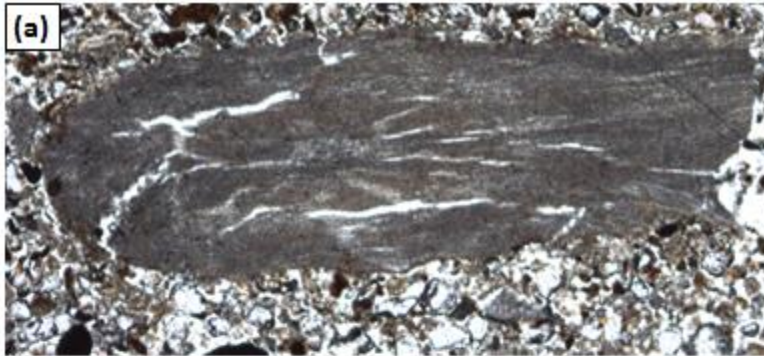


Figure 5.18 (a) Photomicrograph of WW11-09 Area 4. PPL (b) Same as a except XPL. (c) Photomicrograph of Area 4 with FTIR map superimposed. The extent of the map is shown by the black box. Empty squares indicate areas without calcite or without enough signal to identify the material. The colors indicate different $v_3(\text{CO}_3)$ widths. Note the clusters of green (geogenic $v_3(\text{CO}_3)$ widths) on the edges in areas with calcitic coating and/or infilling

Table 5.6 Descriptive statistics of v3 (CO₃) peak widths for areas in WW11-09

Area ID	Average v3 (CO ₃) width at 75% intensity	n	Standard Deviation	Max v3 (CO ₃) width	Min v3 (CO ₃) width	Range	Percentage of Spectra with v3 (CO ₃) Width:				Ash in MM?
							< 78	78 - 95	95 - 125	> 125	
WW11-09 - Area 1	83.5	2574	22.6	175.1	54.2	121	61.4%	26.1%	12.5%	9.6%	Yes
WW11-09 - Area 2	84.7	2175	24.3	164.6	54.2	110	60.3%	22.7%	17.0%	11.3%	Yes
WW11-09 - Area 3	84.7	823	23.0	162.5	51.2	111	56.1%	30.1%	13.7%	10.4%	Yes
WW11-09 - Area 4	78.1	2758	16.5	163.8	45.5	118	74.5%	17.5%	8.0%	4.3%	Yes

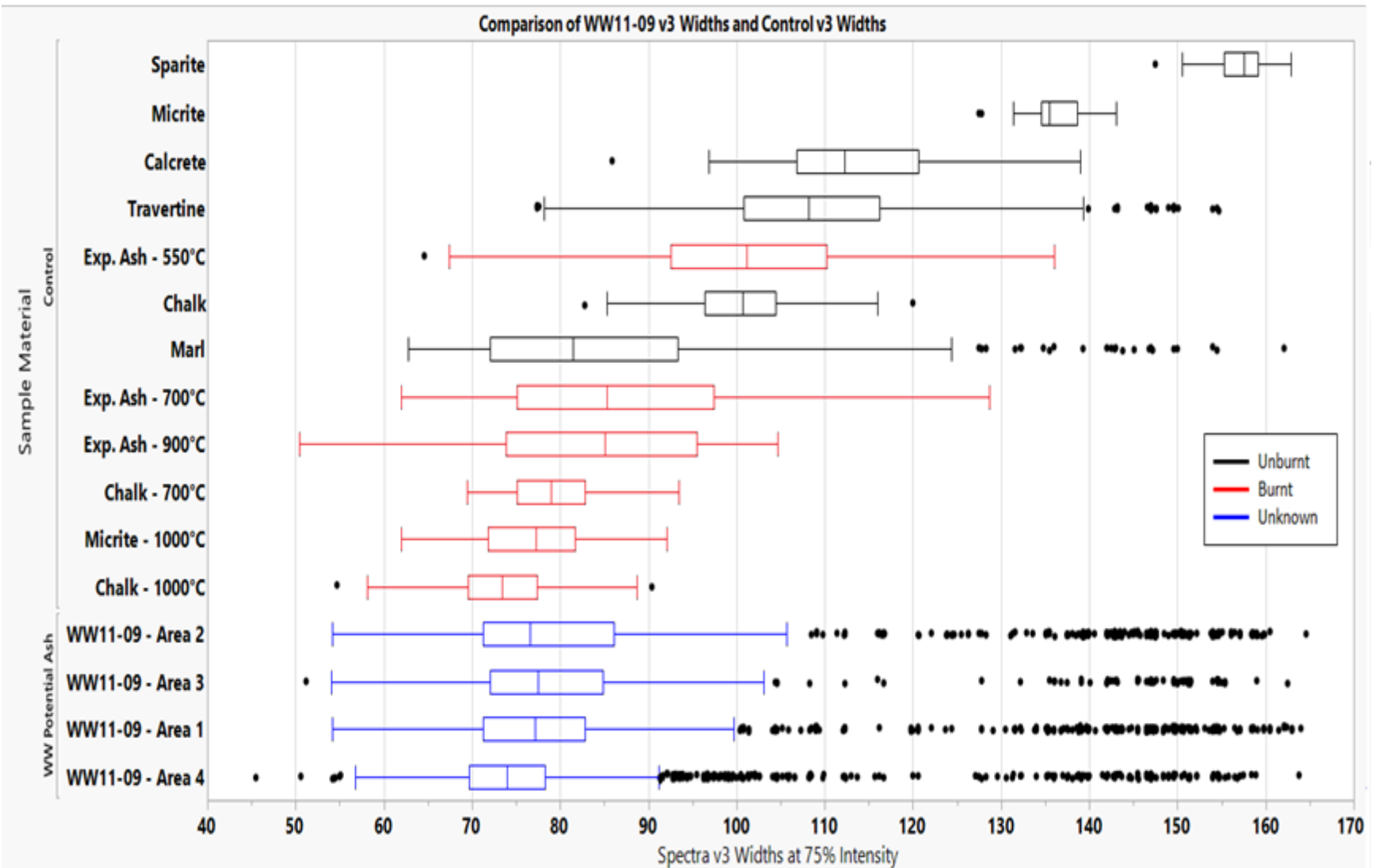


Figure 5.19 v3 (CO₃) widths in WW11-09 areas compared to the control samples

The areas analyzed in thin section WW11-10A are shown in Figure 5.20 and the results of the FTIR-m mapping and v3 (CO₃) analysis for WW11-10A are summarized in Table 5.7. Micromorphology analysis identified Area 1 as a geogenic micritic calcite fragment. The FTIR-m results agreed with that conclusion. The v3 (CO₃) width data of Area 1 did not meet any of the criteria for classification as pyrogenic.

Area 3 does not fit clearly into the pyrogenic or non-pyrogenic category. They were not identified as wood ash from the micromorphology analysis. The micromorphology results identified them as very fine calcite cementation mixed or dissolved into the surrounding clays. Area 3 had an average of 86.8 wavenumbers, and 72% of spectra are less than 95 wavenumbers, which does not fit the standards to confirm pyrogenic material, but are very close to it.

The findings from this sample are inconclusive and include some contradictory results. Area 1 is an example of a definitive non-pyrogenic calcite material within Wonderwerk cave. Both the FTIR-m and micromorphology results suggests that it is geogenic. Despite this, the FTIR-m map includes spectra with v3 (CO₃) widths less than 78 wavenumbers, which was the lowest extent of v3 (CO₃) widths in the unburnt control samples. This demonstrates the heterogeneity of archaeological materials and shows that geogenic materials can have a larger range of widths than originally assumed. It serves as a good addition to the Wonderwerk control samples for any future research. The spectral analyses of Areas 2 indicated that it was pyrogenic. The micromorphology did not identify any distinct wood ash characteristics, but the fine calcite particles and presence of clay indicate that this could be a small marl microfacie.

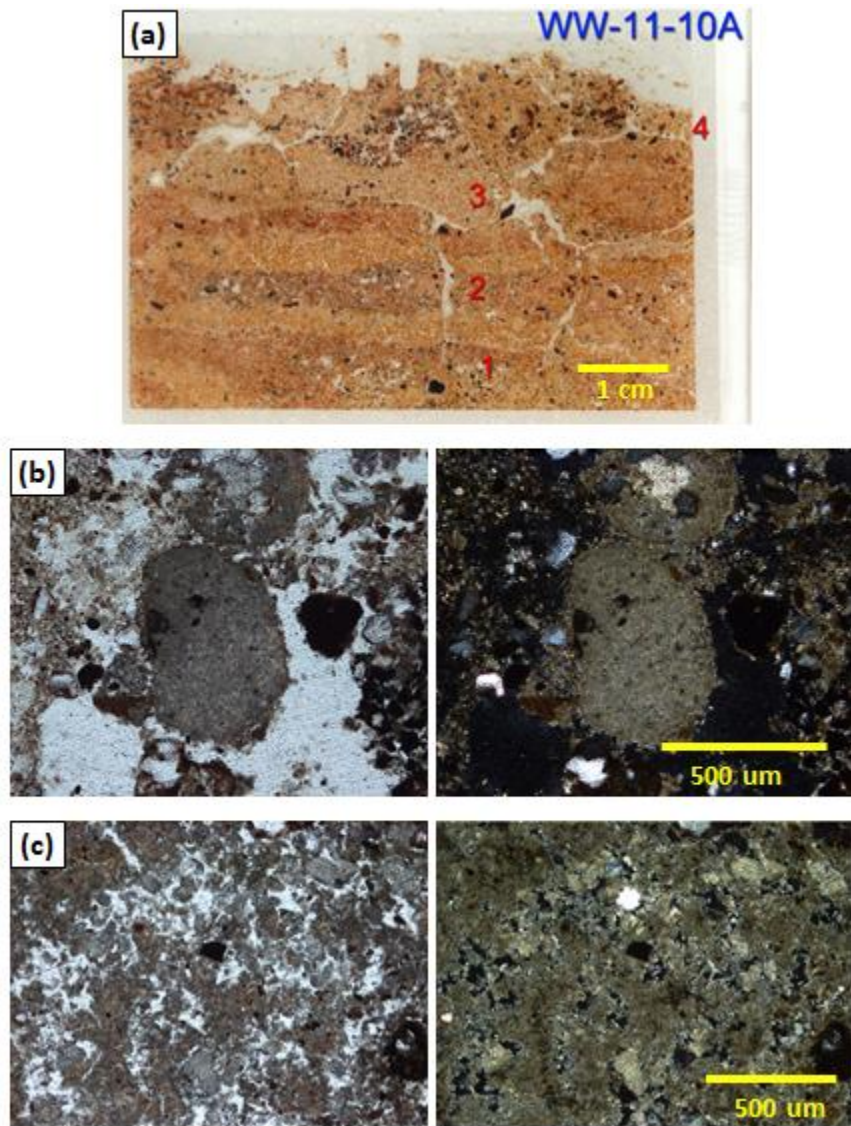


Figure 5.20 (a) Thin section WW11-10A from Layer 10. Areas with calcite are indicated by the boxes and close-ups are provided in b – c. (b) Micrograph of micritic calcite fragment (Area 1). (c) Micrograph area with very fine calcite particles mixed with clays (Area 2).

Table 5.7 Descriptive statistics of v3 (CO₃) peak widths for areas in WW11-10A

Area ID	Average v3 (CO ₃) width at 75% intensity	n	Standard Deviation	Max v3 (CO ₃) width	Min v3 (CO ₃) width	Range	Percentage of Spectra with v3 (CO ₃) Width:				Ash in MM?
							< 78	78 - 95	95 - 125	> 125	
WW11-10A – Area1	94.0	129	12.3	126.3	61.7	65	11.6%	34.9%	52.7%	0.8%	No
WW11-10A – Area3	86.8	334	26.4	172.1	50.4	122	46.7%	25.7%	19.2%	8.4%	No

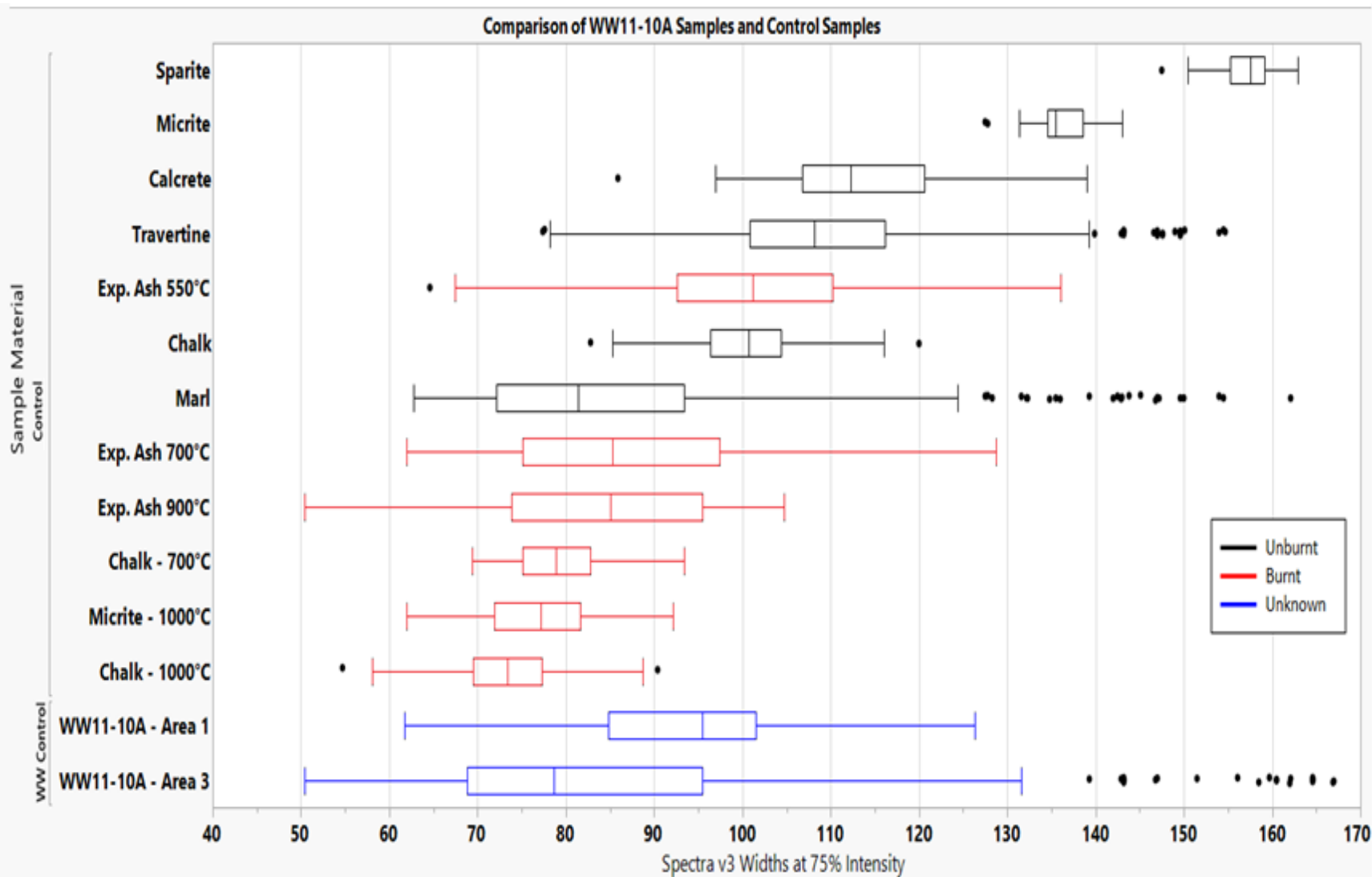


Figure 5.21 v3 (CO₃) widths in WW11-10A areas compared to the control sample

Chapter 6. Discussion and Conclusions

In this chapter, I synthesize the results of my analyses and discuss the limitations and potential confounders of the ν_3 (CO_3) peak width protocol. This leads to proposals for future research that incorporate my results and use the ν_3 (CO_3) peak width protocol in other sites. Finally, I present the implications of my work for our understanding of Wonderwerk Cave, early fire-use, and the role of fire in human evolution.

6.1. General Findings

To summarize the conclusions of this study, spectra collected from a set of known calcite materials, including experimental wood ash, demonstrated that the width of the ν_3 (CO_3) peak width measured at 75% of maximum intensity varies between calcites. A comparison of the peak widths presented convincing data that the average ν_3 (CO_3) peak width and the range of variation of ν_3 (CO_3) peak width within a sample are sufficient to differentiate between calcite types on the basis of formation process. The sequence of calcites from the largest average ν_3 (CO_3) peak width at 75% of maximum intensity to the smallest was roughly equivalent to the sequence of calcites organized on the basis of crystal size and level of atomic order. Specifically, pyrogenic calcite had typical ν_3 (CO_3) peak widths narrower than non-pyrogenic materials, providing that marl could be excluded using other analyses. From the quantitative results of the control samples, I developed the ν_3 (CO_3) peak width protocol which used four criteria to evaluate if spectral analysis with FTIR-m and micromorphology supported an identification of wood ash. Known archaeological ash samples from Oscurusciuto and Wonderwerk Cave fulfilled the criteria, proving that the protocol can be used in prehistoric sites, though it requires good preservation. Using this as a foundation, I identified fragments of ashed plant material in the ESA sediment at Wonderwerk Cave. Out of sixteen potential ash fragments analyzed, eleven fit all four criteria, supporting the identification of ash (Table 6.1).

The results of the FTIR-m analysis indicated that a number of fragments in the Wonderwerk samples which were not conclusively identified as ash using micromorphological analysis were consistent with pyrogenic calcite. This potentially complicates the identification of ash in the cave. Micromorphological analysis relies on the visual identification of plant structures and rhombs composed of micritic calcite in order to identify wood ash. These structures are generally fragile and can be destroyed. It is possible that processes destroy the micromorphological indicators without destroying the molecular indicators that the FTIR-m results come from. In these cases, the ν_3 (CO_3) width protocol is useful second line of evidence to confirm or deny. More research is needed to resolve the discrepancy between the FTIR-m results and the micromorphology results.

As a whole, the results support the identification of wood ash in 1 Mya sediments in Wonderwerk Cave previously reported by Berna et al (2012). I also identified wood ash in new samples collected in 2011 from the same layers of Wonderwerk Cave, suggesting that ash may be present throughout the occupational surface. Although this only confirms the earlier claim, it presents an important secondary line of evidence. Prior to this, it would have been necessary to categorize most wood ash microdeposits in the cave as ambiguous.

The ability to conclusively evaluate potential wood ash features opens a door to future spatial analysis of fire within Wonderwerk Cave. The confirmed microdeposits of ashed plant material combined with the other potential ash features is still a minimal amount, but differences in the abundance and extent of the ash can relate to use of the fire. The greatest concentration of ashed plant material is in WW11-09. Throughout the thin section, there are abundant examples of potential ashed plant fragments, which are very comparable to the known ashed plant fragments. WW11-07 also has frequent examples of similar potential ashed plant fragments, while the similar potential ashed plant fragments in WW05-04 and WW11-10A make up a much smaller proportion of the material. WW11-07 and WW11-09 were taken from the same interface of two layer and the higher frequency of wood ash indicates proximity to the source of the wood ash. These preliminary results suggest a direction to potentially identifying a hearth in the cave.

Table 6.1 Classification of Unknown Archaeological Samples

Area ID	Criteria 1: Spectra < 78	Criteria 2: Average v3 (CO ₃) Width < 87	Criteria 3: 75% of spectra < 95	Criteria 4: Micromorph confirmation	Classification
WW05-04 - Area 1	Yes	No	No	Yes	Likely Wood Ash
WW05-04 - Area 2	Yes	Yes	Yes	Yes	Wood Ash
WW05-04 - Area 3	Yes	Yes	Yes	Yes	Wood Ash
WW05-04 - Area 4	Yes	Yes	Yes	Yes	Wood Ash
WW05-04 - Area 5	Yes	Yes	Yes	Yes	Wood Ash
WW11-07 - Area 1	Yes	No	No	Yes	Likely Wood Ash
WW11-07 - Area 3	Yes	Yes	Yes	Yes	Wood Ash
WW11-07 - Area 4	Yes	Yes	Yes	Yes	Wood Ash
WW11-07 - Area 5	Yes	Yes	Yes	Yes	Wood Ash
WW11-07 - Area 6	Yes	Yes	Yes	No	Unknown
WW11-10A - Area 1	Yes	No	No	No	Geogenic
WW11-10A - Area 3	Yes	No	No	No	Marl/Wood Ash
WW11-09 - Area 1	Yes	Yes	Yes	Yes	Wood Ash
WW11-09 - Area 2	Yes	Yes	Yes	Yes	Wood Ash
WW11-09 - Area 3	Yes	Yes	Yes	Yes	Wood Ash
WW11-09 - Area 4	Yes	Yes	Yes	Yes	Wood Ash

6.2. Reliability of v3 (CO₃) Width as Proxy for Formation Process

The technique developed in this study has the potential to aid in identification of fire in other archaeological sites, both prehistoric and historic. However, there are limitations for how it can be used and what conclusions can be drawn from the results.

It is important to emphasize that the v3 (CO₃) peak width protocol does not divide calcites based on whether they are pyrogenic or geogenic. The v3 (CO₃) width is widest with calcites that have a high level of atomic order and large, stable crystals, and decreases as those decrease. Thus, the separation of calcites is based on these characteristics. Those characteristics (disorder, crystal size) vary based on the formation of the specific sample. Narrow v3 (CO₃) peaks are not an indication of ash, specifically, or even pyrogenic calcite, only that there is a relatively high level of disorder and small

crystals. Any form of calcite that is highly disordered and/or has small crystals will also produce a thin ν_3 (CO_3) peak. This is proven to be the case with marl, which is indistinguishable from pyrogenic materials using solely the ν_3 (CO_3) peak width protocol. In this situation, micromorphology and transmission FTIR-m must be incorporated to identify the clay parts of the marl.

So far, based on the control materials I analyzed, pyrogenic calcite has amounts of disorder and small crystals that are only matched by marl. This does not rule out the existence of other calcitic materials similarly disordered with small crystals. It is possible that dissolved calcite can reform as disordered calcite, due to the presence of magnesium from the dolomitic limestone bedrock in Wonderwerk Cave (Folk 1974; De Groot and Duyvis 1966). Rhizolites that originally formed as clearly geogenic materials may have reformed as disordered ones, or even originally precipitated as disordered ones. However, the lack of a dolomite signal in any of the bedrock within the cave suggests that there is not a strong presence of magnesium within the cave.

While the presence of narrow ν_3 (CO_3) peaks is strong evidence for the presence of fire in the past, the lack of narrow ν_3 (CO_3) peaks does not necessarily mean there was no combustion event. There are a number of potential sources of false negatives. Wet environments will dissolve the ash and destroy the pyrogenic signature. Calcite is highly dissolvable in water, especially the less stable forms such as ash. It will then wash away or re-precipitate as geogenic calcite with a more stable, crystalline structure and no longer preserve the molecular traits picked up by FTIR (Shahack-Gross et al. 2008; Folk 1974; Gillieson 2009). The ν_3 (CO_3) peak width protocol would identify these features as geogenic because of the alteration. I found this in samples where the micromorphology indicated wood ash (specifically known archaeological examples), but the FTIR-m results indicated geogenic. In most of these cases, the micromorphology results included signs of dissolution and precipitation of geogenic calcite within or around the ash deposits.

The range of widths within a single sample make it vital for conclusions to be based not on single spectra, but large groups of spectra. Larger numbers of spectra ensure that the ν_3 (CO_3) widths are a more accurate representation of the variation within that feature. Depending on the length and intensity of maintenance, a fire may produce a combination

of high and low temperature ash because not all of the wood reached the necessary temperature to calcine (Shahack-Gross and Ayalon 2013).

Complementary to comparing large groups of spectra is interpreting the results in conjunction with the microscopic context. Spectra should not be collected at random in a heterogeneous or archaeological sample. Geogenic sources of calcite can be within or next to ash deposits. If a source of identifiable non-pyrogenic calcite is included in a map, the ν_3 (CO_3) widths from the non-pyrogenic calcite should be excluded from analysis.

This new technique should be part of a suite of analyses and is best used to support or reject micromorphological identification of ash, and not as an independent source. Micromorphology remains the most definitive method of identifying combustion features because it can combine context and the identification of a wide range of important materials (and characterize any altered forms of the materials).

6.3. Implications of Fire at Wonderwerk

What does the evidence of fire in an anthropogenic context at Wonderwerk tell us about the relationship of hominins with fire at 1 Mya? Inferring potential hominin behavior requires an understanding of what early interactions and uses of fire would be, and what indicators of these behaviors would survive. Researchers have proposed theoretical schema that could explain how we moved from basic fire-related behavior witnessed in other primates to mastery of pyrotechnology (Pruetz and LaDuke 2010; Chazan in press).

The simplest, and likely earliest, 'uses' of fire would be capitalizing on the benefits of wildfires, including lower transportation costs, naturally cooked food, and high predator visibility (Pruetz and LaDuke 2010). Recently, there have been a number of reports of proto-pyrophiliac behaviors in other primate species, including chimpanzees, baboons, and vervet monkeys (Parker et al. 2016). Vervet monkeys and baboons expand into new areas after a wildfire has swept through to take advantage of better foraging opportunities (Jaffe and Isbell 2009; Herzog et al. 2015; Parker et al. 2016). Chimpanzees demonstrate an understanding of fire behaviour and are potentially able to predict its movements (Pruetz and LaDuke 2010). Pruetz and LaDuke labeled this the 'conceptualization' stage.

From an understanding of fire behavior, it is a small leap to seeking out wildfires on a more frequent basis. These uses of fire are likely to be undetectable in the past, beyond potentially a greater statistical likelihood of finding wildfire evidence in a location with hominin tools.

The first stages of active interaction with fire would include collecting, maintaining, transporting, and extinguishing fires (Pruetz and LaDuke 2010). Chazan (in press) sees this phase as an experimental period which hominins are opportunistically collecting and investigating fire prior to control. He argues for a non-linear process, in which fire-related abilities could be both gained and lost (Chazan in press).

Evidence for experimentation and control of fire is potentially identifiable. Campfires have different properties (shape, duration, fuel) than most wildfires, which leave particular traces in the archaeological record (Bellomo 1993, 1994; Gowlett et al. 1981; Pickering 2012). However, if the use was not habitual, the archaeological evidence for this stage would be inconsistent across sites. Within a site, the lack of constant or repeated use would leave less evidence in the archaeological record.

At some point, there was a shift towards maintenance of fire when benefits of constantly available fire outweighed the expense of gathering fuel. Hominins may or may not have been dependent on fire by maintaining it constantly prior to developing the capability to create it. Habitual use of fire without the ability to create it would have encouraged the long-term maintenance of fire and produced large quantities of fire residues as a result. Thus, this stage may offer the best hope for identifying fire-use and in fact, there are examples of sites where extensive layers of ash support a history of intense, long-term fire maintenance (Albert et al. 2012; Karkanas et al. 2007).

The final stage is the ability to create fire at will. The capability to create fire may have resulted in a decrease of fire residues, because it was not necessary to maintain fires for long periods. The ability would reduce the connection between fire residues and the frequency of fire in an environment and/or season and lead to greater evenness of fire-use across space and time.

The evidence found in Wonderwerk Cave does not exclusively match a single stage, but fitting the evidence to each stage results in a different set of hypotheses for how hominins used the cave which may be testable using information from future excavations. While it is impossible to determine whether humans made the fire, or collected it outside and brought it to the cave, there is an undeniable link between humans and the presence of fire in the cave. This proves that at least some hominins had moved beyond the conceptualization phase of passive association with fire by 1 Mya. If the evidence for fire in Wonderwerk Cave is taken as evidence for human use of fire, it places the control, if not the creation or habitual use, of fire at more than 1 Mya. Recognizing the extent of hominin fire-related behavior and understanding requires a more detailed analysis of how the amount and distribution of ash fits with proposed stages of fire-use.

Before hypothesizing about hominin fire behavior based on the evidence in Wonderwerk Cave, it is necessary to consider how site formation processes effected the preservation of ash and other artifacts of fire. In the case of more recent layers, the results from the LSA fire suggest that bat guano may have promoted the destruction of wood ash in some layers, but guano was not a factor for much of the cave's early occupation. It is possible that factors such as water levels, bioturbation, and/or soil chemistry led to differential preservation of ash, and other indicators of combustion features within the area of analysis and throughout the entire cave. As micromorphological and FTIR analysis has only been done on a small section of the excavated area, it is premature to predict the extent and intensity of fire throughout the cave. If environmental factors are responsible for the pattern of fire residues, the evidence should be seen as a simple indication of presence/absence of fire in an anthropogenic context at 1 Mya. Conclusions beyond that require a detailed understanding of the geological and diagenetic history of the cave on a microscopic scale and multiple proxies of fire-use in order to interpret the pattern of evidence.

If the evidence analyzed so far is representative of the intensity and use of fire, the minimal amounts of burned materials suggest that fire-use in the cave was not on a long-term basis or involve large amounts of fuel. Thus, maintenance of the fire was likely not a primary goal for the inhabitants of the cave. The evidence can be explained in multiple ways. It fits with theories about a stage of experimentation or the early stages of control

of fire, prior to habitual or obligatory use (Pruetz and LaDuke 2010) Chazan in press). The people occupying the cave could not create fire, and were not dependent on it, but they were capable of using fire. According to this hypothesis, the hominins would have opportunistically gathered fire from natural sources (lightning, wildfires), and transported it to the cave. They may have used it for cooking, warmth, protection from predators, but they did not depend on it, and did not or were not able to sustain the fire for long periods of time.

The evidence could also be a reflection of the low-intensity occupation in the cave. Anthropogenic materials are much less common in Wonderwerk than in other, nearby Palaeolithic sites (Horwitz and Chazan 2014). When it was occupied, they used small, short-term combustion features for unknown functions. This would result in a minimal record of fire and fit with the minimal occupational record of the cave. In this scenario, the inhabitants could be habitual and/or obligatory fire-users, in accordance with the Cooking Hypothesis, but the lack of support for maintenance of the cave would necessitate that the occupants had the ability to start fires.

More archaeological evidence is required to test the claims of the cooking hypothesis (Wrangham 1999), but Wonderwerk Cave implies that *Homo erectus* had the cognitive capabilities to use fire, whether or not they used it habitually. The cooking hypothesis had depended, in part, on the explanation that evidence of fire control has been destroyed through taphonomic processes or gone unrecognized due to the difficulty of identifying fire residues. As a single data point, Wonderwerk does not represent the extent of fire-use or the range of variation in fire-related behaviors that existed in all contemporary hominin groups. However, it begins to address the gap of archaeological evidence in the ESA. Because Wonderwerk is a cave environment with hominin occupation, it has better preservation when compared to open-air sites and includes direct evidence of hominin behavior, unlike carnivore deposits or sediment traps. It is therefore one of the most likely places for anthropogenic fire residues to survive. The presence of fire-use in the cave potentially supports an argument of widespread fire-use in the ESA that only survived in exceptional circumstances. Future excavation and sampling can address and narrow down these possibilities.

6.4. Potential Future Research

Having demonstrated that FTIR-m can identify differences in the molecular structure of calcite, it would be useful to better define the range of widths for calcite types. A larger database of control samples would make interpretations more precise and robust. Rhizolite would be one valuable control sample to compare to the wood ash in Wonderwerk Cave.

Future studies could map the extent of combustion features throughout Wonderwerk Cave. The results of this may be able to shed light on the behavior of ancient hominins in the cave and how they interacted with fire. Interpreting the function and behavior in the past is one of the great challenges of archaeology and spatial analysis on this scale is one of the most promising approaches to understand the behavior associated with pyrotechnology.

Within the broader archaeological field, this approach has potential to address a wide range of questions. The quantification of the ν_3 (CO_3) peak width is an approach that can help with a wide range of questions about calcites in archaeological research. While I have focused on wood ash and a binary question of pyrogenic versus not pyrogenic, my protocol has the potential to divide calcites on more fine-grained grounds. For example, because the differences are linked to formation process and environment, a study of the calcite in a stratigraphic sequence may recognize different environmental or climatic conditions at the time of formation. Another interesting strategy would be to use a comprehensive database of local calcites to identify calcite that was imported, or link a specific source of calcite to a use within a site.

The ability to distinguish between high and low temperature ash (if non-ash calcite can be excluded as a possibility) can lead to interpretations about the function of a fire, the fuel and structure of a hearth, and the pyrotechnological abilities involved in pottery and plaster production. Plaster is another form of pyrogenic calcite, and this protocol could characterize the pyrotechnological abilities involved and identify the best preserved line plaster samples for radiocarbon dating.

The creation of a database of ethnoarchaeological samples would be valuable to determine what aspects of fire behavior, if any, can be identified using the v_3 (CO_3) peak width protocol. Here, the ability to distinguish between high and low temperature ash would be extremely relevant to linking ash deposits with behavior. An analysis of the functions and location of ash production and disposal in hunter-gatherer societies could be used to theorize about similar patterns in the archaeological record.

6.5. Conclusions

The research on fire and modern human behavior has been severely curtailed by the lack of archaeological evidence of fire in prehistory. Currently, the data is too incomplete to be used to evaluate theories about when and why pyrotechnology arose. Part of the solution is a multi-proxy, microarchaeological approach to recognize the presence and absence of fire in the archaeological record. With greater precision in recognizing fire, we can interpret the relationship of fire and humans according to seasonality, latitudes, climate, environment, and mobility patterns.

The goal of this study was to first present a new approach for conclusive identification of one element of fire evidence, wood ash, and second, to apply the method and evaluate potential evidence of anthropogenic fire at 1 Mya in Wonderwerk Cave. The results from the analysis of a control set of calcites proved that a combination of micromorphology and FTIR-m spectra could pick up on variances in the crystal size and level of atomic order between calcite types which are caused by different formation process. The ability to identify wood ash on a microscopic scale is a valuable addition to the toolset we use to identify and characterize combustion features.

The v_3 (CO_3) peak width protocol found microdeposits consistent with wood ash in the ESA layers of Wonderwerk Cave. Wood ash is a particularly valuable indicator of fire in this specific situation because the presence of intact fragments implies that the burnt materials are in situ. Thus, the presence of fire residues in the cave is best explained by anthropogenic activity, as other possible causes of fire in the cave have been ruled out.

Conclusions about the pyrotechnological abilities of the cave inhabitants are ambiguous with the current data, but can be refined with spatial analysis of the burnt materials. At present, the small quantity of wood ash even in the samples with the most frequent potential ashed plant fragments may indicate the absence of fire maintenance, because the occupants were capable of creating fire at will, or because the occupants were unable to create fire and unwilling or unable to maintain a fire. The use of fire by hominins in the ESA has implications for our understanding of abstract cognitive abilities in early Homo and raises questions about the role of fire in human evolution.

References

- Addadi, Lia, Sefi Raz, and Steve Weiner
2003 Taking advantage of disorder: amorphous calcium carbonate and its roles in biomineralization. *Advanced Materials* 15(12): 959–970.
- Aiello, Leslie C., and Peter Wheeler
1995 The expensive tissue hypothesis. *Current anthropology* 36(2): 199–221.
- Albert, Rosa M., Francesco Berna, and Paul Goldberg
2012 Insights on Neanderthal fire use at Kebara Cave (Israel) through high resolution study of prehistoric combustion features: Evidence from phytoliths and thin sections. *Quaternary International* 247: 278–293.
- Archibald, Sally, A. Nickless, N. Govender, R. J. Scholes, and Veiko Lehsten
2010 Climate and the inter-annual variability of fire in southern Africa: a meta-analysis using long-term field data and satellite-derived burnt area data. *Global Ecology and Biogeography* 19(6): 794–809.
- Archibald, Sally, A. Carla Staver, and Simon A. Levin
2012 Evolution of human-driven fire regimes in Africa. *Proceedings of the National Academy of Sciences* 109(3): 847–852.
- Barbetti, M., J. D. Clark, F. M. Williams, and M. A. J. Williams
1980 Palaeomagnetism and the Search for Very Ancient Fireplaces in Africa. Results from a Million-year-old Acheulian Site in Ethiopia in Homo Erectus and his Time. Contributions to the origin of Man and his Cultural Development. Vol. 1. *Anthropologie Brno* 18(2–3): 299–304.
- Barbetti, Mike
1986 Traces of fire in the archaeological record, before one million years ago? *Journal of Human Evolution* 15(8): 771–781.
- Bausch, W. M.
1968 Clay Content and Calcite Crystal Size of Limestones. *Sedimentology* 10(1): 71–75.
- Beaumont, Peter B.
2011 The edge: More on fire-making by about 1.7 million years ago at

- Wonderwerk Cave in South Africa. *Current Anthropology* 52(4): 585–595.
- Bellomo, Randy V.
1993 A methodological approach for identifying archaeological evidence of fire resulting from human activities. *Journal of Archaeological Science* 20(5): 525–553.

1994 Methods of determining early hominid behavioral activities associated with the controlled use of fire at FxJj 20 Main, Koobi Fora, Kenya. *Journal of Human Evolution* 27(1): 173–195.
- Bellomo, Randy V., and William F. Kean
1997 Evidence of hominoid-controlled fire at the FxJj 20 site complex, Karari Escarpment. *Koobi Fora Research Project* 5: 224–233.
- Berna, Francesco, Adi Behar, Ruth Shahack-Gross, John Berg, Elisabetta Boaretto, Ayelet Gilboa, Ilan Sharon, Sarel Shalev, Sana Shilstein, and Naama Yahalom-Mack
2007 Sediments exposed to high temperatures: reconstructing pyrotechnological processes in Late Bronze and Iron Age Strata at Tel Dor (Israel). *Journal of Archaeological Science* 34(3): 358–373.
- Berna, Francesco, and Paul Goldberg
2007 Assessing Paleolithic pyrotechnology and associated hominin behavior in Israel. *Israel J Earth Sci* 56: 107–121.
- Berna, Francesco, Paul Goldberg, Liora Kolska Horwitz, James Brink, Sharon Holt, Marion Bamford, and Michael Chazan
2012 Microstratigraphic evidence of in situ fire in the Acheulean strata of Wonderwerk Cave, Northern Cape province, South Africa. *Proceedings of the National Academy of Sciences* 109(20): E1215–E1220.
- Bird, R. Bliege, Douglas W. Bird, Brian F. Coddling, Christopher H. Parker, and James H. Jones
2008 The “fire stick farming” hypothesis: Australian Aboriginal foraging strategies, biodiversity, and anthropogenic fire mosaics. *Proceedings of the National Academy of Sciences* 105(39): 14796–14801.
- Boback, Scott M., Christian L. Cox, Brian D. Ott, Rachel Carmody, Richard W. Wrangham, and Stephen M. Secor
2007 Cooking and grinding reduces the cost of meat digestion. *Comparative*

Biochemistry and Physiology Part A: Molecular & Integrative Physiology 148(3): 651–656.

Brain, C. K., and A. Sillen

1988 Evidence from the Swartkrans cave for the earliest use of fire. *Nature* 336(6198): 464–466.

Brain, Charles Kimberlin

1993 *Swartkrans: A cave's chronicle of early man*. 8. Transvaal Museum.

Brown, Kyle S., Curtis W. Marean, Andy IR Herries, Zenobia Jacobs, Chantal Tribolo, David Braun, David L. Roberts, Michael C. Meyer, and Jocelyn Bernatchez

2009 Fire as an engineering tool of early modern humans. *Science* 325(5942): 859–862.

Canti, Matthew G.

2003 Aspects of the chemical and microscopic characteristics of plant ashes found in archaeological soils. *Catena* 54(3): 339–361.

Carmody, Rachel N., and Richard W. Wrangham

2009 The energetic significance of cooking. *Journal of Human Evolution* 57(4): 379–391.

Chazan, Michael, D. Margaret Avery, Marion K. Bamford, Francesco Berna, James Brink, Yolanda Fernandez-Jalvo, Paul Goldberg, Sharon Holt, Ari Matmon, and Naomi Porat

2012 The Oldowan horizon in Wonderwerk Cave (South Africa): Archaeological, geological, paleontological and paleoclimatic evidence. *Journal of human evolution*.

Chazan, Michael, Hagai Ron, Ari Matmon, Naomi Porat, Paul Goldberg, Royden Yates, Margaret Avery, Alexandra Sumner, and Liora Kolska Horwitz

2008 Radiometric dating of the Earlier Stone Age sequence in excavation I at Wonderwerk Cave, South Africa: preliminary results. *Journal of Human Evolution* 55(1): 1–11.

Chu, Vikki, Lior Regev, Steve Weiner, and Elisabetta Boaretto

2008 Differentiating between anthropogenic calcite in plaster, ash and natural calcite using infrared spectroscopy: implications in archaeology. *Journal of Archaeological Science* 35(4): 905–911.

- Clark, J. D., and J. W. K. Harris
1985 Fire and its roles in early hominid lifeways. *African Archaeological Review* 3(1): 3–27.
- Daniau, Anne-Laure, Francesco d’Errico, and Maria Fernanda Sánchez Goñi
2010 Testing the hypothesis of fire use for ecosystem management by Neanderthal and Upper Palaeolithic modern human populations. *PLoS One* 5(2): e9157.
- De Groot, K., and E. M. Duyvis
1966 Crystal Form of Precipitated Calcium Carbonate as influenced by Adsorbed Magnesium Ions. *Nature* 212(5058): 183–184.
- Dollimore, D.
1987 The thermal decomposition of oxalates. A review. *Thermochimica Acta* 117: 331–363.
- Dunbar, R. I. M., and J. A. J. Gowlett
2014 Fireside Chat: The Impact of Fire on Hominin Socioecology. *Lucy to Language: The Benchmark Papers*: 277.
- Dunbar, Robin IM
2014 How conversations around campfires came to be. *Proceedings of the National Academy of Sciences* 111(39): 14013–14014.
- Folk, Robert L.
1959 Practical petrographic classification of limestones. *AAPG Bulletin* 43(1): 1–38.

1974 The natural history of crystalline calcium carbonate; effect of magnesium content and salinity. *Journal of Sedimentary Research* 44(1): 40–53.
- Giglio, Louis, Ivan Csiszar, and Christopher O. Justice
2006 Global distribution and seasonality of active fires as observed with the Terra and Aqua Moderate Resolution Imaging Spectroradiometer (MODIS) sensors. *Journal of Geophysical Research: Biogeosciences* 111(G2).
- Gillieson, David
2009 *Caves: processes, development and management*. John Wiley & Sons.

- Goldberg, Paul, and Francesco Berna
2010 Micromorphology and context. *Quaternary International* 214(1): 56–62.
- Goldberg, Paul, Francesco Berna, and Michael Chazan
2015 Deposition and diagenesis in the Earlier Stone Age of Wonderwerk Cave, Excavation 1, South Africa. *African Archaeological Review* 32(4): 613–643.
- Goldberg, Paul, and Richard I. Macphail
2009 *Practical and theoretical geoarchaeology*. John Wiley & Sons.
- Goldberg, Paul, S. Weiner, O. Bar-Yosef, Q. Xu, and J. Liu
2001 Site formation processes at Zhoukoudian, China. *Journal of human evolution* 41(5): 483–530.
- Goudsblom, J.
1986 The human monopoly on the use of fire: its origins and conditions. *Human Evolution* 1(6): 517–523.
- Gowlett, J. A. J., J. W. K. Harris, and B. A. Wood
1982 Early hominids and fire at Chesowanja, Kenya (reply).
- Gowlett, John AJ
2006 The early settlement of northern Europe: fire history in the context of climate change and the social brain. *Comptes Rendus Palevol* 5(1): 299–310.
- Gowlett, John AJ, J. W. K. Harris, D. Walton, and B. A. Wood
1981 Early archaeological sites, hominid remains and traces of fire from Chesowanja, Kenya. *Nature* 294: 125–129.
- Herzog, Nicole M., Earl R. Keefe, Christopher H. Parker, and Kristen Hawkes
2015 What's burning got to do with it? Primate foraging opportunities in fire-modified landscapes. *American journal of physical anthropology*.
- Horwitz, L. K., and M. Chazan
2014 An overview of recent research at Wonderwerk Cave, South Africa. In *Proceedings of the 2010 Joint Meeting of the Panafrican Archaeological Congress and the Society of Africanist Archaeologists, Dakar, Senegal*, pp. 2–4.

- Isaac, Glynn
1982 Early hominids and fire at Chesowanja, Kenya.
- Jaffe, Karin Enstam, and Lynne A. Isbell
2009 After the fire: benefits of reduced ground cover for vervet monkeys (*Cercopithecus aethiops*). *American Journal of Primatology* 71(3): 252–260.
- James, Steven R.
1989 Hominid use of fire in the Lower and Middle Pleistocene. *Current Anthropology* 30(1): 1–26.
- Karkanas, P., M. Koumouzelis, J.k. Kozlowski, V. Sitlivy, K. Sobczyk, F. Berna, and S. Weiner
2004 The earliest evidence for clay hearths: Aurignacian features in Klisoura Cave 1, southern Greece. *Antiquity* 78(301): 513–525.
- Karkanas, Panagiotis, Ofer Bar-Yosef, Paul Goldberg, and Steve Weiner
2000 Diagenesis in prehistoric caves: the use of minerals that form in situ to assess the completeness of the archaeological record. *Journal of Archaeological Science* 27(10): 915–929.
- Karkanas, Panagiotis, Ruth Shahack-Gross, Avner Ayalon, Mira Bar-Matthews, Ran Barkai, Amos Frumkin, Avi Gopher, and Mary C. Stiner
2007 Evidence for habitual use of fire at the end of the Lower Paleolithic: Site-formation processes at Qesem Cave, Israel. *Journal of human evolution* 53(2): 197–212.
- Koebnick, Corinna, Carola Strassner, Ingrid Hoffmann, and Claus Leitzmann
1999 Consequences of a long-term raw food diet on body weight and menstruation: results of a questionnaire survey. *Annals of Nutrition and Metabolism* 43(2): 69–79.
- Lane, Melissa D.
1999 Midinfrared optical constants of calcite and their relationship to particle size effects in thermal emission spectra of granular calcite. *Journal of geophysical research* 104(E6): 14099–14108.
- Mallol, Carolina, Cristo M. Hernández, Dan Cabanes, Jorge Machado, Ainara Sistiaga, Leopoldo Pérez, and Bertila Galván
2013 Human actions performed on simple combustion structures: an

- experimental approach to the study of Middle Palaeolithic fire. *Quaternary International* 315: 3–15.
- Mallol, Carolina, Frank W. Marlowe, Brian M. Wood, and Claire C. Porter
2007 Earth, wind, and fire: ethnoarchaeological signals of Hadza fires. *Journal of Archaeological Science* 34(12): 2035–2052.
- Oakley, Kenneth
1956 The earliest fire-makers. *Antiquity* 30(118): 102–107.
- Oakley, Kenneth P.
1961 On man's use of fire, with comments on tool-making and hunting. *Social life of early man* 31: 176e193.
- Organ, Chris, Charles L. Nunn, Zarin Machanda, and Richard W. Wrangham
2011 Phylogenetic rate shifts in feeding time during the evolution of Homo. *Proceedings of the National Academy of Sciences* 108(35): 14555–14559.
- Parfitt, Simon A., René W. Barendregt, Marzia Breda, Ian Candy, Matthew J. Collins, G. Russell Coope, Paul Durbidge, Mike H. Field, Jonathan R. Lee, and Adrian M. Lister
2005 The earliest record of human activity in northern Europe. *Nature* 438(7070): 1008–1012.
- Parker, Christopher H., Earl R. Keefe, Nicole M. Herzog, James F. O'connell, and Kristen Hawkes
2016 The pyrophilic primate hypothesis. *Evolutionary Anthropology: Issues, News, and Reviews* 25(2): 54–63.
- Pickering, Travis Rayne
2012 What's new is old: Comments on (more) archaeological evidence of one-million-year-old fire from South Africa. *South African Journal of Science* 108(5–6): 1–2.
- Poduska, Kristin M., Lior Regev, Elisabetta Boaretto, Lia Addadi, Steve Weiner, Leeor Kronik, and Stefano Curtarolo
2011 Decoupling local disorder and optical effects in infrared spectra: differentiating between calcites with different origins. *Advanced Materials* 23(4): 550–554.

- Poduska, Kristin M., Lior Regev, Francesco Berna, Eugenia Mintz, Ianir Milevski, Stephen Weiner, and Elisabetta Boaretto,
2012 Plaster Characterization at the PPNB site of Yiftahel (Israel) including the use of ¹⁴C: implications for plaster production, preservation and dating” *Radiocarbon* 54(3-4): 887-898
- Pruetz, Jill D., and Thomas C. LaDuke
2010 Brief communication: Reaction to fire by savanna chimpanzees (*Pan troglodytes verus*) at Fongoli, Senegal: Conceptualization of “fire behavior” and the case for a chimpanzee model. *American Journal of Physical Anthropology* 141(4): 646–650.
- Regev, Lior, Kristin M. Poduska, Lia Addadi, Steve Weiner, and Elisabetta Boaretto
2010 Distinguishing between calcites formed by different mechanisms using infrared spectrometry: archaeological applications. *Journal of Archaeological Science* 37(12): 3022–3029.
- Robert, S. Boynton
1979 Chemistry and technology of Lime and Limestone. *A Wiley-Interscience Publication*: 95–158.
- Roebroeks, Wil, and Paola Villa
2011 On the earliest evidence for habitual use of fire in Europe. *Proceedings of the National Academy of Sciences* 108(13): 5209–5214.
- Rolland, N.
2000 Cave occupation, fire-making, hominid/carnivore coevolution, and Middle Pleistocene emergence of home-base settlement systems. *Acta Anthropologica Sinica (Supplement)* 1(9): 209–1.
- Rowlett, Ralph M.
2000 Fire control by *Homo erectus* in East Africa and Asia. *Acta Anthropologica Sinica* 19: 198–208.
- de Ruiter, Darryl J.
2004 Relative abundance, skeletal part representation and accumulating agents of macromammals at Swartkrans. *Swartkrans: a cave’s chronicle of early man. Transvaal Museum, Pretoria*: 265–278.
- Sandgathe, Dennis M., Harold L. Dibble, Paul Goldberg, Shannon P. McPherron, Alain Turq, Laura Niven, and Jamie Hodgkins
2011 Timing of the appearance of habitual fire use. *Proceedings of the National*

Academy of Sciences 108(29): E298–E298.

- Schiegl, Solveig, Paul Goldberg, Ofer Bar-Yosef, and Steve Weiner
1996 Ash deposits in Hayonim and Kebara caves, Israel: macroscopic, microscopic and mineralogical observations, and their archaeological implications. *Journal of archaeological Science* 23(5): 763–781.
- Scott, Andrew C.
2000 The Pre-Quaternary history of fire. *Palaeogeography, palaeoclimatology, palaeoecology* 164(1): 281–329.
- Sergant, Joris, Philippe Crombé, and Yves Perdaen
2006 The “invisible”hearths: a contribution to the discernment of Mesolithic non-structured surface hearths. *Journal of Archaeological Science* 33(7): 999–1007.
- Shahack-Gross, Ruth, and Avner Ayalon
2013 Stable carbon and oxygen isotopic compositions of wood ash: an experimental study with archaeological implications. *Journal of Archaeological Science* 40(1): 570–578.
- Shahack-Gross, Ruth, Avner Ayalon, Paul Goldberg, Yuval Goren, Boaz Ofek, Rivka Rabinovich, and Erella Hovers
2008 Formation processes of cemented features in karstic cave sites revealed using stable oxygen and carbon isotopic analyses: A case study at middle paleolithic Amud Cave, Israel. *Geoarchaeology* 23(1): 43–62.
- Sillen, Andrew, and Thomas Hoering
1993 Chemical characterization of burnt bones from Swartkrans. *Swartkrans: A cave’s chronicle of early man. Pretoria: Transvaal Museum*: 243–249.
- Spagnolo, Vincenzo, Giulia Marciani, Daniele Aureli, Francesco Berna, Paolo Boscato, Filomena Ranaldo, and Annamaria Ronchitelli
Between hearths and volcanic ash: The SU 13 palimpsest of the Oscurusciuto rock shelter (Ginosa – Southern Italy): Analytical and interpretative questions. *Quaternary International*.
- Thieme, Hartmut
1997 Lower Palaeolithic hunting spears from Germany. *Nature* 385(6619): 807–810.

2005 The Lower Palaeolithic art of hunting. *The hominid individual in context*.

Archaeological investigations of Lower and Middle Palaeolithic landscapes, locales and artefacts. Routledge, London New York: 115–132.

- Thompson, T. J. U., Marie Gauthier, and Meez Islam
2009 The application of a new method of Fourier Transform Infrared Spectroscopy to the analysis of burned bone. *Journal of Archaeological Science* 36(3): 910–914.
- Vaquero, Manuel, and Ignasi Pastó
2001 The definition of spatial units in Middle Palaeolithic sites: the hearth-related assemblages. *Journal of Archaeological Science* 28(11): 1209–1220.
- Weiner, Stephen
2010 *Microarchaeology: Beyond the visible archaeological record*. Cambridge University Press.
- Weiner, Stephen, Paul Goldberg, and Ofer Bar-Yosef
2002 Three-Dimensional Distribution of Minerals in the Sediments of Hayonim Cave, Israel: Diagenetic Processes and Archaeological. *Journal of Archaeological Science* 29(11): 1289–1308.
- Weiner, Stephen, Paul Goldberg, and Ofer Bar-Yosef
1993 Bone preservation in Kebara Cave, Israel using on-site Fourier transform infrared spectrometry. *Journal of Archaeological Science* 20(6): 613–627.
- Weiner, Steve, Qinqi Xu, Paul Goldberg, Jinyi Liu, and Ofer Bar-Yosef
1998 Evidence for the Use of Fire at Zhoukoudian, China. *Science* 281(5374): 251–253.
- Whittaker, John C.
2010 *Flintknapping: making and understanding stone tools*. University of Texas Press.
- Wigley, T. M. L.
1973 The incongruent solution of dolomite. *Geochimica et Cosmochimica Acta* 37(5): 1397–1402.
- Wrangham, Richard, and NancyLou Conklin-Brittain
2003 “Cooking as a biological trait.” *Comparative Biochemistry and Physiology Part A: Molecular & Integrative Physiology* 136(1): 35–46.

Wrangham, Richard W., James Holland Jones, Greg Laden, David Pilbeam, and NancyLou Conklin-Brittain
1999 The Raw and the Stolen: Cooking and the Ecology of Human Origins. *Current Anthropology* 40(5): 567–594.

Zink, Katherine D., Daniel E. Lieberman, and Peter W. Lucas
2014 Food material properties and early hominin processing techniques. *Journal of human evolution* 77: 155–166.